Role of Central Nervous System Ceramides and Free Radicals in a Mouse Model of Orofacial Pain

Tang Ning

(MBBS)

Supervisor: Associate Professor Yeo Jin Fei

A THESIS SUBMITTED FOR THE DEGREE OF

DOCTOR OF PHILOSOPHY

DEPARTMENT OF ORAL AND MAXILLOFACIAL SURGERY

FACULTY OF DENTISTRY

NATIONAL UNIVERSITY OF SINGAPORE

2009

ACKNOWLEDGMENTS

First of all, I would like to express my deepest appreciation to my two supervisors, **Associate Professor Yeo Jin Fei** (Department of Oral and Maxillofacial Surgery, Faculty of Dentistry) and **Associate Professor Ong Wei Yi** (Department of Anatomy, Yong Loo Lin School of Medicine). Their guidance, support, and generosity have made me where I am today. They have not only introduced me to an entirely new research field but also are role models for hardworking and commitment to research. Their deep and sustained interest, immense patience and stimulating discussions have been most invaluable in the accomplishment of my research project.

I must also acknowledge my gratitude to **Assistant Professor Chen Peng** and **Dr Zhang En Ming** from Division of Bioengineering, Nanyang Technological University, **Dr Wei Shun Hui** from Singapore Bioimaging Consortium, Biopolis, for their kind suggestions and guidance in my work.

I would like to thank all other staff members, my fellow postgraduate students and vital friends in Histology Lab, Neurobiology Programme, Centre for Life Science, National University of Singapore: **Pan Ning**, **Lim Seok Wei**, **Jinatta Jittiwat**, **Lee Li Yen**, **Lee Hui Wen Lynette**, **Kim Ji Hyun**, **Ma May Thu**, **Poh Kay Wee**, **Chia Wan Jie**, for their help and support in many ways. It was a joyful experience working with all of them.

Last but not least, I would like to take this opportunity to express my heartfelt thanks to my family for their full and endless support, especially my husband, **Dr He Wei**, whose constant encouragement and understanding throughout my study have made this work possible, and to my child, **He Ming Zhe** who brings me so much joy. Without my family, I could not have completed this thesis.

TABLE OF CONTENTS

SUMMARY

Growing evidences have indicated an important role of central nervous system (CNS) lipid mediators and reactive nitrogen species (RNS) in augmenting the sensitivity of sensory neurons and enhancing pain perception. Increased amount of ceramide which is an important sphingolipid signaling molecule and elevated ceramide biosynthetic activity have been shown to contribute to neuronal death in the hippocampus after kainate-induced excitotoxic injury. RNS species such as peroxynitrite ($ONOO^-$) and its derivates can cause lipid oxidation, protein nitration, and DNA damage, leading to changes in the function of signaling molecules.

Intracerebroventricular (ICV) injection of inhibitors to ceramide synthetic enzymes into mice was conducted to elucidate possible role of CNS ceramide in orofacial pain induced by facial carrageenan injection. ICV injection of inhibitors to acid sphingomyelinase (ASMase), neutral sphingomyelinase (NSMase), or serine palmitoyltransferase (SPT) significantly reduced allodynic responses in facial carrageenan injected mice.

An enzyme activity assay was conducted in the mice brain tissue. Increased ASMase activity was found in the left primary somatosensory cortex at 3 days after facial carrageenan injection. And ICV injection of ASMase inhibitor D609 significantly reduced ASMase activity in all parts of brain examined (i.e., left and right brain stem, thalamus, and primary somatosensory cortex). These results provide a further confirmation that D609 alleviates facial allodynia through the action of ASMase.

Since D609 is also found to be a free radical scavenger, phenyl-N-tert-butylnitrone (PBN), a free radical spin trap was ICV injected to elucidate the role of free radicals in nociception. Similar anti-allodynic effect was observed in mice with facial allodynia after PBN treatment. It was also found that C18 ceramide could cause increased hydrogen peroxide production in PC12 cells. This effect could be inhibited by co-treatment with L-type calcium inhibitor (nifedipine), free radical scavengers (D609 or PBN), or mitochondria permeability transition pore blockers (bongkrekic acid or cyclosporine A).

Electrophysiological study showed that ceramide has the ability to directly induce exocytosis in cells using membrane capacitance measurement technique (whole-cell patch clamp) and total internal reflection fluorescence microscopy technique. Effects of ceramide were found to be dependent on the integrity of cell membrane lipid raft, as ceramide could not induce exocytosis in cells depleted of membrane cholesterol. Direct application of ceramide can also cause elevated intracellular calcium concentration in PC12 cells.

The role of other forms of free radicals such as peroxynitrite in orofacial allodynia was also investigated. Mice behavioral studies showed that $ONOO^-$ plays a role in nociception in the CNS in mice with facial allodynia. ICV injection of $ONOO^-$ scavenger FeTPPS significantly reduced allodynia in the facial carrageenan injected mice at 3 days after injection.

In conclusion, the present study showed a possible role of CNS ceramide and $ONOO^-$ in a mouse model of orofacial allodynia.

LIST OF TABLES

LIST OF FIGURES

ABBREVIATIONS

$[Ca^{2+}]_i$	intracellular free calcium concentration
5-HT	serotonin/5-hydroxytryptamine
AMPA	α-amino-3-hydroxyl-5-methyl-4-isoxazole-propionate
ASMase	acid sphingomyelinase
ATP	adenosine triphosphate
cAMP	cyclic adenosine monophosphate
Cer1P	ceramide 1- phosphate
cGMP	cyclic guanosine monophosphate
CGRP	calcitonin gene related peptide
CNS	central nervous system
COX	cyclooxygenase
$cPLA_2$	cytosolic phospholipase A_2
DAG	diacylglycerol
DMEM	Dulbecco's modified eagle medium
DMSO	dimethyl sulfoxide
DRG	dorsal root ganglia
EDTA	ethylenediaminetetraacetic acid
EGFP	enhanced green fluorescence protein
EGTA	ethylene glycol tetraacetic acid
eNOS	endothelial nitric oxide synthase
Fura-2-AM	Fura-2, acetoxymethyl ester
H_2O_2	hydrogen peroxide

IASP	International association for the study of pain
IC50	median inhibition concentration
ICV	intracerebroventricular
iNOS	inducible nitric oxide synthase
IP	intraperitoneal
IP_3	inositol trisphosphate
KRPG	Krebs–Ringer phosphate buffer
M-ß-CD	methyl ß cyclodextrin
mtNOS	mitochondrial nitric oxide synthase
NGF	nerve growth factor
NMDA	N-methyl-D-aspartate
nNOS	neuronal nitric oxide synthase
NO	nitric oxide
NOS	nitric oxide synthase
NPY	neuropeptide Y
NSMase	neutral sphingomyelinase
O_2^-	super oxide anion
$ONOO^-$	peroxynitrite
PBN	phenyl-N-tert-butylnitrone
PC-PLC	phosphatidylcholine-specific phospholipase C
PC12 cell	pheochromocytoma cell
PGE_2	prostaglandin E_2
PKC	protein kinase C

PLA_2	phospholipase A_2
Pr5	the principal or main trigeminal nucleus
RNS	reactive nitrogen species
ROS	reactive oxygen species
S1P	sphingosine 1- phosphate
SI	primary somatosensory cortex
SII	secondary somatosensory cortex
SNARE	soluble N-ethylmaleimide-sensitive factor attachment protein receptor
SOD	superoxide dismutase
Sp5C	spinal trigeminal nucleus caudalis
Sp5I	spinal trigeminal nucleus interpolaris
Sp5O	spinal trigeminal nucleus oralis
$sPLA_2$	secretory phospholipase A_2
SPT	serine palmitoyltransferase
SPTLC1	serine palmitoyltransferase, long chain base subunit 1
TIRFM	total internal reflection fluorescence microscopy
TNF	tumor necrosis factor
TRPV1	transient receptor potential cation channel, subfamily V, member 1
UV	ultraviolet
VPL	ventral posterolateral nucleus of the thalamus
VPM	ventral posteromedial nucleus of the thalamus

PUBLICATIONS

Various portions of the present study have been published in international refereed journals.

1. **Tang N**, Ong WY, Farooqui AA, Yeo JF (2009) Anti-allodynic effect of intracerebroventricularly administered antioxidant and free radical scavenger in a mouse model of orofacial pain. J Orofac Pain 23: 167-173

2. Yeo JF, Ling SF, **Tang N**, Ong WY (2008) Antinociceptive effect of CNS peroxynitrite scavenger in a mouse model of orofacial pain. Exp Brain Res 184: 435-438

3. **Tang N**, Ong WY, Zhang EM, Chen P, Yeo JF (2007) Differential effects of ceramide species on exocytosis in rat PC12 cells. Exp Brain Res 183: 241-247

4. Ong WL, Jiang B, **Tang N**, Ling SF, Yeo JF, Wei S, Farooqui AA, Ong WY (2006) Differential effects of polyunsaturated fatty acids on membrane capacitance and exocytosis in rat pheochromocytoma-12 cells. Neurochem Res 31: 41-48

Chapter I

INTRODUCTION

1. General introduction of pain

1.1. History of pain study and pain definitions

Pain is defined by the International Association for the Study of Pain (IASP, 2008) as “an unpleasant sensory and emotional experience associated with actual or potential tissue damage, or describe in terms of such damage”. It is a protective mechanism for the body and causes a human or animal to take action to remove the pain stimulus.

The earliest scientific history of pain transmission should be René Descartes' reflex theory more than 300 years ago, which proposed a specific pain pathway which carries the information from pain receptors in the peripheral skin to pain center in the brain, indicating that a simple block of the pathway would result in the alleviation of pain. The pain measurement at that time was focused on the pain intensity. Descartes’ reflex theory guided both the study and treatment of pain for centuries till the appearance of the gate control theory of pain (Melzack and Wall 1965), which led to a further investigation into spinal sensitization and central nervous system (CNS) plasticity. The main achievement of the gate control theory of pain is that it led to the recognition that the relationship between pain and stimulus is not a simple sensory response, the processing of pain takes place in at least three levels — at peripheral, spinal, and supraspinal sites. However, recently more studies showed that pain perception is not a mere biophysical process, it is always subjective and influenced by a variety of complicated factors. For example, acute pain can be proportional to the extent of the injury, but also be affected by psychological factors, such as fear, anxiety, cultural background and the meaning of the situation to the person (Sternbach 1975).

A few definitions of pain-related terms are clarified here: Nociception is defined as the neural process of encoding and processing noxious stimuli (Loeser and Treede 2008). It is the afferent activity produced in the peripheral and CNS by stimuli that have the potential to damage tissue. The term "nociception" is often used interchangeably with the term "pain", but technically refers to the transmission of nociceptive information to the brain without reference to the production of emotional or other types of response to the noxious stimulus. Nociceptor is a receptor preferentially sensitive to a noxious stimulus or to a stimulus which would become noxious if prolonged. The most often used two behavioral tests in pain studies are hyperalgesia and allodynia. Hyperalgesia is the increased response to a stimulus which is normally painful. For pain evoked by stimuli that usually are not painful, the term allodynia is preferred. Allodynia is defined as pain due to a stimulus which does not normally provoke pain. In addition, the difference between hyperalgesia and allodynia can also be elucidated in terms of pain hypersensitivity which takes two forms: thresholds are lowered so that stimuli that would normally not produce pain now begin to — allodynia; Responsiveness is increased, so that noxious stimuli produce an exaggerated and prolonged pain — hyperalgesia.

Other somatosensory disorders of increased pain sensation which are often seen in the literature include hyperesthesia, hyperpathia and neuropathy. Hyperesthesia is defined as increased sensitivity to stimulation, excluding the special senses. Hyperesthesia may refer to various modes of cutaneous sensibility including touch and thermal sensation without pain, as well as to pain. Hyperesthesia includes both allodynia and hyperalgesia. Hyperpathia is defined as a painful syndrome characterized by an abnormally painful reaction to a stimulus, especially a repetitive stimulus, as well as an

increased threshold. Neuropathy is a disturbance of function or pathological change in a nerve (IASP, 2008).

1.2. Types of pain

Depending on the nature and time course of the original stimulus, there are three major types of pain that have different neurophysiological mechanisms. However, it is important to know that these types are not exclusive.

1.2.1. Type 1 (Acute nociceptive pain)

The mechanism of type 1 of pain can be viewed as a simple and direct route of transmission centrally toward the thalamus and cortex and subsequently the conscious perception of pain, however there still has possibility of modulation at synaptic relays along the pathway. It is suggested that it is best to use models based on the specificity interpretation of pain mechanisms to explain type 1 pain, that is, the existence within the peripheral and CNS of a series of neuronal elements concerned solely with the processing of these simple noxious elements.

1.2.2. Type 2 (Inflammatory pain)

If a noxious stimulus is very intense or prolonged, leading to tissue damage and inflammation, the afferent flow to the CNS from the injured nociceptors will increase because of the elevated activity and responsiveness of sensitized nociceptors. And nociceptive neurons in the spinal cord also modify their responsiveness in ways that are not merely an expression of the peripheral stimulations.

The subject with type 2 pain can feel spontaneous pain in the injured area, as well

as the undamaged area surrounding the injury site. This changed sensation is known as hyperalgesia, defined as a leftward shift in the stimulus-response function (Figure 1.1). In this situation, normally innocuous stimuli such as brushing and touch, are painful (allodynia), and normally mild pain stimuli like pinprick are much more painful than usual (hyperalgesia). Hyperalgesia in the area of injury is also known as primary hyperalgesia, and the abnormal pain in the "normal" tissue surrounding the damaged site is defined as secondary hyperalgesia.

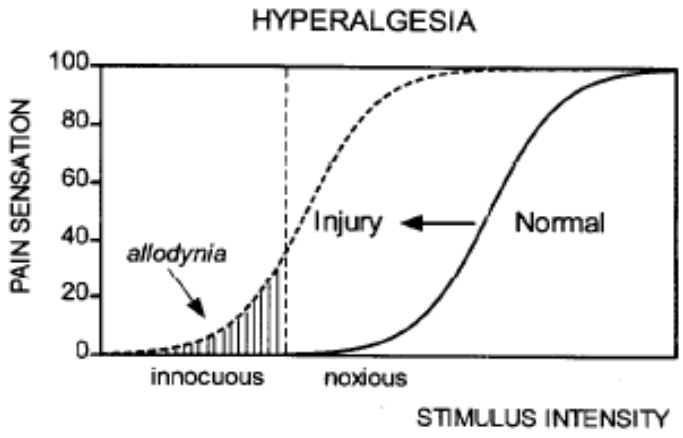

Figure 1.1 Diagram illustrating the changes in pain sensation induced by injury. The normal relationship between stimulus intensity and magnitude of pain sensation is represented by the curve. Pain sensation is only evoked by stimulus intensities in the noxious range (the vertical dotted line indicates the pain threshold). The leftward shift in the curve relating stimuli intensity to pain sensation is called hyperalgesia. Under these conditions, innocuous stimuli evoke pain (allodynia), and stimuli intensities that normally evoke mild pain evoke more intense pain (Cervero and Laird 1996).

1.2.3. Type 3 (Neuropathic pain)

This type of pain is abnormal and is generally the consequence of damage to peripheral nerves or CNS itself, characterized by a lack of correlation. These pains are spontaneous, triggered by innocuous stimuli, or are exaggerated responses to noxious

minor stimuli. These sensations are expressions of substantial changes in the nociception system induced by peripheral or central damages.

1.3. Primary and central sensitization

On the one hand, pain hypersensitivity as an adaptive response facilitates the healing process after an injury because it avoids or minimizes the direct contact with the injured tissue until repair is complete. On the other hand, pain hypersensitivity may persist long after an injury has healed or occur in the absence of any injury. In this case, pain turns to a manifestation of pathological change in the nervous system.

Two mechanisms are known to be involved in pain hypersensitivity — peripheral and central sensitization. “Sensitization” here means the increase in the excitability of neurons, so they are more sensitive to stimuli or sensory inputs.

1.3.1. Peripheral sensitization

Peripheral sensitization refers to a reduction in threshold and an increase in the sensitivity and excitability of the nociceptors terminal (Treede et al. 1992; Julius and Basbaum 2001). Peripheral sensitization contributes to pain hypersensitivity at the site of tissue damage and inflammation, a phenomenon which is also called primary hyperalgesia.

Peripheral sensitization results from the release of numerous inflammatory factors and changes of ion channels in the nociceptor terminal. The inflammatory factors include prostaglandins, adenosine triphosphate (ATP) (Gold et al. 1996), bradykinin (Chahl and Iggo 1977; Cui and Nicol 1995), nerve growth factor (NGF), potassium, leukotrienes,

serotonins, substance P, histamines, thromboxanes, serotonin/5-hydroxytryptamine (5-HT) (Cardenas et al. 2001; Okamoto et al. 2002), endothelin-1 (Gokin et al. 2001; Zhou et al. 2002), platelet-activating factor, protons and free radicals. For example, increased level of substance P is found in the periphery after nerve injury (Donnerer et al. 1993; Carlton et al. 1996). It has been observed that intrathecal injection of substance P, or its close analogues, can produce hyperalgesia to a variety of noxious stimuli (Cridland and Henry 1986).

These inflammatory mediators could phosphorylate G-protein-coupled receptors or tyrosine kinase receptors on nociceptor terminals, activating phospholipase C signaling pathways. Among these receptors, transient receptor potential receptor (TRP) is the one that has been well studied. TRPV1 (transient receptor potential receptor, subfamily V, member 1) can be activated by noxious heat, acid, capsaicin and resiniferatoxin, leading to burning pain or itch. It is found that NGF and bradykinin can induce changes in TRPV1 by activating of cAMP-dependent (cyclic adenosine monophosphate-dependent) protein kinase and Ca^{2+}/phospholipid-dependent kinase, so that a lower temperature (<40 °C) which normally could not activate TRPV1 can now activate this receptor (Chuang et al. 2001).

Transcriptional or translational regulation also contributes to peripheral sensitization. It is found that NGF-induced activation of p38 mitogen-activated protein kinase (MAPK) in primary sensory neurons after peripheral inflammation increases the expression and peripheral transport of TRPV1, exacerbating heat hyperalgesia (Ji et al. 2002). There is evidence that in small DRG (dorsal root ganglia) cells, NGF has the

ability to stimulate an upregulation of $Na_V1.8$, a sensory neuron-specific voltage-gated sodium channel (Bielefeldt et al. 2003).

1.3.2. Central sensitization

Central sensitization refers to the increase in the excitability of CNS neurons, so that normal stimuli produce abnormal responses. Central sensitization is responsible for tactile allodynia (pain in response to light brushing of the skin) and for the spread of pain hypersensitivity resulting in increased susceptibility of tissue adjacent to damaged area, a phenomenon often termed as "secondary hyperalgesia" (Sang et al. 1996; Klede et al. 2003). Many studies on secondary hyperalgesia were conducted with capsaicin, which selectively acts on several types of fine sensory C and Aδ-fibers. Capsaicin causes intense pain and secondary hyperalgesia when applied topically or intradermally (Simone et al. 1989).

Central sensitization has two phases: An immediate but relatively transient phase and a slower onset but longer-lasting phase. Central sensitization is associated with enhanced responses to excitatory amino acids and decreased responses to inhibitory amino acids. The mechanism of the increase in responses to excitatory amino acids includes phosphorylation of NR1 subunits of N-methyl-D-aspartate (NMDA) receptors and GluR1 subunits of α-amino-3-hydroxyl-5-methyl-4-isoxazole-propionate (AMPA) receptors (Willis 2009).

In the early phase of central sensitization, signaling molecules including glutamate, neuropeptides [eg., substance P and calcitonin gene related peptide (CGRP)] and synaptic modulators are released from synapses in the spinal cord upon receiving

signals from the nociceptors, activating intracellular signaling pathways that could lead to the phosphorylation of membrane receptors and channels, especially NMDA (Cheng et al. 2008) and AMPA receptors. Glutamate plays a major role in the process of central sensitization (DeLeo 2006). These changes could increase the efficacy of synaptic transmission between primary and secondary neurons in the nociception pathway, thereby increasing the excitability of the neurons. Central sensitization also depends on activation of several protein kinases and other enzymes, such as nitric oxide synthase. This process is regulated by protein phosphatases. Central sensitization can be regarded as a spinal cord form of long-term potentiation (Willis 2009).

The later phase of central sensitization is transcription-dependent. It is mediated by increased protein production. Proteins involved in this process include dynorphin (Malan et al. 2000; Ossipov et al. 2000), an endogenous opioid that increases neuronal excitability, and cyclooxygenase-2 (COX-2) (Burns et al. 2006; Levy et al. 2008), the enzyme that produces prostaglandin E_2.

2. General introduction of orofacial pain

Similar brain structures are involved in the process of nociception and related expression of nociceptive behaviors in humans and animal models (Chang and Shyu 2001). For example, trigeminal sensory nuclei are involved in nociceptive activity in orofacial pain. Lesions or injections of analgesic chemicals into these levels can interfere with nociceptive behavior (Takemura et al. 1993).

2.1. Anatomy basis of orofacial pain

2.1.1. Trigeminal nerves

Trigeminal nerve (the fifth cranial nerve) is primarily a sensory nerve, it also has certain motor functions such as biting, chewing, and swallowing. Trigeminal nerve has three divisions according to the different innervation area. They are ophthalmic, maxillary and mandibular division (Figure 1.2). Each division supplies to a distinct area on the head, face, the adjacent mucosal and meningeal tissues (Usunoff et al. 1997).

The ophthalmic nerve innervates the forehead, upper eyelid, cornea and conjunctiva, dorsum of the nose, mucous membranes of the nasal vestibule and frontal sinus, and the cranial dura. The maxillary nerve innervates the lower eyelid, anterior portion of the temple, paranasal sinuses, upper lip and cheek, nose, oral mucosa of the upper mouth, pharynx, gums, maxillary teeth, hard palate, soft palate, and cranial dura. The mandibular nerve has both sensory and motor components. The motor mandibular component innervates the muscles of mastication, the temporalis, masseter, lateral and medial pterygoids, mylohyoid, the anterior belly of the digastric muscle, the tensors

tympani and veli palatini. The sensory component of mandibular nerve innervates the lower lip and chin, posterior portion of the temple, external auditory meatus and tympanic membrane, external ear teeth of the lower jaw, oral mucosa of the cheeks and the floor of the mouth, anterior two thirds of the tongue, temporomandibular joint and cranial dura.

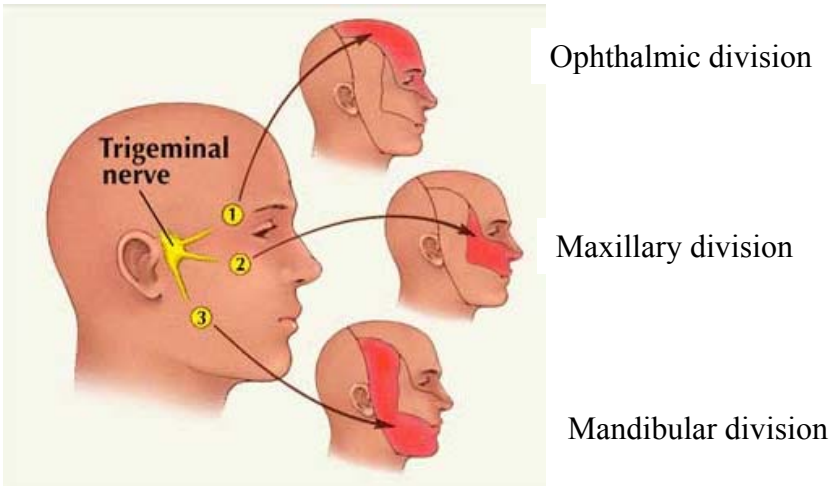

Figure 1.2 Dermatome distribution of the trigeminal nerve (modified from Hinrichsen, 2008).

2.1.2. Trigeminal ganglion

The three branches of trigeminal nerve converge on the trigeminal ganglion, which contains cell bodies of incoming sensory nerve fibers. Fibers from trigeminal ganglion project to different trigeminal nucleus in brain stem. The trigeminal ganglion lies in the Meckel's cave in the dura mater near the apex of the petrous part of the temporal bone. Ganglion cells are pseudounipolar and their somata are tightly wrapped by satellite cells, with some showing complex interdigitations with neuronal membrane (Beaver et al. 1965).

A large number of peptides are known to be present in the trigeminal ganglion. These include calcitonin gene related peptide (CGRP), substance P, somatostatin, galanin and enkephalins (Del Fiacco and Quartu 1994; Quartu and Del Fiacco 1994). It has been found that CGRP exists in the majority of neurons from rat trigeminal ganglia, together with exocytotic SNAREs (soluble N-ethylmaleimide-sensitive factor attachment protein receptor) and synaptotagmin (Meng et al. 2007). Nearly half the human ganglion cells contain CGRP, and around 15% containing substance P, and some showing co-localization of these two (Helme and Fletcher 1983; Quartu et al. 1992).

2.1.3. Sensory trigeminal nucleus

Sensory fibers from trigeminal nerve as well as other cranial nerves— facial nerve (cranial nerve VII), glossopharyngeal nerve (cranial nerve IX) and vagus nerve (cranial nerve X) terminate in the trigeminal nucleus, which thus contains a complete sensory map of the face and mouth. The trigeminal nucleus extends throughout the entire brain stem, from the midbrain to the medulla, continues into the spinal cord and merges with the dorsal horn cells. The nucleus is divided anatomically into three parts. From caudal to rostral, they are the spinal trigeminal nucleus, the main trigeminal nucleus, and the mesencephalic trigeminal nucleus (Figure 1.3).

The major neural transmitter throughout the sensory complex is glutamate, with NMDA and non-NMDA receptors at all levels (Magnusson et al. 1987; Tallaksen-Greene et al. 1992; Petralia et al. 1994). In addition, peptides such as substance P and CGRP are also important neural transmitters in the sensory trigeminal nucleus (Sessle 2000).

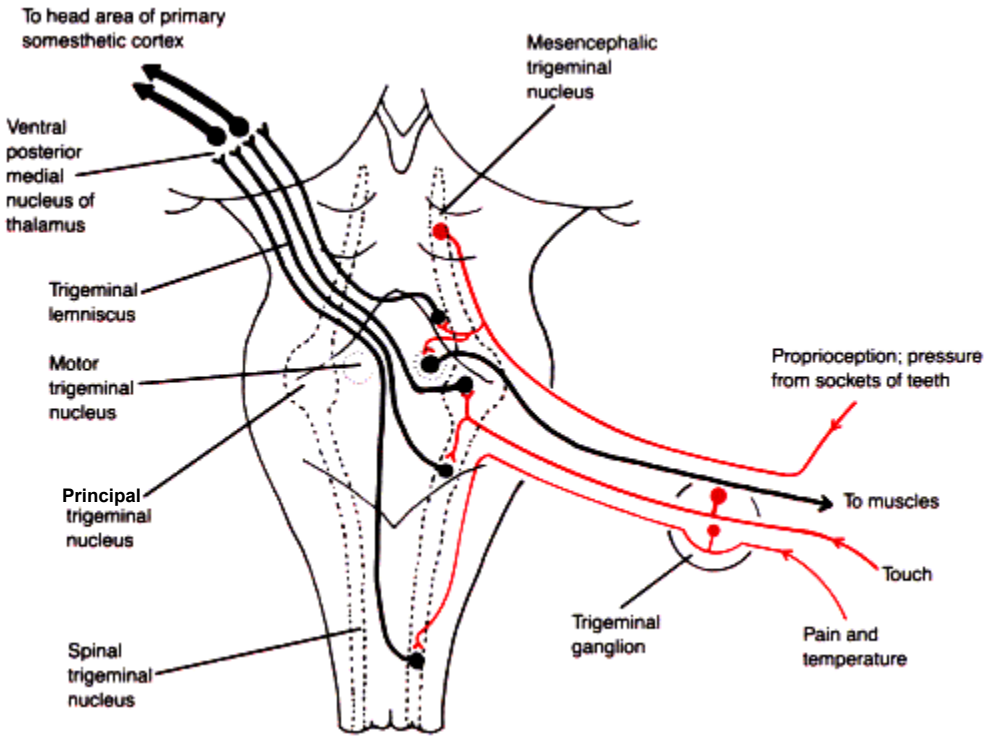

Figure 1.3 Distribution of sensory trigeminal nucleus (modified from Snell 2006).

Spinal trigeminal nucleus

The spinal trigeminal nucleus receives fibers carrying pain/temperature sensation from the face, i.e., fibers from cranial nerves V, VII, IX, and X. These fibers are grouped together and can be identified as the spinal tract of the trigeminal nucleus, which parallels the spinal trigeminal nucleus itself. The spinal trigeminal nuclei are further subdivided into three groups– oralis (Sp5O), interpolaris (Sp5I) and caudalis (Sp5C) (Capra and Dessem 1992). From the spinal trigeminal nucleus, secondary fibers cross the midline and ascend via the trigeminothalamic tract to the contralateral thalamus. The trigeminothalamic tract runs parallel to the spinothalamic tract carrying pain/temperature

sensation from rest of the body. Besides the thalamus, the spinal trigeminal nucleus also sends pain/temperature information to the mesencephalon and the reticular formation of the brainstem.

It has been proposed Sp5O is particularly important for processing information about short duration nociceptive stimuli, whereas Sp5C is more important for processing tonic nociceptive information (Raboisson et al. 1995). Clinical findings are consistent with results from animal experiments indicating that Sp5C is the most important component of the trigeminal nuclear complex for perception of noxious stimuli applied to craniofacial region (Broton et al. 1988; Dohrn et al. 1994; Sessle 2000). The afferents terminating in Sp5C contain neuropeptides and amino acids that have been implicated as excitatory neurotransmitters or neuromodulators (e.g. substance P, glutamate, nitric oxide) in central nociceptive transmission (Sessle 2000). For instance, NK1, an antagonist of the substance P receptor, blocks c-fos expression induced by noxious chemical stimulation of dural afferents (Shepheard et al. 1995).

Main trigeminal nucleus

The principal or main trigeminal nucleus (Pr5) receives touch/position sensation from face via cranial nerves V, VII, IX, and X. It is located in the pons, close to the entry site of the trigeminal nerve. Animal studies have shown that neurons in Pr5 are mechanoreceptive with low thresholds and small receptive fields (Jacquin et al. 1988). From the main trigeminal nucleus, secondary fibers cross the midline and ascend in the trigeminal lemniscus to the contralateral thalamus. The trigeminal lemniscus runs parallel

to the medial lemniscus carrying touch/position information from the rest of the body to the thalamus.

Some sensory information from the teeth and jaws is also projected from the main trigeminal nucleus to the ipsilateral thalamus, via the small dorsal trigeminal tract. Thus touch/position information from the teeth and jaws is represented bilaterally in the thalamus, and hence in the cortex (Brodal 2004).

Mesencephalic trigeminal nucleus

The mesencephalic trigeminal nucleus is not a real "nucleus." It is actually a sensory ganglion imbedded in the brainstem. Only certain types of sensory fibers have cell bodies in the mesencephalic nucleus: proprioceptor fibers from the jaw, and mechanoreceptor fibers from the teeth. Some of these incoming fibers go to the motor trigeminal nucleus, thus entirely bypassing the pathways for conscious perception. Other incoming fibers from the teeth and jaws go to the main trigeminal nucleus. As mentioned above, these information are projected bilaterally to the thalamus, and then to the cortex for conscious perception (Brodal 2004).

2.1.4. Pathways to the thalamus and the cortex

The ventral posterolateral nucleus (VPL) nucleus of the thalamus receives touch/position information from the body, while touch/position information from the face is sent to the ventral posteromedial nucleus (VPM) nucleus of the thalamus. Information from VPL and VPM is then projected to the primary somatosensory cortex (SI) in the postcentral gyrus of the parietal lobe. Information from SI is sent to the secondary

somatosensory cortex (SII) in the parietal lobe. In general, information from one side of the body is represented on the opposite side in SI, but on both sides in SII (Brodal 2004).

Pain/temperature information is also sent to the VPL (body) and VPM (face) of the thalamus. From the thalamus, both pain/temperature and touch/position information is projected onto SI. The main difference between touch/position and pain/temperature sensation transmission is that the latter is also sent to additional thalamic nuclei and areas of cortex. Some pain/temperature fibers are sent to the medial dorsal thalamic nucleus, then to the anterior cingulate cortex. Other fibers are relayed to the ventromedial nucleus of the thalamus, then to the insular cortex. Finally, some fibers are sent to the intralaminar nuclei of the thalamus via the reticular formation. The intralaminar nuclei projections diffuse to all parts of the cerebral cortex (Brodal 2004).

2.2. Orofacial pain

The diagnosis of orofacial pain is complicated because of the region's density of anatomical structures, rich innervations and high vascularity. Orofacial pain is defined by the American Academy of Orofacial Pain (AAOP) as "pain conditions that are associated with the hard and soft tissues of the head, face, neck, and all the intraoral structures" (Okeson 1996). Most prevalent pain in this area originates from the teeth and their surrounding structures. Pain from these areas can be caused by local injury resulting from trauma, infection or neoplasms.

The ill-defined category of atypical oral and facial pain includes a variety of pain descriptions like phantom tooth pain (Turp 2005), atypical odontalgia (Grushka et al. 2003; Baad-Hansen et al. 2005), atypical facial neuralgia (Marbach et al. 1982; Aguggia

2005), and the burning mouth syndrome (Grushka et al. 2003). The pain in these cases usually has a burning quality that occasionally intensifies to produce throbbing sensation. The pain is not triggered by remote stimuli, but may be intensified by stimulation of the affected area itself.

2.3. Animal model of orofacial pain

The understanding of neural mechanisms of both acute and chronic pain syndromes has been improved a lot by the usage of animal models. These animal models provide quantitative assessments of hypersensitivity that are correlated to pain in human. Although currently it is not possible to scientifically prove whether an animal is in pain or not and how painful they are, it can still be inferred from physical and behavioral reactions.

Acute inflammatory pain models normally involve injection of an irritant substance into a joint or hind paw of animals. The chronic neuropathic pain models usually involve surgical manipulation of a nerve. Behavioral testing approaches can be classified by the method of stimulation (thermal, chemical, or mechanical) and by the type of stimulus (noxious compared with non-noxious). The two behavioral tests that are most often used in chronic pain studies are hyperalgesia (increased sensitivity to a noxious stimulus) and allodynia (increased sensitivity to a non-noxious stimulus). Reactions produced by a noxious stimulus can fall into two categories— responses organized by lower hierarchical areas of the CNS, such as withdrawal reflexes and cardiovascular changes, and more integrated complex responses requiring supraspinal input, such as tactile hypersensitivity or learned conditioned responses (DeLeo 2006).

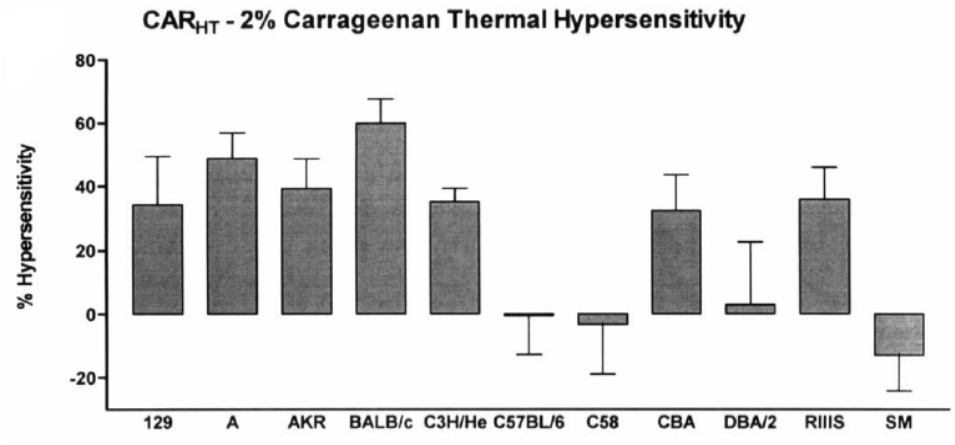

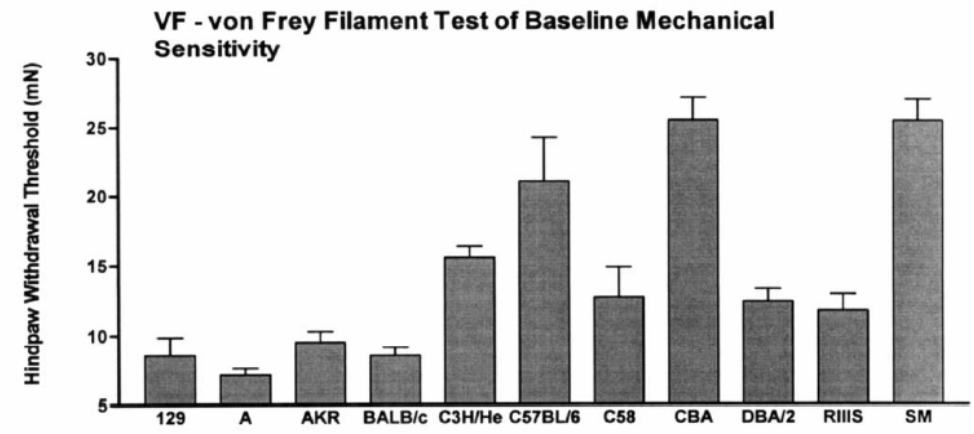

Figure 1.4 Responses of different mouse strains to different behavioral measures of nociception**.** Genotype significantly affected the performance in nociceptive measures. No mice strain is consistently highest or lowest in these assays (Mogil et al. 1999).

Standard evaluation methods currently in use include the hot-plate and tail-flick tests (Le Bars et al. 2001) and the use of von Frey hair to assess mechanical allodynia. Models of inflammation that produce more persistent pain include the injection of carrageenan or complete Freud's adjuvant into the footpad (Iadarola et al. 1988) or into the joint of the limb of animals (Schaible et al. 1987), or facial carrageenan injections (Ng and Ong 2001; Yeo et al. 2004; Vahidy et al. 2006).

Increasing attention has been paid to behavior genetics of the laboratory animals, especially mice. It has been found to have a great deal of response variability to mechanical, chemical or thermal stimulus among different mouse strains (Figure 1.4) (Mogil et al. 1999). In this study, Balb/c and C57BL/6J mice were chosen for the study of carrageenan induced orofacial pain according to studies from other researchers (Mogil et al. 1999; Yeo et al. 2004). A von Frey hair filament was used to test the response of facial allodynia induced by facial carrageenan injection.

Lambda carrageenan used to induce orofacial pain in mice in the present study is a mucopolysaccharide derived from the Irish sea moss. It produces inflammation, hypersensitivity, and some apparent spontaneous pain with a peak effect at 3-5 hours after injection to the rat hind paw (Tonussi and Ferreira 1992). After injection of carrageenan into the footpad, the cutaneous inflammation appeared within 2 hours and peaked at 6-8 hours. Hyperalgesia and edema were present for approximately 1 week to 10 days. The physiological and biochemical effects are limited to the affected limb (Iadarola et al. 1988). Although unilateral injuries have been reported to alter sensitivity in remote locations including contralateral sites (Levine et al. 1985), carrageenan does not appear to produce changes in nociceptive threshold in the contralateral hind paw of the rat (Kayser and Guilbaud 1987).

In addition, carrageenan has been found to have the ability to induce the release of inflammatory factors. For example, it has been shown that elevated interleukin-6 level appears in the circulating blood 3 hours after carrageenan injection. Carrageenan injection into the hind paw also induces the release of prostaglandin E_2 (PGE_2) from

isolated blood vessels of the CNS, as well as the induction of cyclooxygenase-2 (COX-2) and microsomal prostaglandin E synthase. It also causes nuclear translocation of signal transducer and activator of transcription 3 in vascular endothelial cells of the CNS (Oka et al. 2007).

3. General introduction of sphingolipids

3.1. Structure and classification of sphingolipids

Sphingolipids are a class of complex lipids derived from the aliphatic amino alcohol sphingosine. They contain an amide-linked fatty acid and a long-chain (sphingoid) base that are important structural components of cell membranes. Different combinations of sphingoid long-chain bases, fatty acids and head group moieties lead to a large number of sphingolipids and glycosphingolipids. The basic structure of sphingosine is shown in Figure 1.5.

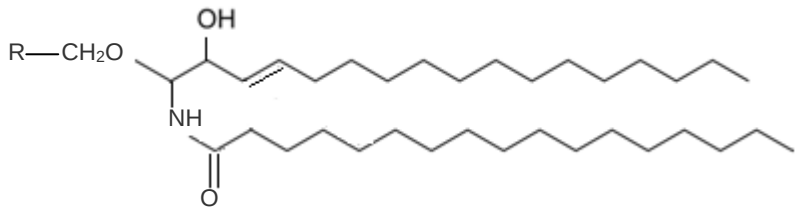

Figure 1.5 General chemical structures of sphingolipids. Different substituents (R) give: H— ceramide; Phosphocholine— sphingomyelins; Sugar— glycosphingolipids.

There are mainly three types of sphingolipids: ceramides, sphingomyelins and glycosphingolipids (Figure 1.5). Ceramides consist simply of a fatty acid chain attached through an amide linkage to sphingosine. The fatty acid chain length of ceramide can vary from 2 to 28 carbons, while C16 to C24 ceramides are most abundant in mammalian cells. These fatty acids can be either saturated or unsaturated, and sometimes may contain a hydroxyl group at the C-2 position (K-hydroxy fatty acid) or on the terminal C atom (g-hydroxy fatty acid) (Kolesnick and Hannun 1999; Cremesti et al. 2002; Kolesnick 2002). Figure 1.6 illustrates examples of structures of two different ceramide species.

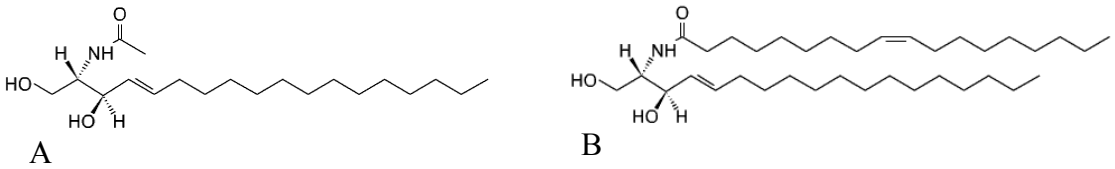

Figure 1.6 Structure of N-Acetoyl-D-erythro-Sphingosine (C2 Ceramide) (A) and N-Oleoyl-D-erythro-Sphingosine (C18:1 Ceramide) (B).

Sphingomyelins have a phosphorylcholine or phosphoroethanolamine esterified to the hydroxy group of a ceramide. Glycosphingolipids have one or more sugar residues joined in a β-glycosidic linkage at the 1-hydroxyl position of ceramide. Glycosphingolipids consist of cerebrosides and gangliosides. Cerebrosides have a single glucose or galactose at the 1-hydroxy position. Gangliosides have at least three sugars, while one of which must be sialic acid.

3.2. Biosynthesis of sphingolipids

Sphingolipids are synthesized in the endoplasmic reticulum and Golgi apparatus, and enriched in the plasma membrane and endosomes, where they perform many of their functions. Transport of sphingolipids is via vesicles and monomeric transport in the cytosol. Sphingolipids are absent from mitochondria and the endoplasmic reticulum, but constitute a 20-35 molar fraction of the plasma membrane lipids (van Meer and Lisman 2002).

The metabolic pathways of sphingolipids are shown in Figure 1.7. It is difficult to determine the specific role for each sphingolipid since sphingolipid metabolites are interconvertible. It has been reported that the various enzymes involved in the metabolism of the sphingolipids are regulated by physiological stimuli such as growth

factors and stress (Spiegel et al. 1998; Pettus et al. 2003) and might also be involved in some pathological conditions.

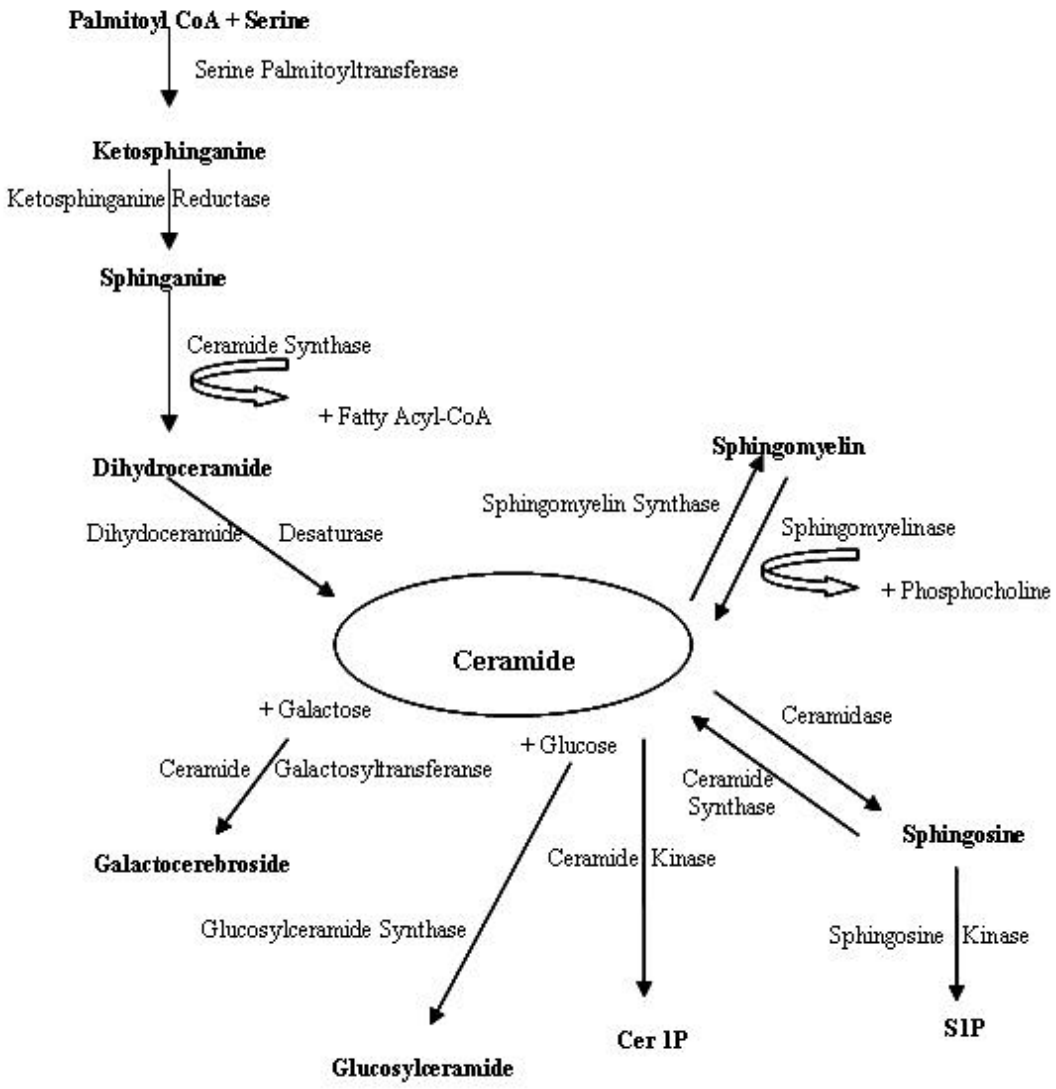

Figure 1.7 Biosynthesis of sphingolipids (Colombaioni and Garcia-Gil 2004).

The *de novo* pathway of ceramide synthesis can be triggered by agonist stimulations such as TNF-α and chemotherapeutic agents, with ceramide generated by this pathway having the capability of exerting biological actions (Xu et al. 1998). Condensation of

serine and palmitoyl CoA by serine palmitoyltransferase (SPT) initiates the pathway leading to ceramide generation. SPT is the first and rate-limiting enzyme in the pathway (Merrill et al. 1985; Merrill and Wang 1986; Perry et al. 2000).

The sphingomyelinases are the most heavily studied enzymes in ceramide metabolism. Five distinct enzymes have been identified so far, based upon their pH optima, cellular localization, and cation dependence. They are Zn^{2+} dependent acid sphingomyelinase (ASMase), ASMase splice variant, Mg^{2+}-independent neutral sphingomyelinase (NSMase), Mg^{2+}-dependent NSMase and alkaline sphingomyelinase. Among these, Mg^{2+}-independent NSMase and the lysosomal ASMase are the best studied for their roles in ceramide generation (Pettus et al. 2002). Sphingomyelin is hydrolyzed by sphingomyelinase to form ceramide and phosphocholine. ASMase is found in lysosomes, it has been also observed in caveoli and/or lipid rafts, which are microdomain of the plasma membrane that are rich in sphingomyelin (Pettus et al. 2002). ASMase can be activated by a large number of stimuli such as UV light, pathogens like *P. aeruginosa* and rhinoviruses, many receptors including CD95, CD28, TNF, interleukin-1 receptor and platelet-activating factor receptor (Gulbins and Li 2006).

3.3. Biological effects of sphingolipids

Sphingolipids are important structural protective components of the membrane lipid bilayer by forming a mechanically stable and chemically resistant outer leaflet of the plasma membrane. Briefly, biological membranes primarily consist of sphingolipids, cholesterol, and other (glycerol)phospholipids. The most prevalent component of the sphingolipid fraction in the cell membrane is sphingomyelin.

Sphingolipids are one of main important structural components of lipid raft on the cell membrane. Lipid rafts are a special domain in the cell membrane which can bind proteins, exerting various important functions like signal transduction, cytoskeletal organization, membrane trafficking, and pathogen entry (Simons and Ikonen 1997; Brown and London 1998). The theory of "lipid raft'' hypothesis suggests that sphingolipids and cholesterol cluster into discrete regions of the cell membrane (Simons and Ikonen 1997). These sphingolipid and cholesterol rich domains are termed ''lipid rafts'' because they exist in a less fluid and more ordered state compared to glycerophospholipid-rich domains of the membrane. It is shown that cholesterol interacts tightly with sphingomyelin through hydrogen-bonding between the C-3 hydroxyl group of cholesterol and the sphingosine moiety of sphingomyelin, forming the basis for lipid raft (Kolesnick et al. 2000). Studies on model membranes clearly illustrate the phenomenon of clustering and segregation of sphingolipids, cholesterol and certain types of glycerophospholipids in the cell membrane, and evidence also showed the existence of raft-type domains in living cells (Friedrichson and Kurzchalia 1998; Varma and Mayor 1998; Pralle et al. 2000; Dietrich et al. 2001).

Many well known signaling proteins have been shown to either reside in or be transferred into or out of the rafts during the process of signal transmission. These signaling proteins include epidermal growth factor receptor, insulin receptor, G proteins, Ras, nitric oxide synthase, and TNF-α receptor (Smart et al. 1999). The localization of these proteins in lipid rafts, which is affected by the cytoskeleton, influences the efficacy and potency of both neurotransmitter receptors and transporters. In addition, the effect of

lipid rafts on neurotransmitter signaling has also been implicated in many neurological and psychiatric diseases (Allen et al. 2007).

Besides that, sphingolipids themselves are also considered as signaling molecules which are involved in the control of cellular processes such as proliferation, growth, migration, differentiation, senescence, and apoptosis (Kolesnick and Kronke 1998; Spiegel et al. 1998; Hannun and Luberto 2000; Cuvillier 2002; Hannun and Obeid 2002; Malisan and Testi 2002). Sphingolipids can either act as first messengers binding to a seven-spanning G protein-coupled receptor subfamily, or as intracellular second messengers, capable of interacting with a multiplicity of targets. In addition, sphingolipid metabolites generated in cells are capable of modifying the activity of a number of proteins, including receptors, ion channels and enzymes as well as intracellular calcium levels (Colombaioni and Garcia-Gil 2004).

3.3.1. Sphingolipids as second messengers

It is found that sphingosine directly inhibits voltage-gated calcium channels in pituitary cells (Titievsky et al. 1998). It also inhibits cytosolic Ca^{2+}-dependent NOS activity in rat cerebellar granule cells, probably interfering with the calmodulin-dependent activation of the enzyme (Viani et al. 1999). Sphingosine 1-phosphate (S1P) and ceramide 1-phosphate (Cer1P) are able to stimulate neutral ceramidase *in vitro* (Usta et al. 2001). It is postulated that Cer1P might be involved in inflammatory reactions by acting on phospholipase A_2 (PLA_2) during glial cell injury. PLA_2 regulates the generation of pro-inflammatory mediators through COX and lipoxygenase pathways. Cer1P interacts directly with cytosolic PLA_2 ($cPLA_2$), inducing

the activation and translocation of $cPLA_2$ from the cytosol to the Golgi apparatus/perinuclear regions (Pettus et al. 2003). After ischemia or chronic injury in an amyotrophic lateral sclerosis transgenic model, the increased $cPLA_2$ level is accompanied by elevated intracellular ceramide levels (Herr et al. 1999; Stephenson et al. 1999; Cutler et al. 2002).

3.3.2. Sphingolipids affect Ca^{2+} mobilization in neural cells

Sphingolipid metabolites, especially S1P, are capable of mobilizing intracellular calcium. It can induce Ca^{2+} release via inositol triphosphate (IP_3), or by a direct action on intracellular Ca^{2+} stores (Ghosh et al. 1990; Meyer zu Heringdorf et al. 1998). Evidence has shown that TNF induces sphingomyelinase activation and transient Ca^{2+} -dependent inward currents in the dorsal root ganglia neurons. Intracellular flash photolysis of caged sphingosine can trigger similar currents. Likewise, extracellular S1P also evokes a transient rise in intracellular calcium concentration in neurons (Pollock et al. 2002).

Both extracellular receptors and intracellular action of sphingolipid metabolites might be involved in Ca^{2+} mobilization. The application of lysophosphatidic acid to neuroblastoma cells would lead to Ca^{2+} mobilization, which is dependent on the production of S1P within cells (Young et al. 2000). In rat brain synaptosomes, glucosylsphingosine mobilizes calcium via IP_3 receptor and sarcoplasmic/endoplasmic reticulum Ca^{2+}/ATPase (Lloyd-Evans et al. 2003a; Lloyd-Evans et al. 2003b). Elevated levels of intracellular glucosylceramide would lead to an increase in Ca^{2+} release from

intracellular stores in the hippocampal neurons, in response to glutamate or caffeine (Korkotian et al. 1999).

3.3.3. Sphingolipids affect excitability and neurotransmitter release

Sphingolipid metabolites such as ceramide, Cer1P, sphingosine, and S1P could modulate the excitability and transmitter release in the CNS. It is possible that Cer1P plays a role in regulating neurotransmitter secretion by increasing the fusibility of the vesicle membranes (Bajjalieh et al. 1989). It is now known that Cer1P facilitates calcium entry through voltage gated calcium channels and increases the probability of opening these channels (Tornquist et al. 2004). On the other hand, sphingosine inhibits voltage gated calcium channels in the pituitary cells (Titievsky et al. 1998). Ceramide is also involved in the modulation of ion currents and neurotransmitter release. For instance, both TNF-α which could activate sphingomyelinase, and ceramide analogues decrease the current induced by glutamate and increase the activity of L type Ca^{2+} channels in hippocampal cells (Furukawa and Mattson 1998).

Sphingolipids can increase neuronal excitability by decreasing K^+ current. This leads to the depolarization of the cell membrane and the activation of voltage gated Ca^{2+} or Na^+ channels. It is found that ceramide analogues block inward rectifier I_K and/ or Ca^{2+}-activated K^+ [BK_{Ca}] in a number of cells including neuroblastoma, GH3 cells (Wu et al. 2001) and sensory cells (Zhang and Zhou 2002). However, effects of ceramide on I_K might be cell-specific since it has an inhibitory effect in some cell types such as rat pinealocytes, oligodendrocytes, sensory neurons and neuroblastoma cells (Chik et al. 2001; Wu et al. 2001; Zhang and Zhou 2002), but an opposite effect in cortical neurons

(Yu et al. 1999). So far it is still not clear whether these effects are due to ceramide or its metabolites, such as sphingosine or S1P.

In addition, the excitability modulation by sphingolipids can also be done through regulating the target channels on the plasma membrane. The number of acetylcholine receptors in the plasma membrane can be decreased by 45.5% after the inhibition of ceramide synthase (Roccamo et al. 1999). It is found that small rafts are necessary for the activity of Kv1.3, which localizes to small, sphingolipid- and cholesterol-enriched rafts in the cell membrane. The formation of large ceramide-enriched platforms by the fusion of these small rafts upon the stimulation of sphingomyelinase or C16 ceramide, results in the clustering of this voltage dependent K channel and the inhibition of its activity (Bock et al. 2003).

3.4. Biological and biophysical effects of ceramides

A large number of intracellular targets of ceramides have been investigated. For example, ceramide amplifies the action of TNF-α by stimulating acid and neutral sphingomyelinases and by inhibiting sphingomyelin synthase (Vivekananda et al. 2001). In addition, it has been found that ceramide upregulates expression of $cPLA_2$ and COX-2 and causes a significant increase in the levels of reactive oxygen species (ROS) in primary hippocampal cells (Prasad et al. 2008).

Recent studies have suggested that some effects of ceramide are mediated by its unique structure. Ceramide is capable of forming extensive hydrogen bonds in the phospholipid bilayer due to its polar headgroup, amide linkage, as well as the hydroxyl groups of sphingosine and the fatty acid chain. The tight interactions between ceramide

molecules enable the separation of ceramide-rich and -poor microdomains within the cell membrane. Ceramides have poor affinity for cholesterol and phospholipids in bilayers, and these form ceramide-enriched microdomains (Kolesnick et al. 2000). These properties affect the ordering of lipids in the membrane, tending to destabilize them and cause efflux, fusion, or budding of vesicles (Cremesti et al. 2002).

Ceramide can mediate membrane fusion or fission by inducing a negative curvature because of its relatively small polar headgroup (conical shape), which favors vesicle formation. The changes in the membrane curvature will lead to the alteration of the structure of enzymes residing in the membrane, either through activating or inhibiting them. Recent studies have indicated that membrane fusion is critical for many cellular processes (Kolesnick et al. 2000). It has been demonstrated that ceramide facilitates vesicle aggregation and the release of vesicle contents when added to model membrane (Ruiz-Arguello et al. 1998; Holopainen et al. 2000; Montes et al. 2002). Besides model membranes, endocytic vesicles formation has been observed in ATP-depleted macrophages after treating with exogenous sphingomyelinase or ceramide (Zhang et al. 1998).

Owing to its extensive hydrogen-bonding capacity, ceramide has also been shown to induce pore formation in model phospholipid bilayers (Siskind and Colombini 2000). This might account for the postulated functions of ceramide. Ceramide is generated at the plasma membrane upon receptor aggregation induced by stress or agonist. This could lead to the local alteration in the plasma membrane permeability barrier. The changes in permeability and fluidity of cell membrane will lead to conformational changes in

membrane-associated enzymes or receptors, increase movement of proteins into or from rafts, induce ion fluxes, as well as alter the movement of lipids, and activating specific local signaling cascades. An activated receptor can also be trapped in rafts, and this stabilizes the interaction with the receptor ligand (Gulbins and Li 2006).

The receptor clustering by the fusion of very small rafts to larger platform via the generation of ceramide leads to a high density of receptors that seems to be required for effective transmission of the signal into cells. Although ceramide-enriched membrane platforms are not part of the specific signaling cascade of the activated receptor molecule, these domains greatly facilitate and amplify signaling. This concept is consistent with the finding that ceramide-enriched membrane platforms amplify the signaling via CD95 by approximately 100-fold (Grassme et al. 2003).

3.5. Sphingolipids in pain perception

Growing evidences have indicated a role of lipids, including eicosanoids, diacylglycerols, lysophosphatidic acids and ceramides, in augmenting the sensitivity of sensory neurons and enhancing pain perception, as second messengers in signaling pathways or putative inflammatory mediators that activate either surface receptors or ion channels in sensory neurons.

It has become more evident in recent years that sphingolipids are involved in nociception. *In vitro* studies have shown that NGF activates sphingomyelinases and increases the production of ceramides through p75 receptor (Dobrowsky et al. 1994; Brann et al. 1999). Both NGF and TNF-α alter the sensitivity of sensory neurons (Parada et al. 2003; Petruska and Mendell 2004). Peripheral nerve injury and inflammation lead

to an increase in the expression of p75 and p55 receptors in the dorsal root ganglia and the dorsal spinal cord (Cho et al. 1996; Ohtori et al. 2004). In isolated sensory neurons, C2 ceramide increases the number of evoked action potential, this phenomenon appears to be secondary to the augmentation of TTX-resistant Na^+ channels and the inhibition of delayed rectifier K^+ channels (Zhang et al. 2002). In a similar manner, exposing sensory neurons to NGF augments action-potential firing, increases the activity of TTX-resistant channels and inhibits K^+ channel activity. These effects are attenuated by inhibiting neutral sphingomyelinase and blocked by pre-treatment with an antibody to the p75 receptor to the cells (Zhang and Zhou 2002; Zhang and Nicol 2004).

Sphingolipids are also shown to mediate peripheral sensitization directly. Intradermal injection of C2 ceramide or TNF-α into the dorsal hind paw of the rat results in hyperalgesia (Joseph and Levine 2004). TNF-α induced hyperalgesia can be blocked by pre-injection of a neutral sphingomyelinase inhibitor (Joseph and Levine 2004), suggesting that TNF-α induced hyperalgesia is mediated by the activation of the ceramide signaling pathway.

4. Role of free radicals in nociception

Under normal conditions, reactive oxygen species (ROS) and reactive nitrogen species (RNS) are by-products of normal metabolic processes, and they function as physiological signaling molecules (Grisham et al. 1999). However, in pathological conditions, the excessive increase in ROS, such as super oxide anion (O_2^-), hydrogen peroxide (H_2O_2), hydroxyl radicals, and RNS, such as nitric oxide (NO) and peroxynitrite ($ONOO^-$), could lead to cell death and tissue damage (Endemann and Schiffrin 2004).

4.1. Role of nitric oxide in nociception

NO is a molecule with 11 valence electrons, 6 from oxygen and 5 from nitrogen, with an unpaired electron in the last orbital, making NO a free radical ($^{\bullet}NO$). Hence, NO is thermodynamically unstable and tends to react with other molecules. Moreover, NO-mediated pathogenicity largely depends on the formation of secondary intermediates such as nitrites (NO_2^-), nitrates (NO_3^-) and $ONOO^-$ that are more reactive and toxic than NO itself (Beckman and Koppenol 1996; Radi 2004). The presence of oxidants such as superoxide radicals (O_2^-), H_2O_2, and transition metal centers are required for the formation of RNS from $^{\bullet}NO$. The concentration of these oxidants can be increased either by $^{\bullet}NO$ itself or by the same mediators that upregulate $^{\bullet}NO$ production.

NO can be synthesized by a family of enzymes— nitric oxide synthase (NOS) which is present in most cells of the body. Important biological roles of NO have been identified in various systems. For example, NO has been shown to be an important neurotransmitter in the nervous system (Bredt and Snyder 1992). Four members of the NOS family have been identified: endothelial NOS (eNOS), neuronal NOS (nNOS),

inducible NOS (iNOS) and mitochondrial NOS (mtNOS). nNOS and eNOS are Ca^{2+}-calmodulin-dependent enzymes expressed in mammalian cells (Mungrue et al. 2003), and the generation of NO via these two enzymes last only a few minutes. In contrast, iNOS is Ca^{2+}-calmodulin-independent and its regulation depends on *de novo* synthesis (Ebadi and Sharma 2003). iNOS is not normally expressed in the brain, but inflammatory mediators such as lipopolysaccharide and cytokines will induce its expression in microglia and astrocytes (Murphy 2000), and possibly in neurons (Heneka and Feinstein 2001). Once expressed, iNOS would produce high levels of NO continuously.

NO and superoxide are normal signaling molecules at low concentrations, but at high concentrations, they are key cytotoxic molecules of innate immune defence against pathogens (Davies 1999; Floyd 1999; Murphy 2000; Forman and Torres 2002). They are also involved in the pathology of many brain diseases, including ischemia, trauma, inflammatory and neurodegenerative diseases, as well as aging of the brain (Floyd 1999; Murphy 2000; Brown and Bal-Price 2003; Zekry et al. 2003; Block et al. 2007). Numerous studies have indicated NO as a biological mediator in various conditions. However, in this thesis, the author would be placing more emphasis on the role of NO on nociception in the CNS.

It is reported that intrathecal injection of NO donor causes spinally mediated hyperalgesia (Kitto et al. 1992), and blockage of NO synthesis eliminates hyperalgesia (Yamamoto et al. 1993; Meller et al. 1996) as well as formalin-induced hyperalgesia (Wiertelak et al. 1994). Furthermore, inhibition of spinal NO synthesis also blocks

NMDA-induced hyperalgesia (Kitto et al. 1992; Malmberg and Yaksh 1993) and thermal hyperalgesia resulting from nerve injury (Meller et al. 1992). Inhibition of spinal NO synthesis results in anti-nociception in rats with their paw injected with formalin (Roche et al. 1996). It is reported that c-fos positive neurons in superficial laminae of the caudal part of the spinal nucleus of the trigeminal nerve which receive the primary afferents from the trigeminal ganglion, are modulated by NO diffused from adjacent NOS positive neurons. Moreover, the NOS positive neurons are most likely local circuit neurons (Yeo et al. 1997; Leong et al. 2000).

4.2. Role of superoxide in nociception

Superoxide can be formed from activated polymorphonuclear leucocytes, endothelial cells and mitochondrial electron flux, and normal cellular respiration (McCord and Omar 1993; Lenaz 2001). The biological reactivity of superoxide is tightly controlled by SOD (superoxide dismutase). More superoxide will be produced during acute and chronic inflammations, resulting in superoxide-mediated injury (Fridovich 1999; Muscoli et al. 2003).

Important pro-inflammatory roles for superoxide include: (i) endothelial cell damage and increased microvascular permeability (Droy-Lefaix et al. 1991; Haglind et al. 1994); (ii) up-regulation of adhesion molecules such as ICAM-1 (intercellular adhesion molecule 1) and P-selectin that recruit neutrophils to sites of inflammation (Salvemini et al. 1999; Salvemini et al. 2001); (iii) lipid peroxidation and oxidation; and (iv) DNA damage (Dix et al. 1996). Superoxide also activates redox-sensitive transcription factors including NF-κB (nuclear factor κB) and AP-1 (activator protein 1) that in turn regulate

genes encoding various pro-inflammatory and pro-nociceptive cytokines (Gius et al. 1999; Salvemini et al. 2001; Haddad and Land 2002; Matata and Galinanes 2002; McInnis et al. 2002; Ndengele et al. 2005).

It is reported that intraplantar injection of carrageenan to rats causes nitrotyrosine formation and hyperalgesia. This effect can be blocked by a SOD mimetic M40403. It is also shown that at the time of peak hyperalgesia, endogenous manganese SOD is nitrated and subsequently deactivated at the spinal cord, hence lose its capacity to remove superoxide (Wang et al. 2004). It is suggested that ROS mediates the development and the maintenance of capsaicin-induced-hyperalgesia in mice, mainly through central sensitization. And the elevation of spinal ROS is most likely due to increased production of mitochondrial superoxide in the dorsal horn neurons (Schwartz et al. 2008).

Recent results have demonstrated that the removal of superoxide and superoxide-derivatives is effective in inhibiting peripheral and central sensitization associated with severe pain. Superoxide scavengers have been shown to be effective in reducing acute inflammatory pain (Wang et al. 2004; Nishiyama and Ogawa 2005), glutamate-induced hyperalgesia (Muscoli et al. 2004), neuropathic pain (Tal 1996; Chuang et al. 2001; Kim et al. 2004; Kim et al. 2006; Naik et al. 2006; Park et al. 2006), trigeminal pain and temporomandibular joint dysfunction (Viggiano et al. 2005).

4.3. Role of peroxynitrite in nociception

Peroxynitrite can be formed through the interaction between superoxide and nitric oxide *in situ* (Beckman et al. 1990) (Figure 1.8). Removal of peroxynitrite results in cytoprotective and anti-inflammatory effects (Misko et al. 1998; Salvemini et al. 1998a;

Salvemini et al. 1998b). The most important property of peroxynitrite in inflammation is its ability to nitrate protein tyrosine groups, resulting in modification of the functional activity of key proteins (Fries et al. 2003; Muscoli et al. 2003; Radi 2004; Wang et al. 2004) (Figure 1.8). Another mechanism of nitration is via H_2O_2 and myeloperoxidase (Eiserich et al. 1998). Nitration and inactivation of manganese-complexed SOD also play a role in the development of peripheral and central pain sensitization (Muscoli et al. 2004; Wang et al. 2004).

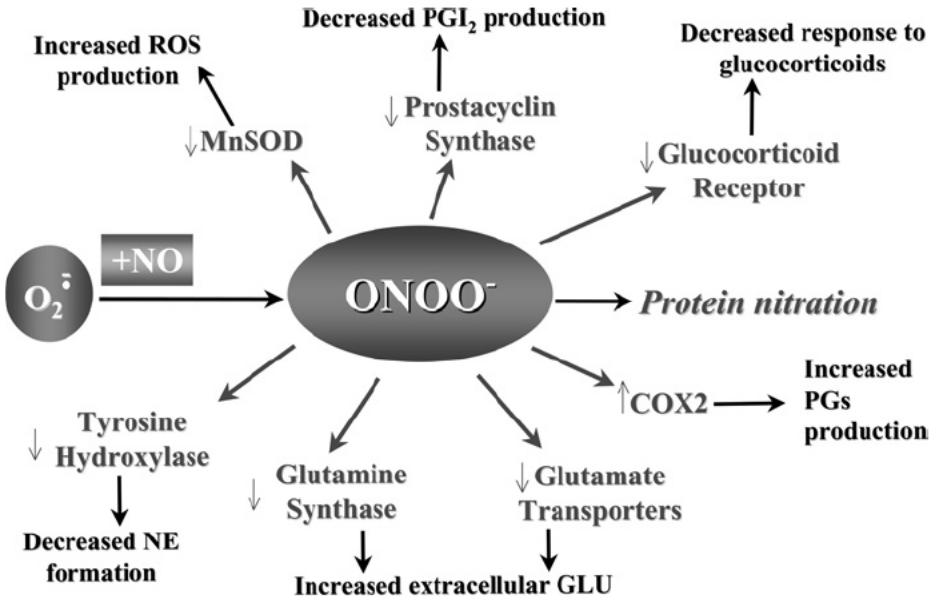

Figure 1.8 Peroxynitrite-mediated tyrosine nitration plays a key role in inflammation and pain. Nitration can be focused on specific tyrosine residues on proteins, resulting in loss (↓) or gain (↑) of protein function (Cassina et al. 2000; Salvemini et al. 2006).

Protein nitration of specific tyrosine residues results in structural modification, and loss or gain of protein function (Cassina et al. 2000; Balafanova et al. 2002; Vadseth et al. 2004). For example, nitration of cytochrome c, voltage-dependent ion channel, and ATPase disrupts mitochondrial metabolism, and this in turn triggers apoptotic signaling

of cell death (Radi et al. 2002; Turko and Murad 2003). The enhanced peroxidative activity of nitrated cytochrome c may further contribute to oxidative damage (Cassina et al. 2000; Radi et al. 2002). In addition, nitration of glutamate transporters by peroxynitrite inhibits their ability to transport glutamate from the synaptic cleft to the neurons, where it is then metabolized to non-toxic glutamine by glutamine synthase (Kennedy et al. 1974). The latter can also be nitrated by peroxynitrite and lose its enzymatic activity (Minana et al. 1997; Gorg et al. 2005). As a consequence, the accumulated glutamate in the synaptic cleft will lead to neurotoxicity. Peroxynitrite can nitrate tyrosine residues present on the NMDA receptor subunits, leading to constant potentiation of synaptic currents, calcium influx and ultimately neuronal excitotoxicity (Mishra and Delivoria-Papadopoulos 1999; Zanelli et al. 2000; 2002).

4.4. Interaction between sphingolipids and ROS/RNS

It has been reported that ROS/ RNS are involved in sphingolipid metabolism. For example, sphingomyelinases and ceramidase activities are affected by the depletion of cellular reduced glutathione due to increased ROS and RNS levels (Huwiler et al. 1999; Mansat-de Mas et al. 1999; De Nadai et al. 2000; Qiu et al. 2003). On the other hand, sphingolipids including ceramide, sphingosine, and S1P can regulate cellular redox homeostasis through the regulation of NADPH oxidase (Garcia-Ruiz et al. 1997; Zhang et al. 2003), mitochondrial integrity (Garcia-Ruiz et al. 1997), NOS (Viani et al. 2001; Won et al. 2004), and antioxidant enzymes (Macmillan-Crow and Cruthirds 2001; Iwai et al. 2003).

4.4.1. Regulation of sphingolipid metabolism by oxidative stress

Exogenous or endogenous NO has been shown to inhibit TNF-α-mediated apoptosis via inhibiting acid sphingomyelinase (ASMase) and decreasing ceramide generation (De Nadai et al. 2000; Bulotta et al. 2001). NO also increases the level of cyclic guanosine monophosphate (cGMP) and activates cGMP-dependent protein kinase which is thought to inhibit ASMase (Barsacchi et al. 2002; Falcone et al. 2004). It is also reported that sodium nitroprusside, a NO donor, increases sphingomyelin hydrolysis and ceramide generation through the activation of neutral sphingomyelinase (NSMase) (Takeda et al. 1999).

4.4.2. Regulation of redox potential by sphingolipids

Increasing evidences suggest that certain sphingolipids such as ceramides or its glycosyl derivates, are able to induce cellular oxidative stress via various mechanisms. Ceramide and sphingosine are potential activators for mitochondrial dysfunction, leading to an increased production of O_2^-, abnormal electron transfer, mitochondrial lipid peroxidation, opening permeability transition pore, and cytochrome c release. Ceramide can activate the gene expression of redox enzymes (i.e., iNOS and manganese-complexed SOD) through receptor clustering, recruitment of signaling enzymes, and activation of certain protein kinases (i.e., PKC_ζ and kinase suppressor of Ras). The ceramide-activated signaling cascades, together with its derivatives such as glucosyl-ceramide and lactosyl-ceramide, may be involved in the regulation of NADPH oxidase activity. Ceramide is also able to inhibit the action of eNOS through NADPH-mediated O_2^- generation, leading to the formation of $ONOO^-$ (Won and Singh 2006).

Chapter II

AIMS OF THE PRESENT STUDY

Lipid mediators including phospholipids and lysophospholipids play important roles in the normal physiology of the brain. However, relatively little is known about whether CNS ceramides could also play a role in orofacial allodynia. The present study was therefore carried out to evaluate possible effects of CNS sphingomyelinase and/or ceramides in a mouse facial carrageenan injection model of orofacial pain.

Previous study showed that increased ceramides were found in rat hippocampus after kainate-induced excitotoxic injury (Guan et al. 2006). Such changes could be due to increased neuronal excitation caused by kainite injection. Similar increases in neuronal excitation could also occur in the CNS during hyperalgesia (Gibbs et al. 2006). It was postulated that CNS ceramides — member of sphingolipid family— might also play a role in carrageenan induced facial allodynia. The first part of study was then carried out to examine whether the inhibition of CNS ceramide formation was effective in reducing orofacial allodynia after facial carrageenan injection. It was found that acid sphingomyelinase inhibitor D609 was effective in reducing allodynia.

Electrophysiological study of the role of ceramides in inducing exocytosis was then performed to provide possible mechanistic explanation for the effects of ceramides on orofacial allodynia. Various ceramide species were examined for their ability to induce membrane capacitance changes and whether ceramides could reduce the number of subplasmalemmal vesicles in PC12 cells.

Since D609 is also a free radical scavenger besides being an ASMase inhibitor, a possible role of CNS free radicals in facial allodynia was further examined using the spin

trap/ free radical scavenger PBN. It was found that intracerebroventricular (ICV) injection of PBN was effective in reducing orofacial allodynia after facial carrageenan injection.

Previous study showed an increase in microglial activity after formalin-induced facial allodynia (Yeo et al. 2001). Since microglia produces NO, which could combine with superoxide to form peroxynitrite, it was postulated that CNS peroxynitrite could play a role in facial allodynia. The last part of study was then carried out using ICV injections of $ONOO^-$ donor and scavenger to elucidate the effects of CNS peroxynitrite on nociception, in an orofacial pain model induced by facial carrageenan injection.

Chapter III

EXPERIMENTAL STUDIES

Chapter 3.1 Possible Effects of CNS Ceramides on Allodynia Induced by Facial Carrageenan Injection

1. Introduction

An increasing number of lipids, including eicosanoids, diacylglycerols, lysophosphatidic acids and sphingolipids have been implicated in increasing the sensitivity of sensory neurons and enhancing pain perception. Many of these lipids are second messengers in signaling pathways of sensory neurons (Colombaioni and Garcia-Gil 2004; Park and Vasko 2005). For example, one class of lipid mediators, the acylethanolamides, inhibits pain response, while the others appear to enhance pain sensitivity (Malan and Porreca 2005). Among these lipids, ceramides have been recently found to be important signaling molecules in diverse cellular processes.

Ceramides are generated via hydrolysis of sphingomyelin by sphingomyelinases or *de novo* synthesis through enzymes such as serine palmitoyltransferase (SPT) or ceramide synthase (Kolesnick and Hannun 1999). Ceramide can be phosphorylated by ceramide kinase to Cer1P, or metabolized by ceramidase to sphingosine, which can then be phosphorylated by sphingosine kinase to S1P. All the above compounds can affect cell signaling. Exposure of cultured rat dorsal root ganglion neurons to C2 ceramide, or intracellular perfusion with bacterial sphingomyelinase produced a 3-4 folds increase in the number of action potentials (Zhang et al. 2002). This might be due to the enhancement of a tetrodotoxin-resistant sodium current and/or reduction in outward potassium current, by ceramide or S1P, in these neurons (Zhang et al. 2006). S1P also contributes to depolarization induced neurotransmitter release in PC12 cells (Alemany et al. 2001). In addition, enhancement of calcium entry through voltage dependent calcium channels has been reported, after the addition of ceramide 1-phosphate (Cer1P)

(Tornquist et al. 2004). In humans, mutations in SPTLC1 (Serine palmitoyltransferase, long chain base subunit 1) which encodes serine palmitoyltransferase (SPT) have been detected in patients with hereditary sensory neuropathy type I (Dawkins et al. 2001). These observations provide direct evidence for a connection between altered ceramide metabolism and somatosensation.

An increased level of ceramide species such as C18:0, C24:1 and C24:0 ceramide have been found by non-targeted lipid profiling (lipidomic analysis) of rat hippocampus after kainate-induced excitotoxic injury (Guan et al. 2006). Treatment of hippocampal slice cultures with SPT inhibitor myriocin or L-cycloserine resulted in modulation of the ceramide production (He et al. 2007). These results suggest that besides breakdown of sphingomyelin, some of increased ceramide could have been produced as a result of *de novo* synthesis. Such changes could be due to increased neuronal excitation after injection of kainate. Similar increases in neuronal excitation could also occur in the CNS during hyperalgesia (Gibbs et al. 2006), although at present little is known about the role of ceramide in these conditions.

The present study was therefore carried out, by reducing the CNS ceramide production through direct injection of inhibitors to sphingomyelinases or SPT into the third ventricle of the brain, to elucidate a possible role of CNS ceramides in a mouse model of orofacial pain induced by facial carrageenan injection (Yeo et al. 2004).

2. Materials and methods

2.1. Behavioral experiment

2.1.1. Animal groups and chemicals

Treatment		Enzyme	Solvent	Concentration	n
With facial carrageenan injection	D609	ASMase and PC-PLC	Saline	2 mM	7
				0.2 mM	7
				0.02 mM	7
	PtdIns3,5P_2	ASMase	Saline	2 mM	7
				0.2 mM	7
				0.02 mM	7
	GW4869	NSMase	100% DMSO	2 mM	4
				0.2 mM	4
				0.02 mM	4
	L-cycloserine	SPT	Saline	2 mM	5
				0.2 mM	4
				0.02 mM	4
	Myriocin	SPT	Saline	2 mM	5
				0.2 mM	4
				0.02 mM	4
	Saline	Vehicle control			8
	100%DMSO	Vehicle control			4
Facial carrageenan injection only					6
Without facial carrageenan injection	Saline	Vehicle control			4
	100%DMSO	Vehicle control			4
	D609	ASMase	Saline	2 mM	4
	GW4869	NSMase	100% DMSO	2 mM	4
	L-cycloserine	SPT	Saline	2 mM	4
Summary				23 groups	118 mice

Table 3.1 Treatment groups of Balb/c mice.

Altogether 118 adult male Balb/C mice, about 6-8 weeks of age and weighing approximately 20-30 g each were purchased from the Laboratory Animals Centre, Sembawang, Singapore. All measures were taken to minimize pain or discomfort, and experiments were conducted in accordance with international standards on animal welfare and compliant with standards defined by the European Communities Council Directive of 24 November 1986 (86/609/EEC). These mice were randomly divided into 23 groups, with 4 to 8 mice per group. Eighteen groups were used to study the effects of various inhibitors on facial carrageenan induced allodynia. Five groups were used to test effects of inhibitors on normal somatosensation (Table 3.1).

Chemicals used for behavioral assessment are shown in Table 3.1. O-Tricyclo [5.2.1.02,6] dec-9-yl dithiocarbonate potassium salt (D609), GW4869, L-cycloserine, and myriocin were purchased from Sigma, St Louis, USA. D-myo-phosphatidylinositol 3,5-bisphosphate (PtdIns3,5P_2) was from Echelon, Salt Lake City, USA.

The enzyme inhibitors used in the present study are thought to have fairly specific actions, except acid sphingomyelinase (ASMase) inhibitors. Neutral sphingomyelinase (NSMase) inhibitor GW4869 is a cell-permeable, symmetrical dihydroimidazolo-amide compound that acts as a potent, specific, non-competitive inhibitor of NSMase (Luberto et al. 2002). L-cycloserine and myriocin are commonly used inhibitors for serine palmitoyltransferase (SPT) (Holleran et al. 1990; Miyake et al. 1995).

Thus far, no specific ASMase inhibitor has been found. Commercially available ASMase inhibitors such as D609, imipramine, desipramine, PtdIns3,5P_2 are not specific

for the ASMase, imipramine and desipramine are anti-depression drugs, and PtdIns3,5P_2 is a second messenger involved in a number of cellular signaling processes. D609 is a xanthogenate derivative with a variety of biological effects, including antiviral, antitumor, and anti-inflammatory activities (Zhou et al. 2001). It inhibits phosphatidylcholine-specific phospholipase C (PC-PLC) (Tschaikowsky et al. 1994), as well as ASMase activities (Simarro et al. 1999; Koishi et al. 2002; Strle et al. 2004). It is also a potent antioxidant, with the ability to scavenge intracellular reduced glutathione and inhibit intracellular ROS accumulation in cells (Zhou et al. 2001; Lauderback et al. 2003; Sultana et al. 2004). The median inhibition concentration (IC50) of D609 was 50~100 μg/ml *in vitro* (Kahle et al. 1998; Luberto and Hannun 1998). The concentrations of D609 injected were thus 1/10, 1 and 10 times of the IC50 (50 μg/ml). D609 has a relatively long half-life of 1.5 days (Kahle et al. 1998). PtdIns3,5P_2 and a similar analog PtdIns3,4,5P_3 have been shown to be inhibitor of ASMase (Kolzer et al. 2003; Testai et al. 2004). The half life of PtdIns3,5P_2 is about 2-5 hours (Brearley and Hanke 1995), however, its IC50 *in vivo* or *in vitro* has not been investigated so far.

2.1.2. Behavioral assessment

Mice were assessed for behavioral responses to von Frey hair (Touch-Test Sensory Evaluator, North Coast Medical, Morgan Hill, USA) stimulation applied to the right maxillary area at 1 day before injections, 6 hours, 1 day and 3 days after intracerebroventricular (ICV) injection and facial carrageenan injection. The von Frey hair filament delivering ~ 1 g force (4.08 log units) was used. A coding system was used

to blind the investigator to the nature of the surgical procedures performed on individual animals.

Chemicals administered via ICV injections did not produce any gross abnormalities in behavior or locomotion after mice woke up from anesthesia. The time point of 6 hours after injection was chosen because at that time, mice would be fully awake, and moved freely without obvious motor deficits. In addition, pilot observations showed that the number of responses to von Frey hair stimulation peaked at 3 to 4 days after facial carrageenan injection, hence, testing of effects of different chemicals was extended up to that time, i.e., 3 days after facial carrageenan injection.

The mice were tested individually in a deep rectangular stainless steel tank (60 × 40 × 25 cm^3). Mice were habituated to the movements of von Frey hair and the experimental environment for 5 to 10 min before testing. The mechanical stimulations were administered only when the mice were in a non-locomotion state, with four paws placed on the ground, neither moving nor freezing, but exhibiting sniffing behavior. A new stimulus was applied at least 30 seconds after the previous stimulation (Vos et al. 1994). Directed facial grooming, i.e. uninterrupted series of face-wash strokes directed to the stimulated maxillary area, was used as an indicator of unilateral facial pain in freely moving mice (Vos et al. 1998).

Twenty probes were delivered to each mouse to obtain sufficient number of responses to reduce variability among individual animals in each group. The total number of face wash strokes after the delivery of 20 probes was noted for each mouse, and the mean and standard deviation of each group were calculated. Possible differences between

the means were elucidated using one-way ANOVA with Bonferroni's multiple comparison post hoc test (SPSS 12.0 for Windows software).

2.1.3. Intracerebroventricular injection

Intracerebroventricular (ICV) injections were carried out as previously described (Yeo et al. 2004). The anesthesia used in the present study was a mixture of 7.5% ketamine and 10% medetomidine, administered via intraperitoneal (IP) injection. Each mouse was injected with a volume of 0.1 ml per 10 g body weight.

Mice were deeply anaesthetized, and the operation site was prepared by clipping the fur and swapping with alcohol. Each mouse was then fixed on a stereotaxic apparatus. The cranial was exposed via a midline incision. A small bur hole (approximately 2 mm diameter) was then made on the skull around the area of the third ventricle, and 5 μl of solution was injected slowly in 5 minutes. The coordinates were: 0.7 mm caudal to bregma, 1.0 mm lateral to the midline, 3.0 mm from the surface of the cerebral cortex. The wound was then closed with sutures.

2.1.4. Facial carrageenan injection

λ-carrageenan (Sigma, St Louis, USA) was suspended in sterilized saline at a concentration of 40 mg/ml. Fifty microliter of carrageenan suspension was subcutaneously injected into the right maxilla area of the mice to study the effects of these inhibitors on allodynia (Table 3.1).

2.2. ASMase activity assay and PC-PLC activity assay

2.2.1. Animals and tissue harvesting

Twenty-one Balb/c mice, randomly divided to 3 equal groups, were used to test ASMase and PC-PLC activity changes in brain after facial carrageenan injection and ICV injection of D609. Seven mice received ICV injection of 5 μl of 2 mM D609 and right facial carrageenan injection, seven received ICV injection of 5 μl of saline plus right facial carrageenan injection, the last seven were without any treatment (untreated control). ICV injection and facial carrageenan injection were carried out as previously described (chapter 3.1, page 51).

Mice were deeply anesthetized and sacrificed by decapitation 3 days after ICV and facial injections. The left and right halves of the brain stem (containing the trigeminal nucleus), the left and right thalamus (containing the ventral posterior nucleus of the thalamus), and the left and right primary somatosensory cortex (SI) (barrel field) were dissected out by referring to a mouse atlas, to roughly scan the ASMase and phosphatidylcholine-specific phospholipase C (PC-PLC) activities in different parts of brain.

2.2.2. Enzyme activity assay

Tissue samples were homogenized in 0.25% Triton X-100, the homogenate was centrifuged (10,000g for 5 min at 4 °C) and protein concentrations of supernatant was determined by Bio-Rad protein assay (Bio-Rad, California, USA.) (Bradford 1976). The remaining supernatant was used for enzyme activity assay using commercial kits—

Amplex red sphingomyelinase assay kit and Amplex red phosphatidylcholine-specific phospholipase C assay kit (both from Molecular Probes, Eugene, Oregon, USA).

Sphingomyelinase hydrolyzes sphingomyelin to ceramide and phosphocholine. PC-PLC converts the phosphatidylcholine (lecithin) substrate to form phosphocholine and diacylglycerol. Phosphocholine is then hydrolyzed by alkaline phosphatase to phosphate and choline, which is oxidized by choline oxidase to betaine and H_2O_2. H_2O_2 then reacts with 10-acetyl-3,7-dihydroxyphenoxazine (Amplex Red reagent) to produce highly fluorescent resorufin, which is detected by fluorescence emission at 590 nm.

The ASMase activity assay was carried out by following the product manual from the company. Each sample was diluted in 50 mM sodium acetate (pH 5.0) and sodium acetate was used as a negative control. A volume of 100 µl was used for each reaction. 10 µl of 5 mM sphingomyelin was added to each sample or negative control and incubated at 37 °C for one hour. 100 µl of 0.4 U/ml sphingomyelinase and 10 µM H_2O_2 were used as positive controls. After that, 100 µl of the samples and controls were transferred into separate wells of a 96 well fluorescence microplate. Ten microliter of the 5 mM sphingomyelin solution was added to each positive control. Reactions were began by adding 100 µl of the working solution [100 µM Amplex® Red reagent containing 2 U/ml HRP, 0.2 U/ml choline oxidase and 8 U/ml alkaline phosphatase in 100 mM Tris-HCl (pH 8.0)] to each microplate well containing the samples and controls. The microplate was then incubated for 30 minutes at 37 °C, protected from light.

The PC-PLC activity assay was carried out by following the product manual from the company. Each sample was diluted in reaction buffer (50 mM Tris-HCl, pH 7.4, 140

mM NaCl, 10 mM dimethylglutarate, 2 mM $CaCl_2$). PC-PLC (0.1 U/ml) solution and H_2O_2 (10 μM) in reaction buffer were positive controls. Reaction buffer without PC-PLC was used as a negative control. A volume of 100 μl was used for each reaction. 100 μl of the diluted samples and controls were pipetted into separate wells of 96 well fluorescence microplate. reactions were began by adding 100 μl of working solution (400 μM Amplex® Red reagent containing 2 U/ml HRP, 8 U/ml alkaline phosphatase, 0.2 U/ml choline oxidase and 1 mM lecithin in reaction buffer) to each microplate well containing the samples and controls. The microplate was then incubated for 30 minutes at 37 °C, protected from light.

Fluorescence reading was measured using a fluorescence microplate reader (Tecan, Grödig/Salzburg, Austria). The fluorescence was excited at 530 nm and emission was detected at 590 nm. Each measurement was corrected for background fluorescence by subtracting the values derived from the negative control. Each assay was performed in duplicate and results were normalized by protein concentration. Possible differences between the means were elucidated using one way ANOVA test with Bonferroni's multiple comparison post-hoc test (SPSS 12.0 for Windows software).

2.3. The effect of free radical spin trap phenyl-N-tert-butylnitrone (PBN) on facial allodynia

PBN is one of the most commonly used spin traps (Lee at al. 2007). The biological half-life of PBN in rats is 134 min (Chen et al. 1990; Lee et al. 2007). PBN was freshly prepared before injection and dissolved in saline at a concentration of 40 mg/ml. This dose of PBN was modified from previous study (Lee et al. 2007).

Fourteen adult male Balb/c mice were used to study the effect of PBN (Sigma, St Louis, USA) in carrageenan injected mice. Mice were randomly divided into two groups with seven each. The mice were assessed for behavioral responses to von Frey hair stimulation before treatments, and 3 days after facial carrageenan injection. At the third day after facial carrageenan injection, mice received ICV injection of 5 μl of PBN or saline (vehicle control) after the behavior test, 6 hours later when the mice were fully awake and did not produce any gross abnormalities in behavior or locomotion, mice received the behavior assessment again. Mice were also received the behavior assessment 1 day after ICV injection of PBN or saline. The method of behavior test, ICV injection and facial carrageenan injection were the same as previously described (chapter 3.1, page 49-51).

2.4. Intracellular H_2O_2 production in PC12 cells induced by ceramides

2.4.1. Cells and chemicals

PC12 cells (pheochromocytoma cells) were cultured in RPMI Medium supplemented with 10% fetal bovine serum and 1% penicillin/ streptomycin (Gibco, Invitrogen, Carlsbad, CA). The cells were plated in 35 mm Petri dishes, and maintained in an incubator at 37 ^{0}C, 100% humidity, with 95% air and 5% CO_2.

Chemicals	Source	Final Concentration	Solvent
C18 ceramide	Avanti Polar Lipids, Alabaster, USA	10 μM, 50 μM, 100 μM	DMSO
Nifedipine	Sigma, St Louis, USA	10 μM	DMSO
Bongkrekic acid (BKA)	Sigma, St Louis, USA	1 μM	KRPG
Cyclosporine A (CsA)	Sigma, St Louis, USA	1 μM	KRPG
D609	Sigma, St Louis, USA	50 μM	KRPG
phenyl-N-tert-butylnitrone (PBN)	Sigma, St Louis, USA	1 mM	KRPG

Table 3.2 Chemicals used in H_2O_2 assay. Abbreviation: KRPG: Krebs-Ringer phosphate buffer.

2.4.2. H_2O_2 assay in PC12 cells

First, effects of different concentration of C18 ceramide on the H_2O_2 production in PC12 cells were tested, i.e., 10 μM, 50 μM, 100 μM (final concentration). C18 ceramide level was found to be increased in rat hippocampus after kainate-induced excitotoxic injury using the method of non-targeted lipid profiling (lipidomic analysis) (Guan et al. 2006). It was observed that 100 μM C18 ceramide was the one which significantly increased the production of H_2O_2, C18 ceramide with this concentration was then chosen to further investigate the possible underlying mechanisms. L-type calcium channel inhibitor nifedipine, mitochondria permeability transition pore blockers bongkrekic acid and cyclosporine A, free radical scavengers D609 and PBN were used to test whether they can influence the effect of C18 ceramide on H_2O_2 production (Table 3.2). The vehicle of ceramides, DMSO, was used as negative control. Untreated PC12 cells were also used as another negative control.

The H_2O_2 assay in PC12 cells was carried out using a commercial available kit--Amplex® Red Hydrogen Peroxide/ Peroxidase Assay kit (Molecular Probes, Eugene, Oregon USA). The method was modified from the product manual provided by the company and is as follows: The reaction mixture contained 50 μM Amplex Red reagent and 0.1 U/ml HRP in KRPG (145 mM NaCl, 5.7 mM Na_3PO_4, 4.86 mM KCl, 0.54 mM $CaCl_2$, 1.22 mM MgSO4, 5.5 mM glucose, pH 7.35). One hundred microliter of the reaction mixture was pipetted into each microplate well (Greiner 96 well plate, black for fluorescence) and pre-warmed at 37 °C for 10 minutes. Ten microliter of chemical solution/mixture was then added into each microplate well. Each treatment was repeated several times (no less than four times). The final concentrations of each chemical were listed in Table 3.2. For non-treatment negative control, only 10 μl KRPG was added to the microplate well.

Cell density was counted using a hemacytometer and trypan blue, and a cell suspension with a density of 1.5×10^6 cells/ml in Krebs-Ringer phosphate buffer (KRPG) was obtained. The reaction was started by adding 10 μl of cells suspension to each microplate well containing chemical solution or 10 μl KRPG, i.e. 1.5×10^4 cells in each microplate well with a final volume of 120 μl in each well. For background control, only 20 μl of KRPG was added (without PC12 cells). The microplate was incubated at 37 °C for three hours. The absolute fluorescence reading was then recorded using a fluorescence microplate reader (Tecan, Grödig / Salzburg, Austria) equipped for excitation at 530 nm and emission detection at 590 nm, and normalized by subtracting the value derived from the background control. Possible differences between the means were

elucidated using one way ANOVA test with Bonferroni's multiple comparison post-hoc test (SPSS 12.0 for Windows software).

3. Results

3.1. Behavioral experiment

3.1.1. Effects of vehicle controls on facial carrageenan injected mice

Mice showed significantly increased face wash strokes at 1 day and 3 days after facial carrageenan injection, or facial carrageenan plus ICV saline injection, compared to before injection and 6 hours after injection (Figure 3.1A, B, Table 3.3), indicating allodynia.

Mice injected with 100% DMSO plus carrageenan showed significantly increased face wash strokes at 3 days after injections, compared to the same group before injections, 6 hours and 1 day after injections (Figure 3.1C, Table 3.3), indicating allodynia.

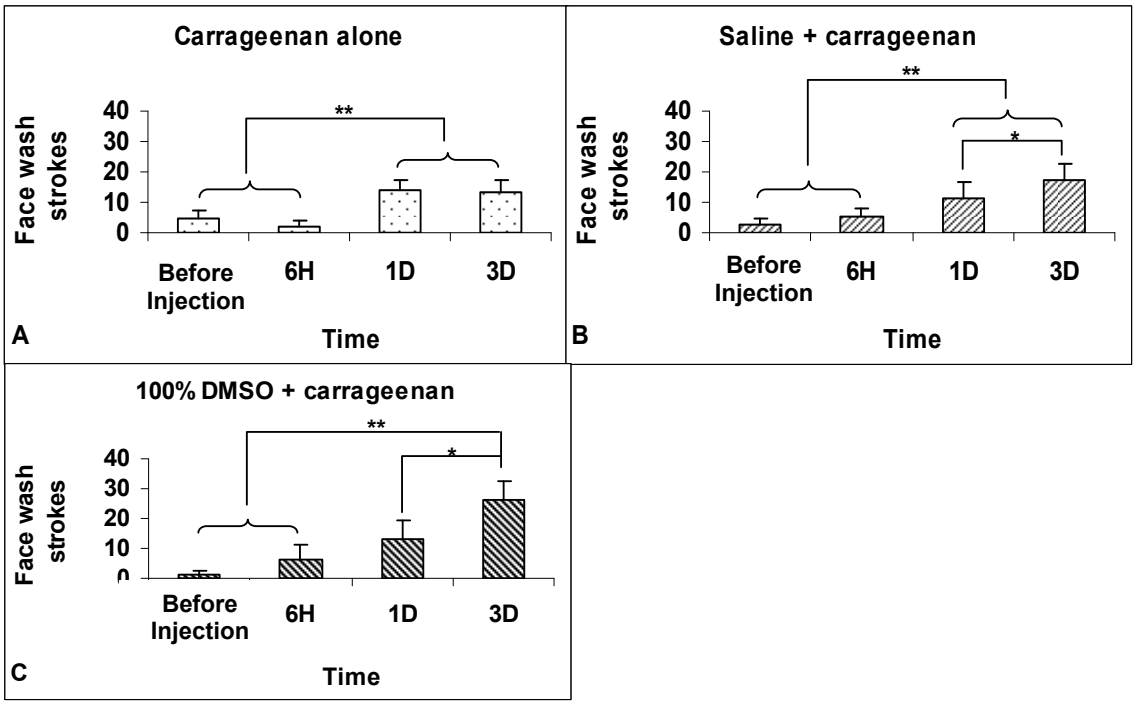

Figure 3.1 Effect of vehicle controls on facial allodynia in mice. A: Effect of facial carrageenan injection. B: Effect of ICV saline plus facial carrageenan injection. C: Effect of ICV injection of 100% DMSO plus facial carrageenan injection. All control groups showed significant allodynic effect at 3 days after injection, compared with before injection and 6 hours after injections. Data was shown in Mean ± SD. * indicates $P<0.05$; ** indicates $P<0.01$.

Treatment	n	Before Injection	6H	1D	3D
Carrageenan alone	6	4.5 ± 2.8	2.2 ± 2.0	14.2 ± 3.3	13.2 ± 4.1
Saline + carrageenan	8	3.0 ± 2.0	5.1 ± 2.8	11.2 ± 5.4	17.5 ± 5.3
100% DMSO + carrageenan	4	1.5 ± 1.3	6.5 ± 4.9	13.0 ± 6.3	26.2 ± 6.6

Table 3.3 Number of face wash strokes in control groups. Mean ± SD of the number of face wash strokes in each group at different time point is presented.

3.1.2. Effects of ASMase inhibitors on carrageenan injected mice

Mice injected with 2 mM D609 plus carrageenan, showed significantly fewer face wash strokes, compared to mice injected with saline and the two lower doses of D609, at 1 day and 3 day post-injection (Figure 3.2, Table 3.4).

Mice injected with 2 mM PtdIns3,5P_2 showed significantly fewer face wash strokes at 3 day after injections, compared to those injected with saline plus carrageenan (Figure 3.3, Table 3.5).

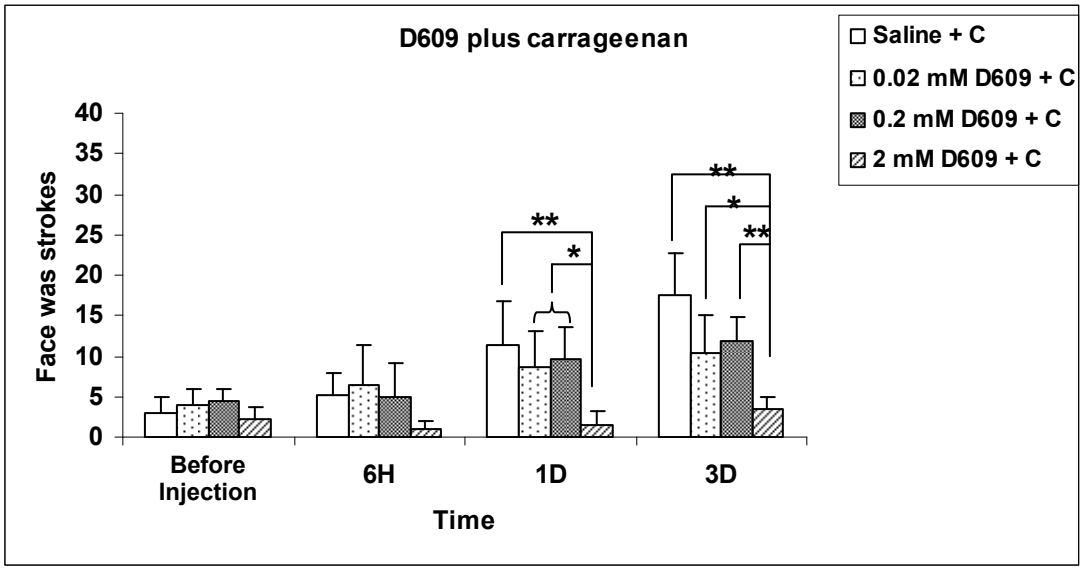

Figure 3.2 Effect of ASMase inhibitor D609 on facial allodynia in mice. Mice injected with 2 mM D609 showed significantly reduced allodynic effect at 1 day and 3 days after injection, compared with saline injected mice, and the two lower doses of D609 injected mice. Abbreviation: C: carrageenan. * indicates P<0.05; ** indicates P<0.01.

Treatment	n	Before Injection	6H	1D	3D
Saline + C	8	3.0 ± 2.0	5.1 ± 2.8	11.2 ± 5.4$^{\wedge\wedge\#\#}$	17.5 ± 5.3$^{\wedge\wedge\#\#\&}$
0.02 mM D609 + C	7	4.0 ± 1.8	6.4 ± 4.8	8.6 ±4.6	10.4 ± 4.5$^{\wedge}$
0.2 mM D609 + C	7	4.4 ± 1.5	4.8 ± 4.2	9.7 ± 4.0$^{\wedge}$	11.8 ± 2.8$^{\wedge\wedge\#\#}$
2 mM D609 + C	7	2.1 ± 1.5	1.0 ± 1.0	1.6 ± 1.6	3.4 ± 1.4$^{\#}$

Table 3.4 Number of face wash strokes after D609 plus carrageenan injection. Mean ± SD of each group is shown. Abbreviation: C: carrageenan. ^ indicates significant difference compared with before injection within the same treatment group (^: P<0.05; ^^: P<0.01). # indicates significant difference compared with 6 hours after injection within the same treatment group (#: P<0.05; ##: P<0.01). & indicates significant difference compared with 1 day after injection within the same treatment group (&: P<0.05).

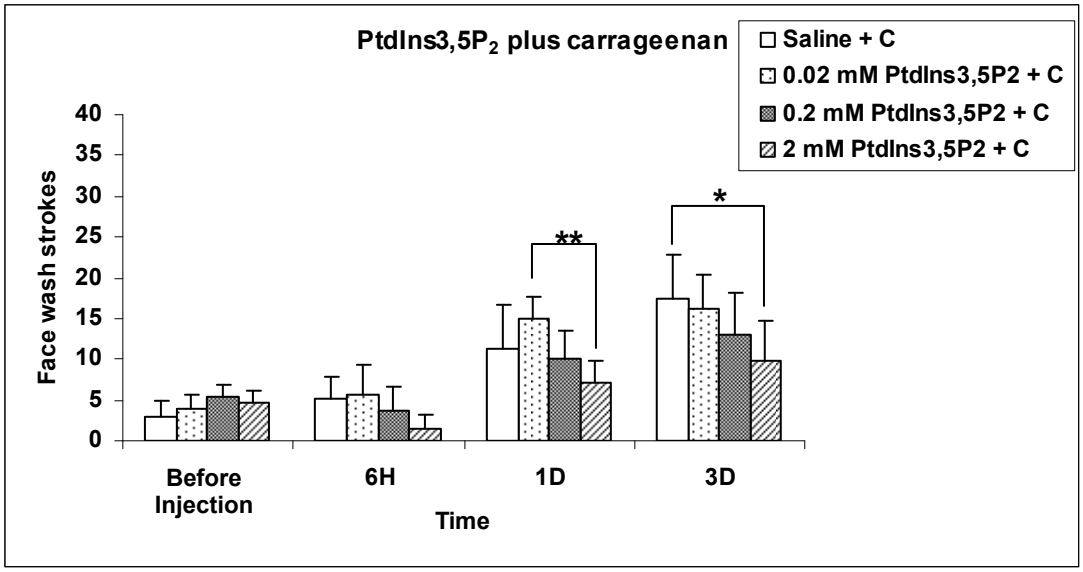

Figure 3.3 Effect of ASMase inhibitor PtdIns3,5P_2 on facial allodynia in mice. Mice injected with 2 mM PtdIns3,5P_2 showed significantly reduced allodynic effect at 3 days after injection, compared with saline injected mice. Abbreviation: C: carrageenan. * indicates P<0.05; ** indicates P<0.01.

Treatment	n	Before Injection	6H	1D	3D
Saline + C	8	3.0 ± 2.0	5.1 ± 2.8	11.2 ± 5.4$^{\wedge\wedge\#\#}$	17.5 ± 5.3$^{\wedge\wedge\#\#\&}$
0.02 mM PtdIns3,5P_2 + C	7	4.0 ± 1.7	5.7 ± 3.5	15 ± 2.8$^{\wedge\wedge\#\#}$	16.1 ± 4.3$^{\wedge\wedge\#\#}$
0.2 mM PtdIns3,5P_2 + C	7	5.3 ± 1.6	3.6 ± 3.0	10 ± 3.5$^{\#}$	13 ± 5.2$^{\wedge\#\#}$
2 mM PtdIns3,5P_2 + C	7	4.7 ± 1.5	1.6 ± 1.5	7 ± 2.9$^{\#}$	9.8 ± 4.8$^{\wedge\#\#}$

Table 3.5 Number of face wash strokes after PtdIns3,5P_2 plus carrageenan injection. Mean ± SD of each group is shown here. Abbreviation: C: carrageenan. ^ indicates significant difference compared with before injection within the same treatment group (^: P<0.05; ^^: P<0.01). # indicates significant difference compared with 6 hours after injection within the same treatment group (#: P<0.05; ##: P<0.01). & indicates significant difference compared with 1 day after injection within the same treatment group (&: P<0.05).

3.1.3. Effect of NSMase inhibitor on carrageenan injected mice

Mice injected with 2 mM and 0.2 mM GW4869 showed significantly reduced allodynia compared with DMSO injected mice at 3 days after injection (Figure 3.4, Table 3.6).

3.1.4. Effect of SPT inhibitor on carrageenan injected mice

Mice injected with 2 mM and 0.2 mM L-cycloserine showed significantly reduced allodynia compared with saline injected mice at 3 days after injection (Figure 3.5A, Table 3.7).

Mice injected with myriocin (all 3 doses i.e., 0.02 mM, 0.2 mM and 2 mM) showed significantly reduced allodynia compared with DMSO injected mice at 3 days after injection (Figure 3.5B, Table 3.7).

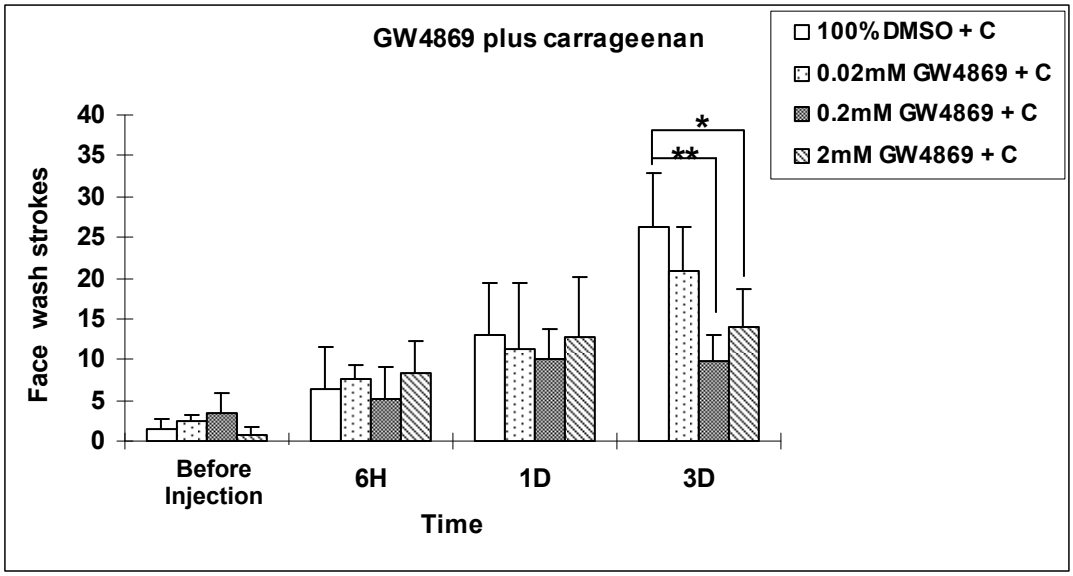

Figure 3.4 Effect of NSMase inhibitor GW4869 on facial allodynia in mice. Mice injected with 2 mM and 0.2 mM GW4869 showed significantly reduced allodynia compared with DMSO injected mice at 3 days after injection. Abbreviation: C: carrageenan. * indicates P<0.05; ** indicates P<0.01.

Treatment	n	Before Injection	6H	1D	3D
100% DMSO + C	4	1.5 ± 1.3	6.5 ± 4.9	13 ± 6.3	26.2 ± 6.5$^{\wedge\wedge\#\#\&}$
0.02 mM GW4869 + C	4	2.5 ± 0.6	7.5 ± 1.7	11.2 ± 8.0	20.7 ± 5.5$^{\wedge\wedge\#}$
0.2 mM GW4869 + C	4	3.5 ± 2.4	5.2 ± 3.8	10.0 ± 3.7	9.7 ± 3.2
2 mM GW4869 + C	4	0.8 ± 1.0	8.2 ± 4.1	12.8 ± 7.4$^{\wedge}$	14 ± 4.8$^{\wedge}$

Table 3.6 Number of face wash strokes after GW4869 plus carrageenan injection. Mean ± SD of each group is shown here. Abbreviation: C: carrageenan. ^ indicates significant difference compared with before injection within the same treatment group (^: P<0.05; ^^: P<0.01). # indicates significant difference compared with 6 hours after injection within the same treatment group (#: P<0.05; ##: P<0.01). & indicates significant difference compared with 1 day after injection within the same treatment group (&: P<0.05).

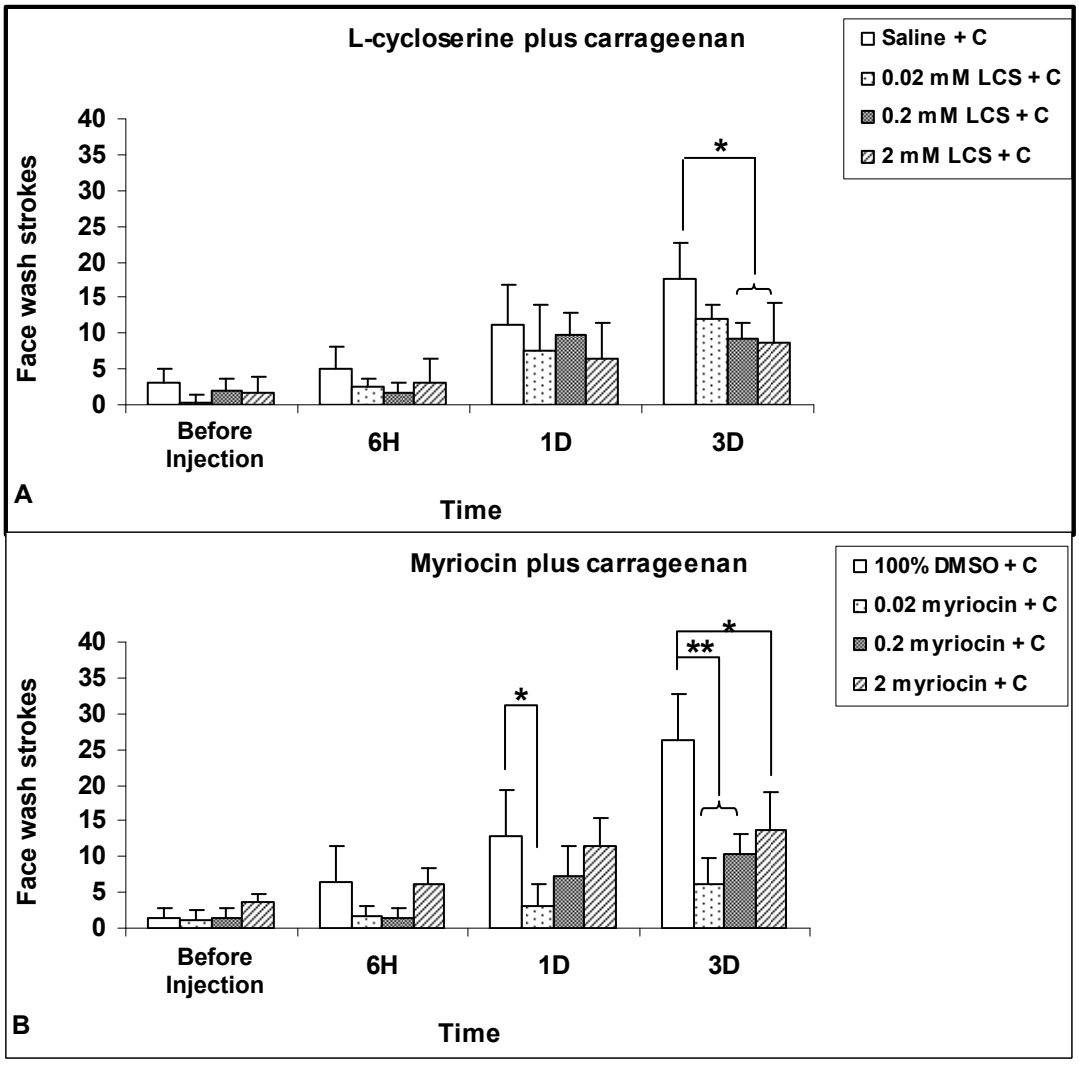

Figure 3.5 Effects of SPT inhibitor L-cycloserine and myriocin on facial allodynia in mice. A: Mice injected with 2 mM and 0.2 mM L-cycloserine showed significantly reduced allodynia compared with saline injected mice at 3 days after injection. B: Mice injected with all 3 doses of myriocin showed significantly reduced allodynia compared with DMSO injected mice at 3 days after injection. Abbreviations: LCS: L-cycloserine. C: carrageenan. * indicates $P<0.05$; ** indicates $P<0.01$.

Treatment	n	Before Injection	6H	1D	3D
Saline + C	8	3.0 ± 2.0	5.1 ± 2.8	11.2 ± 5.4$^{\wedge\wedge\#\#}$	17.5 ± 5.3$^{\wedge\wedge\#\#\&}$
0.02 mM L-cycloserine + C	4	0.4 ± 0.9	2.6 ± 1.1	7.6 ± 6.5$^{\wedge}$	12.0 ± 2.0$^{\wedge\wedge\#\#}$
0.2 mM L-cycloserine + C	4	2.0 ± 1.6	1.8 ± 1.2	9.8 ± 3.1$^{\wedge\wedge\#\#}$	9.2 ± 2.2$^{\wedge\wedge\#\#}$
2 mM L-cycloserine + C	5	1.6 ± 2.3	3.2 ± 3.3	6.4 ± 5.2	8.6 ± 5.6
100% DMSO + C	4	1.5 ± 1.3	6.5 ± 4.9	13 ± 6.3	26.2 ± 6.5$^{\wedge\wedge\#\#\&}$
0.02 mM myriocin + C	4	1.0 ± 1.4	1.8 ± 1.3	3.0 ± 3.2	6.2 ± 3.5
0.2 mM myriocin + C	4	1.5 ± 1.3	1.5 ± 1.3	7.2 ± 4.3	10.2 ± 2.9$^{\wedge\wedge\#\#}$
2 mM myriocin + C	5	3.6 ± 1.1	6.2 ± 2.2	11.6 ± 3.7$^{\wedge}$	13.8 ± 5.3$^{\wedge\wedge\#}$

Table 3.7 Number of face wash strokes after L-cycloserine or myriocin plus carrageenan injection. Mean ± SD of each group is shown in this table. Abbreviation: C: carrageenan. ^ indicates significant difference compared with before injection within the same treatment group (^: P<0.05; ^^: P<0.01). # indicates significant difference compared with 6 hours after injection within the same treatment group (#: P<0.05; ##: P<0.01). & indicates significant difference compared with 1 day after injection within the same treatment group (&: P<0.05).

3.1.5. Effects of ICV injection of inhibitors on mice without carrageenan injection

Several compounds were chosen to test their effects on intact mice, i.e., mice without facial carrageenan injection. There were no significant differences in the number of responses between any two groups at any time point, which meant that ICV injection of D609, GW4869, or L-cycloserine might not affect normal somatosensation of mice (Table 3.8)

Treatment without carrageenan	n	Before Injection	6H	1D	3D
Saline	4	1.8 ± 2.4	3.0 ± 26	3.0 ± 2.2	7.2 ± 2.9
100% DMSO	4	2.2 ± 2.2	4.2 ± 1.5	6.0 ± 4.4	3.8± 3.3
2 mM D609	4	5.2 ± 1.7	4.5 ± 2.5	5.2 ± 1.7	7.0 ± 7.4
2 mM GW4869	4	3.0 ± 0.0	2.8 ± 0.5	6.0 ± 3.6	8.2 ± 3.8
2 mM L-cycloserine	4	1.8 ± 2.1	2.5 ± 1.3	2.0 ± 0.0	5.8 ± 4.1

Table 3.8 Number of face wash strokes in mice without facial carrageenan injection. Data is shown in Mean ± SD. Mice injected with inhibitors showed no statistical difference in the number of face wash strokes compared with vehicle injected mice at any time point.

3.2. ASMase activity and PC-PLC activity assay after ICV D609 injection

D609 was chosen for further study of ASMase/ PC-PLC activity assay because it showed the most obvious effect in reducing allodynia caused by facial carrageenan injection among all inhibitors in the mice pain behavior experiment.

No significant differences in PC-PLC activity were observed among ICV D609 plus facial carrageenan injected mice, ICV saline plus facial carrageenan injected mice and untreated mice (Figure 3.6A). ASMase activity was significantly increased in the left SI in mice with ICV saline plus facial carrageenan injection, compared to untreated mice at 3 days after injection. Decreased ASMase activity was observed in all investigated parts of the brain, i.e. brain stem, thalamus, somatosensory cortex in the ICV D609 plus facial carrageenan injected mice, compared to the untreated mice and vehicle injected mice (Figure 3.6B).

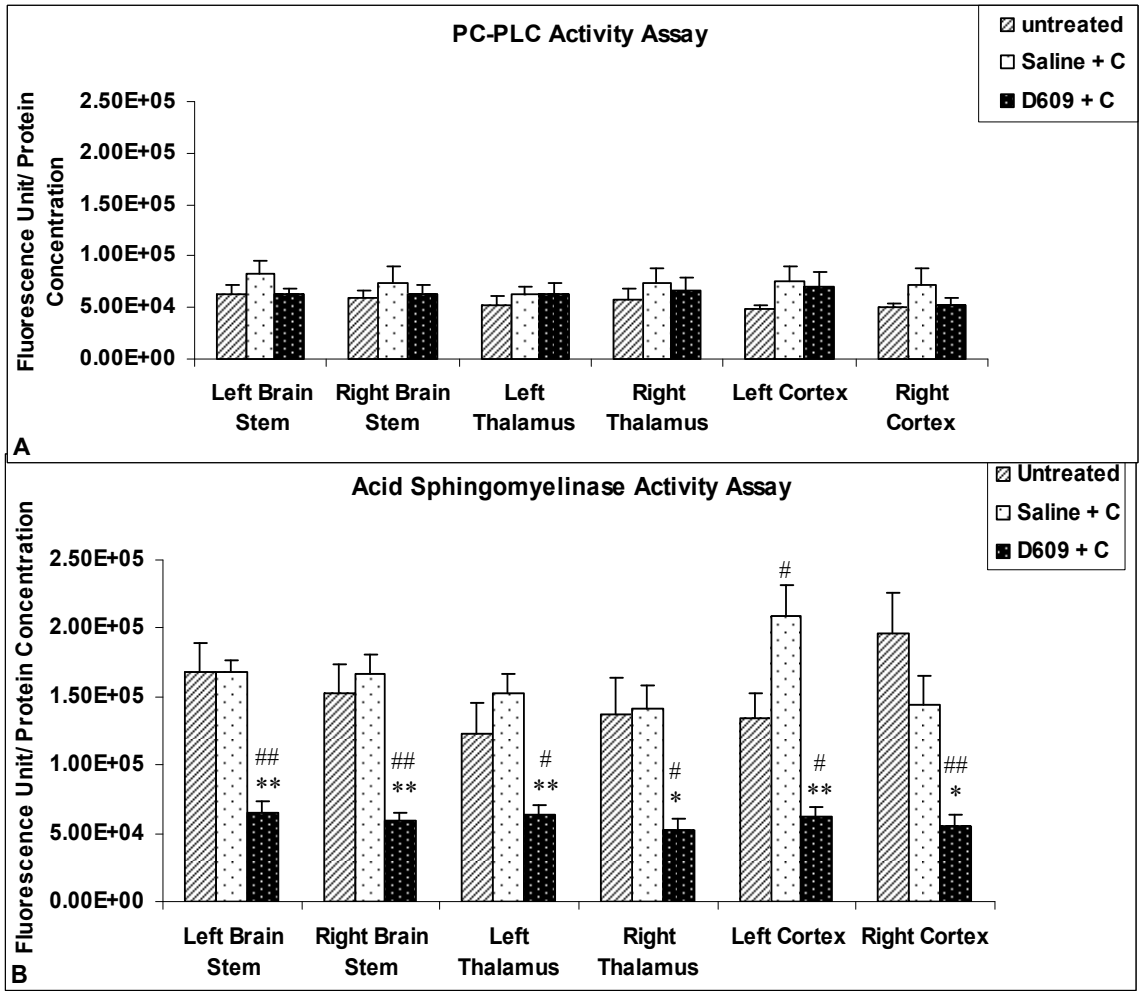

Figure 3.6 ASMase and PC-PLC activity in different parts of brain. A: No PC-PLC activity differences were observed among D609 plus carrageenan injected, saline plus carrageenan injected, and untreated mice. B: Significantly increased fluorescence reading was observed in the left primary somatosensory cortex after saline plus carrageenan injection, compared with untreated mice. ICV injection of D609 resulted in significant reduction in fluorescence reading in all the selected parts of the brain. Data is shown in Mean ± SE. n=7 for each treatment group. # indicates significant difference compared with untreated group (#: $P<0.05$; ##: $P<0.01$). * indicates significant difference compared with saline plus carrageenan injected group (*: $P<0.05$; **: $P<0.01$). Abbreviation: C: facial carrageenan injection.

3.3. Effect of free radical scavenger PBN on facial allodynia

Mice injected with carrageenan showed significantly increased face wash strokes on the third day after injection, indicating allodynia. The number of face wash strokes decreased significantly at 6 hours after ICV injection of PBN. At 1 day after ICV PBN injection, the number of responses slightly increased, but still significantly fewer compared with before ICV injection. In contrast, no significant decrease in the number of face wash strokes was found after ICV injection of saline. There was also a significant difference in the number of face wash strokes between PBN injected mice and saline injected mice at 6 hours after ICV injections (Figure 3.7, Table 3.9).

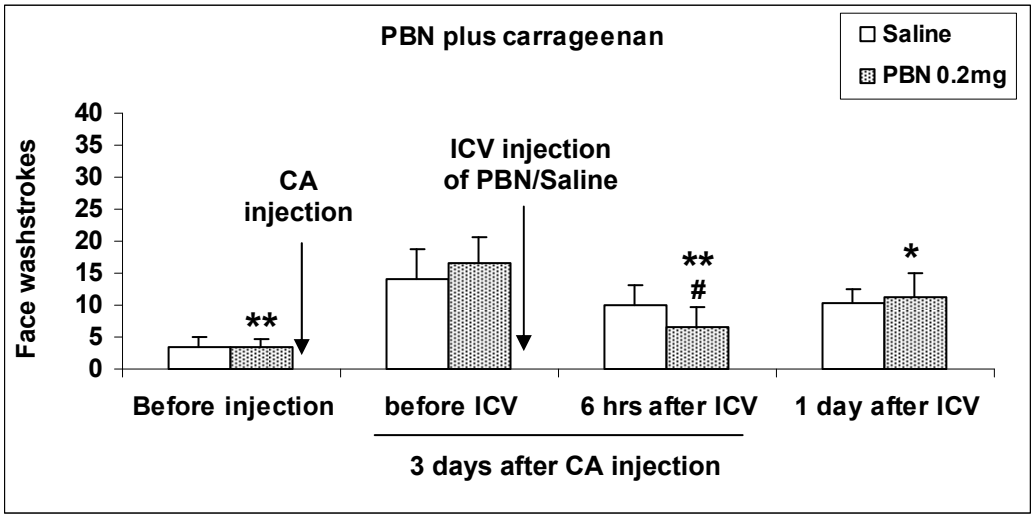

Figure 3.7 Effect of free radical scavenger PBN on carrageenan induced facial allodynia. ICV PBN injection significantly reduced the number of face wash strokes in mice with facial allodynia. # indicates significant difference compared to saline injected mice at the same time point ($P<0.05$). * indicates significant difference compared with before ICV PBN injection (3 days after facial carrageenan injection) (*: $P<0.05$; **: $P<0.01$). Abbreviation: CA: carrageenan.

Treatment	n	Before Injection	3 days after facial carrageenan injection		1 day after ICV injection
			before ICV injection	6 h after ICV injection	
Saline + carrageenan	7	3.6 ±1.3	14.1 ± 4.6**	10.1 ± 3.0**	10.3 ± 2.3**
PBN + carrageenan	7	3.4 ±1.1	16.7± 3.9**	6.6 ± 3.1££	11.3 ± 3.6£

Table 3.9 Number of face wash strokes after PBN injection. Mean ± SD of face wash strokes of each group is shown here. * indicates significant difference compared with before injection within the same treatment group (*: P<0.05; **: P<0.01). £ indicates significant difference compared with before ICV injection on the third post-carrageenan injection day, within the same treatment group (£: P<0.05; ££: P<0.01).

3.4. Intracellular H_2O_2 production induced by C18 ceramide in PC12 cells

Three hours after treatment, the amount of H_2O_2 produced in 100 μM C18 ceramide treated cells was significantly higher than vehicle (DMSO) treated cells (Figure 3.8). This effect can be inhibited by co-incubation with L-type calcium channel inhibitor nifedipine, free radical scavenger D609 and PBN, or mitochondria permeability transition pore blockers bongkrekic acid and cyclosporine A (Figure 3.9).

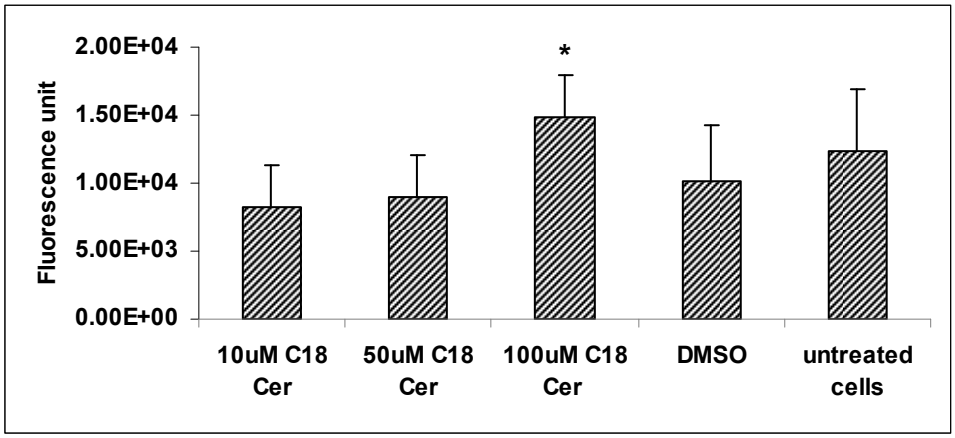

Figure 3.8 C18 ceramide's effects on intracellular H_2O_2 production in PC12 cells. C18 ceramide at different concentration was added to PC12 cells. Three hours after addition of C18 ceramide, H_2O_2 produced in 100 μM C18 ceramide treated cells was much more than vehicle (DMSO) treated cells. * indicates significant difference compared with DMSO treated cells ($P<0.05$). Data is shown in Mean ± SD. Abbreviation: Cer: ceramide.

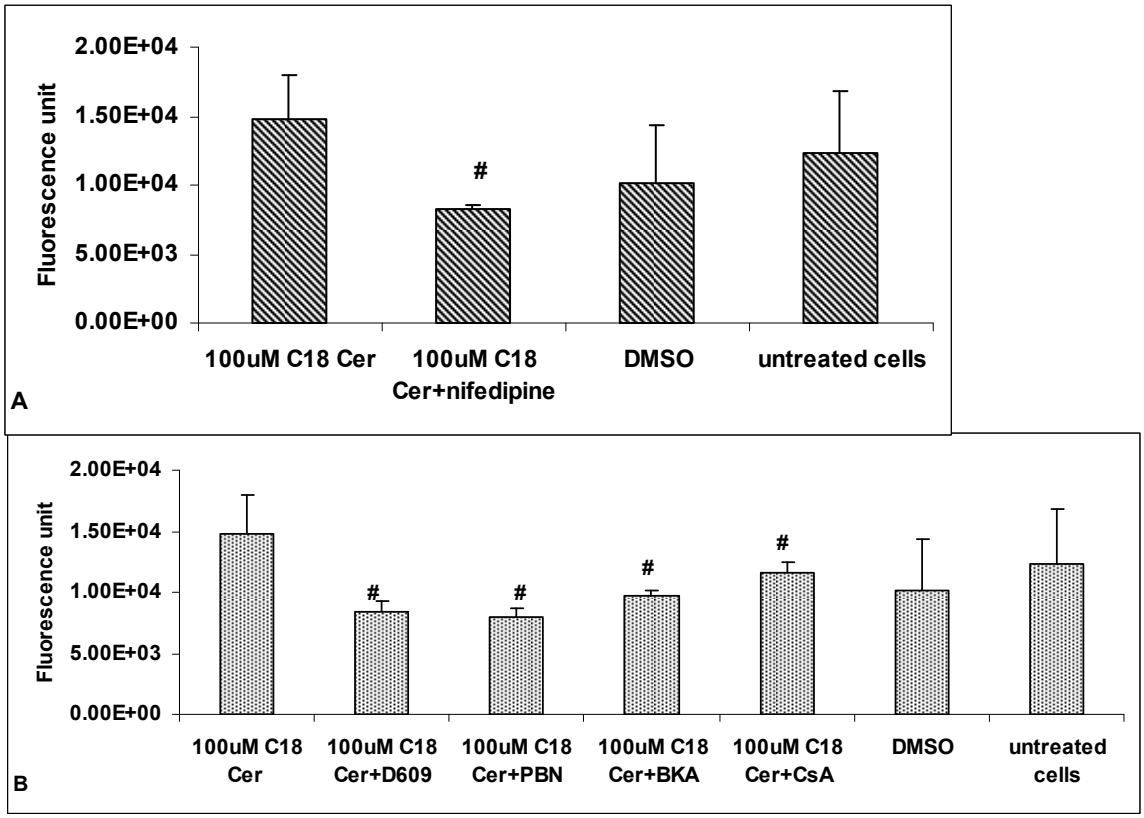

Figure 3.9 C18 ceramide's effects on intracellular H_2O_2 production are affected by other factors. A: Nifedipine caused decreased H_2O_2 production induced by 100 μM C18 ceramide in PC12 cells. B: D609, PBN, bongkrekic acid or cyclosporine A caused decreased H_2O_2 production induced by 100 μM C18 ceramide in PC12 cells. Abbreviations: Cer: ceramide; BKA: bongkrekic acid; CsA: cyclosporine A. Data is shown in Mean ± SD. # indicates significant difference compared with 100 μM C18 ceramide treated cells ($P<0.05$).

4. Discussion

The present study was carried out using inhibitors to sphingomyelinase or SPT to elucidate a possible role of CNS ceramide in nociception in a mouse model of orofacial pain. It was found that ICV injection of inhibitors to ASMase, NSMase or SPT, significantly reduced responses to von Frey hair stimulation at 3 days after facial carrageenan injection, indicating a possible role of ceramide in CNS nociception. The results added to a previous finding, in which peripheral injection of the sphingomyelinase inhibitor GW4869 markedly attenuated TNF-α-induced hyperalgesia in rats (Joseph and Levine 2004). No differences in the number of responses were detected before and after injection of inhibitors and vehicles in the absence of facial carrageenan injection. This suggests that these enzymes play a role during allodynia, but not normal somatosensation.

Acid sphingomyelinase in secretory vesicles is released when the latter fuse with the cell membrane (Grassme et al. 1997; Grassme et al. 2001). This brings the enzyme to the outer leaflet of the cell membrane and its substrate, sphingomyelin (Emmelot and Van Hoeven 1975; Merrill and Jones 1990). In comparison, neutral sphingomyelinase is localized to the endoplasmic reticulum and nucleus (Fensome et al. 2000; Neuberger et al. 2000; Rodrigues-Lima et al. 2000; Mizutani et al. 2001) and might exert its effect at these locations. The observation that inhibitors to SPT inhibited allodynia also indicates a possible role for *de novo* ceramide synthesis in allodynia after facial carrageenan injection. The effects of the above inhibitors are expected to occur in the spinal trigeminal nucleus that relays pain from the orofacial region, but could also occur in other parts of the central pain pathway, since compounds could diffuse throughout the brain

after ICV injection. Direct injection of the compounds into the brainstem was not attempted in this study as they could be lethal.

From the behavior test results, it was found that ASMase inhibitor D609, was the one that could reduce facial allodynia most obviously. However, the anti-allodynic effect of D609 might be due to other effects since it is not specific. For example, it might be due to PC-PLC, which is also known to be involved in the development of hyperalgesia (Galeotti et al. 2006; Joseph et al. 2007). PC-PLC hydrolyzes phosphatidylcholine to produce diacylglycerol (DAG), which is an important regulator of PKC (Newton 1997). PKC has been shown to affect pain transmission. Intrathecal injection of PKC inhibitor also significantly reduced the formalin induced central sensitization (Coderre 1992) or substance P mediated hyperalgesia (Wajima et al. 2000) in rats. However, this possibility is not supported by the finding since no changes of PC-PLC activity were observed in the brain after ICV D609/ facial carrageenan injection.

The possibility that D609 reduces mechanical allodynia by inhibiting ASMase is supported by the finding of significantly reduced ASMase activity in all the selected regions of the brain after D609 injection. It was also found that ASMase activity increased significantly in left primary somatosensory cortex (SI) after saline plus carrageenan injection, but not in the other selected parts of brain. The reason might be that the sampled region (the left and right part of medulla oblongata, ventral posterior nucleus of the thalamus, and primary somatosensory cortex) process non-nociceptive information as well as nociceptive signals.

It is postulated that even minute changes of ceramide might be sufficient to induce significant amplification of downstream signaling molecules/ second messengers. Ceramide molecules have the tendency to spontaneously self associate to small ceramide-enriched membrane microdomains (Kolesnick et al. 2000) and these microdomains spontaneously fuse to large ceramide-enriched macrodomains or platforms (Holopainen et al. 1998; Kolesnick et al. 2000; Nurminen et al. 2002). The fusion of small rafts might cluster receptor molecules in the membrane raft (Roccamo et al. 1999), or result in conformational changes of the receptor molecules on binding to ligands. It has been observed that ceramide-enriched membrane platforms amplify signaling via CD95 by around 100 folds (Grassme et al. 2003). It is postulated that increased clustering of glutamate receptors into lipid rafts of central nociceptive neurons could potentiate synaptic transmission through these neurons (Hering et al. 2003).

Another possibility is that D609 modulates allodynia transmission due to its antioxidant properties. D609 is one of the derivatives of xanthates, which scavenges hydroxyl radicals and hydrogen peroxide, reacting with electrophilic products of lipid oxidation in a manner similar to glutathione (Zhou et al. 2001; Lauderback et al. 2003). It has been shown to reduce free radical-induced changes in synaptosomal lipid peroxidation, protein oxidation, intracellular ROS accumulation, and apoptosis (Lauderback et al. 2003; Sultana et al. 2004; Perluigi et al. 2006). The notion that CNS free radicals are important in inducing mechanical allodynia is supported by the fact that injection of the spin trap / free radical scavenger, PBN, significantly reduced mechanical allodynia after ICV injection. Intrathecal or ICV injection of PBN has also been shown to

reduce secondary hyperalgesia caused by intradermal injection of capsaicin into the rat paw (Lee et al. 2007). Other studies have shown reduction in inflammatory pain after intrathecal injection of the SOD mimetic M40403 (Wang et al. 2004) or TEMPOL (Lee et al. 2007; Schwartz et al. 2008). It is proposed that caspase signaling, ROS production, and ceramide generation are closely associated with the pathogenesis of neuropathic and inflammatory pain in rats (Joseph and Levine 2004; Joseph and Levine 2006).

In addition, ceramide and its metabolites including S1P, or Cer1P are important signaling molecules that not only facilitate neurotransmission (Colombaioni and Garcia-Gil 2004; Farooqui et al. 2007) but also modulate PLA_2 and COX activities, which regulate the production of free radicals and ROS levels (Farooqui et al. 2007) and may contribute to pathogenesis of neuropathic and inflammatory pain in rats. This is supported by the finding that C18 ceramide directly caused an increased H_2O_2 production in PC12 cells. Furthermore, sphingomyelinase itself can also induce NO release / iNOS mRNA expression in cultured rat brain microglia (Yang et al. 2001).

In conclusion, ICV injections of inhibitors that reduce CNS ceramide generation are effective in reducing mechanical allodynia after facial carrageenan injection. The results could point to a role of CNS sphingolipids and free radicals in inflammatory pain from the orofacial region.

Chapter 3.2 Effects of Ceramides on Exocytosis and Intracellular Calcium Concentration

1. Introduction

Ceramides are a class of sphingolipids involved in diverse cellular processes such as apoptosis, growth arrest and differentiation (Hannun and Obeid 2002). They have a fatty acid chain of varied length, saturation and hydroxylation, bound to an amino group of a sphingoid base via amide linkage. The fatty acid chain can vary between two to twenty eight carbons, while C16 to C24 ceramides are the most abundant species in mammalian cells. Ceramides could be generated either through *de novo* synthesis by serine palmitoyltransferase or ceramide synthase, or through hydrolysis of cellular sphingomyelin via acid or neutral sphingomyelinases (Kolesnick and Hannun 1999). Ceramide and cholesterol enriched membrane platforms or "lipid rafts" on the cell membrane cluster receptor molecules, and recruit intracellular signaling molecules to the aggregated receptors (Gulbins and Li 2006). Lipid rafts also cluster members of the SNARE family of proteins, involved in exocytosis (Chamberlain et al. 2001; Salaun et al. 2005; Gil et al. 2006).

Changes in lipid composition and conformation of cell membranes can cause enhanced fusion of synaptic vesicles, and release of neurotransmitters (Rossetto et al. 2006). Such fusion of synaptic vesicles with the plasma membrane during exocytosis may be detected by membrane capacitance measurements under voltage-clamp conditions (Chen and Gillis 2000; Chik et al. 2001; Sun and Wu 2001; Di et al. 2002; Klyachko and Jackson 2002; Sun et al. 2002; Zhang and Zhou 2002). These measurements enable high time-resolution quantitation of exocytosis and neurotransmitter release (Sun and Wu 2001). Using this technique, it was found that

external application of secretory phospholipase A_2 ($sPLA_2$) resulted in increased exocytosis in PC12 cells or cultured hippocampal neurons (Wei et al. 2003). Exocytosis can also be analyzed using total internal reflection fluorescence microscopy (TIRFM). The aqueous phase immediately adjacent to a glass interface is selectively illuminated in this technique, thus enabling direct, real time visualization of a pool of fluorescently labeled vesicles that are close to the cell membrane (Allersma et al. 2004).

Increase in several ceramide species has been shown by non-targeted lipid profiling (lipidomics) of the rat hippocampus after kainate lesions (Guan et al. 2006). Ceramide could affect the function of the cell membrane / lipid rafts, but thus far, little is known about whether ceramide species could have direct effect on exocytosis. The present study was then carried out to determine possible effects of various ceramide species on exocytosis in cells.

2. Materials and methods

Ceramides used in this investigation have fatty acid chains ranging from 2 to 20 carbons and could be dissolved in dimethyl sulfoxide (DMSO) (Table 3.10). These ceramide species were chosen because of their ready commercial availability, and solubility in DMSO. Species such as C24 ceramide, which is insoluble even in DMSO, were not included in this study.

Ceramides (Abbreviations)	Full name	Source
C2 ceramide	N-acetyl-D-sphingosine	Sigma-Aldrich, St Louis, USA
C6 ceramide	N-hexanoyl-D-sphingosine	Sigma-Aldrich, St Louis, USA
C16 ceramide	N- palmitoyl-D--erythro-spingosine	Avanti Polar Lipids, Alabaster, USA
C18 ceramide	N-stearoyl-D-erythro-sphingosine	Avanti Polar Lipids, Alabaster, USA
C20 ceramide	N-arachidoyl –D-erythro-sphingosine	Avanti Polar Lipids, Alabaster, USA

Table 3.10 Ceramide species used in patch clamp and TIRFM experiment.

2.1. Cell membrane capacitance measurements

2.1.1. Cell culture

PC12 cells (pheochromocytoma cells) were cultured in RPMI medium supplemented with 10% fetal bovine serum and 1% penicillin/ streptomycin (Gibco, Invitrogen, Carlsbad, CA). Cells were plated in 35 mm Petri dishes, and maintained in an incubator at 37 ^{0}C, 100% humidity, with 95% air and 5% CO_2.

Primary cultures of hippocampal neurons were prepared from 1 to 3-days-old Wistar rat pups. They were deeply anesthetized and decapitated. The brains were rapidly removed and transferred to 75 mm Petri dishes containing ice cold Hanks' balanced salt solution. The left and right hippocampi were dissected out under sterile conditions, and incubated with 2 ml of 0.05% trypsin-EDTA (ethylenediaminetetraacetic acid) at 37 °C for 10 min. The tissues were washed twice with PBS, and then transferred into Dulbecco's Modified Eagle medium (DMEM) supplemented with 10% fetal bovine serum and 1% penicillin/streptomycin. A cell suspension was prepared by titration with a flame-polished Pasteur pipette. The cells were plated on 35 mm Petri dishes at a final density of approximately 5×10^5 cells per cm^2. They were maintained in an incubator at 37 °C, 100% humidity and 95% air and 5% CO_2. The culture medium was changed to fresh medium on the second day in culture and half the medium was changed every two days. They were analyzed after 5-7 days. All procedures involving animals were approved by the Institutional Animal Care and Use Committee.

2.1.2. Lipid raft disruption by methyl ß cyclodextrin

Some of the cultured cells were treated with methyl ß cyclodextrin (M-ß-CD) (Sigma-Aldrich, St Louis, MI) prior to the capacitance measurements. This chemical is known to decrease cholesterol content of the cell membrane, resulting in disruption of the function of lipid rafts (Ko et al. 2005; Sun et al. 2005; Shvartsman et al. 2006). M-ß-CD was dissolved in serum free culture medium at a concentration of 10 mM. Cells were incubated with 10 mM M-ß-CD in serum free culture medium for 10 min at 37 °C, and washed twice with PBS before patch clamp experiments.

2.1.3. Solutions for patch clamp recording

The cell culture medium was changed to 2 ml of external solution/bath solution prior to the patch clamp experiments.

The external solution/bath solution contained (in mM): 150 NaCl, 2.8 KCl, 10 $CaCl_2$, 1 $MgCl_2$, 10 HEPES and 2 mg/ml glucose, pH 7.2 with 310 mOsm.

The internal solution for glass pipettes contained (in mM): 130 K-gluconate, 2 NaCl, 20 HEPES, 4 $MgCl_2$• $6H_2O$, 4 Na_2ATP•$2.5H_2O$, 0.4 NaGTP and 1 EGTA.

Ceramides were dissolved in DMSO to a concentration of 5 mM, and further diluted with external solution to a concentration of 2 mM. A solution of 40% DMSO in external solution was used as vehicle control. During cell membrane capacitance measurement, 2 µl of ceramide solution / DMSO vehicle was added to the external solution, near a stably "whole cell" voltage clamped cell for capacitance measurements. The final concentration of ceramides in the vicinity of the cell was estimated to be 2 µM.

2.1.4. Whole-cell patch clamp recording

Capacitance measurements during patch clamp conditions enable high time-resolution quantitation of exocytosis and neurotransmitter release (Sun and Wu 2001). An EPC-9 patch-clamp amplifier was used together with the Pulse software package (HEKA Electronics, Germany) in capacitance measurement. Capacitance measurements were performed on the cells while applying ceramides externally, using the Lindau-Neher technique implemented as the `sine+dc' mode (Gillis 1995) of the software lock-in extension of Pulse. This allowed long duration capacitance

measurements in a single sweep. A 1000 Hz, 50 mV peak-to-peak sinusoid voltage stimulus was superimposed onto a DC holding potential of -70 mV.

Glass pipettes for the patch clamp recording had an outer diameter of 1.5 mm, and an inner diameter of 0.84 mm (World Precision Instruments, 1B150F-4, FL, USA). Pipettes were pulled into two with relatively blunt tip using a multi-stage micropipette puller (Sutter Instrument, Model P-97, CA, USA). Pipettes were then firepolished using a microforge (Narishige, MF-830, Tokyo, Japan) to promote gigaohm seals and to reduce the possibility of tip penetration into the cell during seal formation.

Capacitance measurements were carried out on PC12 cells or hippocampal neurons under whole-cell voltage clamp conditions, using 3-7 MOhm pipettes. First, an individual cell with normal appearance, without bulbs attached was chosen under microscope for patch clamp recording. Firepolished glass pipette filled with internal solution was mounted and secured over a silver electrode at the pipette holder. A positive pressure was applied to the pipette to maintain the cleanliness of the internal walls of pipette as the pipette approached the cell. A manipulator was used to control the movement of the pipette towards the location of the selected cell. Upon touching the bath solution, a current response to the voltage held at the electrode was seen on the monitor. Once the pipette touches the cell, a gentle suction was applied until the current response became essentially zero with two small spikes in place of the previous start. The holding potential in the electrode was changed gradually to -70 mV to speed up the giga-seal configuration formation when the recorded resistance of the cell membrane was in the gigaohm range. Capacitance compensation (termed as Fast Capacitance Compensation) was applied to cancel capacitive currents. A further suction was applied for whole cell

configuration, until similar current spikes are observed as in the case of a "giga-seal". Capacitance compensation (termed as Slow Capacitance Compensation) was then applied to cancel this capacitive current. If the membrane resistance was still in the gigaohms range, the whole cell configuration was reached. Only cells that were stably voltage clamped were analyzed, that means, a series resistance of less than 20 mega ohms, with no sudden changes of more than 10%.

The recording of capacitance lasted for 5 seconds after addition of ceramide while the cell was in a "stabilized" position. The capacitance value was normalized to the one immediately before ceramide treatment. This was to take into account slight differences in initial capacitances, between cells of different sizes. Ten to thirteen cells were analyzed for each treatment. A non-parametric test (Spearman's rank correlation test) was used to determine any correlation between capacitance and time (SPSS 12.0 for Windows software). A positive correlation denotes increase in membrane capacitance with time after application of ceramide, indicating exocytosis. $P < 0.05$ was considered significant.

2.2. Total internal reflection fluorescence microscopy (TIRFM)

2.2.1. Cells and plasmids

PC12 cells were cultured in DMEM supplemented with 10% horse serum (Gibco) and 5% fetal bovine serum at 37 ºC and 5% CO_2. Neuropeptide Y (NPY)–enhanced green fluorescence protein (EGFP) plasmid was a kind gift from Dr. Wolf Almers (Vollum Institute, Oregon Health Sciences University). Cells were plated onto poly-L-lysine (Sigma, St Louis, USA) coated glass coverslips and transfected with 1 μg of NPY-EGFP

plasmid using SuperFect Transfection Reagent (QIAGEN GmbH, Germany), 1-2 days before the imaging experiments.

2.2.2. TIRFM

The buffer solution contained (in mM): 150 NaCl, 5.4 KCl, 2 $MgCl_2$, 1.8 $CaCl_2$, 5 mM glucose, and 10 HEPES (pH 7.4). This solution, containing 2 μM of various ceramide species (diluted from 2 mM stock in 40% (v/v) DMSO) or 0.04% (v/v) DMSO vehicle control, was infused to the imaging chamber. In the zero Ca^{2+} experiment, $CaCl_2$ was replaced by 5 mM ethylene glycol tetraacetic acid (EGTA). Total internal-reflection fluorescence microscopy was carried out using a Zeiss Axiovert 200 inverted microscope. EGFP was excited by 488 nm laser and the emission light was collected at 520 nm. Time-lapse digital images were acquired at 1 Hz by a CCD camera with exposure time of 18 ms, and image stacks were analyzed using MetaMorph 6.3 software (Universal Imaging, Downingtown, PA). Four cells were analyzed for each treatment, except for the EGTA calcium chelation experiment (6 cells).

2.3. Intracellular free calcium level measurement

2.3.1. Cell culture

PC12 cells were cultured in RPMI Medium supplemented with 10% fetal bovine serum and 1% penicillin/ streptomycin (Gibco, Invitrogen, Carlsbad, CA). Cells were plated in 35 mm Fluorodish (FD35PDL, World precision Instruments, Sarasota, FL, US). The glass bottom of Fluorodish is coated with poly-D-lysine. Cells were maintained in an incubator at 37 ^{0}C, 100% humidity, with 95% air and 5% CO_2.

2.3.2. Intracellular calcium level measurements

Before the measurement of intracellular free calcium concentration ($[Ca^{2+}]_i$), PC12 cells were loaded with Fura-2-AM (Fura-2, acetoxymethyl ester) (Invitrogen, Eugene, OR, USA), which is a high affinity and membrane-permeable, intracellular calcium indicator that is radiometric and UV light excitable. Fura-2-AM was dissolved in anhydrous DMSO at 1 mM and stored at 4 °C in small aliquots, avoiding of light. PC12 cells were incubated with 5 μM fura-2-AM in HEPES buffer (20 mM HEPES, 115 mM NaCl, 5.4 mM KCl, 1.8 mM $CaCl_2$, 0.8 mM $MgCl_2$, 13.8 mM glucose, pH 7.4) for 1 hour at 37 °C. Fura-2-AM loaded cells were washed twice with HEPES buffer and incubated for an additional 30 minutes to allow for cellular esterase cleavage of the acetoxymethyl moiety and intracellular trapping of the free acid Fura-2-AM indicator.

Intracellular free calcium level measurement was carried out by following previously established procedures (Pal et al. 1999; De et al. 2003) using dual wavelength fluorescent measurements with imaging-based detection system. Fluorodish with PC12 cells loaded with Fura-2-AM was mounted on an Olympus IX71 inverted microscope. The fluorescence excitation source was a 150 W Xenon arc lamp (OptoSource Arc Lamp, Cairn Research Limited, Kent, UK). Alternating excitation wavelengths of 340 and 380 nm were generated using OptoScan Monochromator (Cairn Research Limited, Kent, UK), and 510 nm emission was acquired using a Fura filter cube (XF-04-2, Omega Optical Inc., VT, USA) with a dichroic at 400 nm. Alternating emissions from 340 and 380 nm excitation were captured with a CoolSNAP HQ2 digital CCD camera (Photometrics, AZ, USA). Image pairs for each wavelength were captured and digitized at 10 s intervals. Image acquisition and processing were computer-controlled using

Metamorph software version 7.0.4. Using this image analysis software, regions of interest were selected for each PC12 cell in the field, on average more than 10 cells were selected in each dish. The ratio of emission intensity (340/380) for individual region/cell was calculated. The relative $[Ca^{2+}]_i$ across time was indicated as the normalized value of emission intensity (340/380), that means, each value was divided by the first value of recording. This was to take into account possible differences in initial $[Ca^{2+}]_i$ concentration in different cells. Two microliter of 2 mM C18 ceramide was added to fura-2-AM loaded PC12 cells at 390 s from the start of recording, the final concentration of C18 ceramide was estimated as 2 μM. In another group of PC12 cells, after loading with the fura-2-AM, PC12 cells were incubated with L-type calcium channel blocker nifedipine at a concentration of 1 μM in HEPES buffer for 15 min at 37 °C. Then 2 μM of C18 ceramide was added to fluorodish at 390 s from the start of fura-2-AM image recording.

3. Results

3.1. Capacitance measurements

3.1.1. Capacitance changes after adding ceramides to PC12 cells

Significant increase in membrane capacitance with time was observed in PC12 cells after external addition of C2, C6, and C18 ceramides ($P < 0.05$). This is an indicator of exocytosis since membrane capacitance is proportional to cell surface area and is increased upon fusion of secretory vesicles with the plasma membrane. In contrast, no increase in capacitance was observed after addition of C16 and C20 ceramides, or DMSO

vehicle (Figure 3.11, Table 3.11). Figure 3.10 shows a typical recording of capacitance change after adding C18 ceramide to PC12 cell.

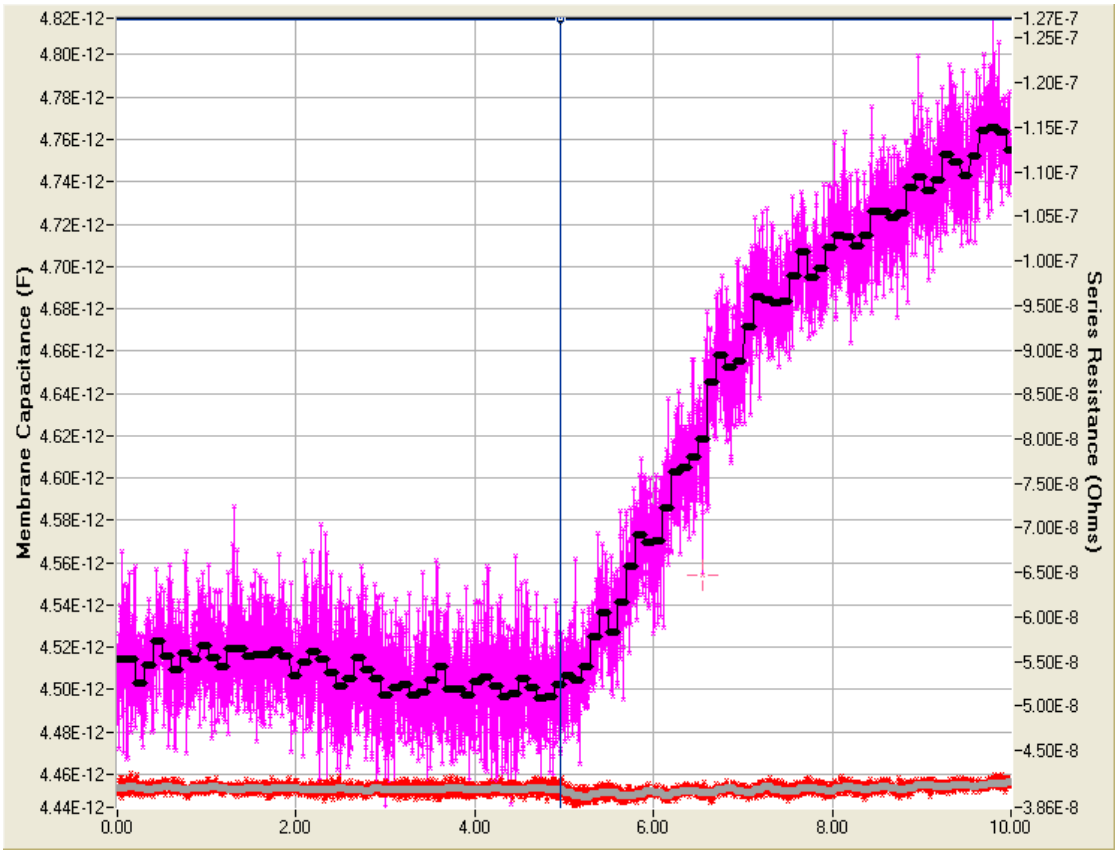

Figure 3.10 Typical recording of capacitance changes after addition of C18 ceramide to PC12 cell. The X axis indicates time (s). The left Y axis indicates membrane capacitance (F), the right Y axis indicates series resistance (Ohms). The pink wave represents membrane capacitance; the red wave represents series resistance. An average of membrane capacitance or series resistance was calculated every 100 ms respectively. Vertical blue line indicates the time point of adding ceramides to PC12 cells. There was an increase in membrane capacitance after adding C18 ceramide to PC12 cell.

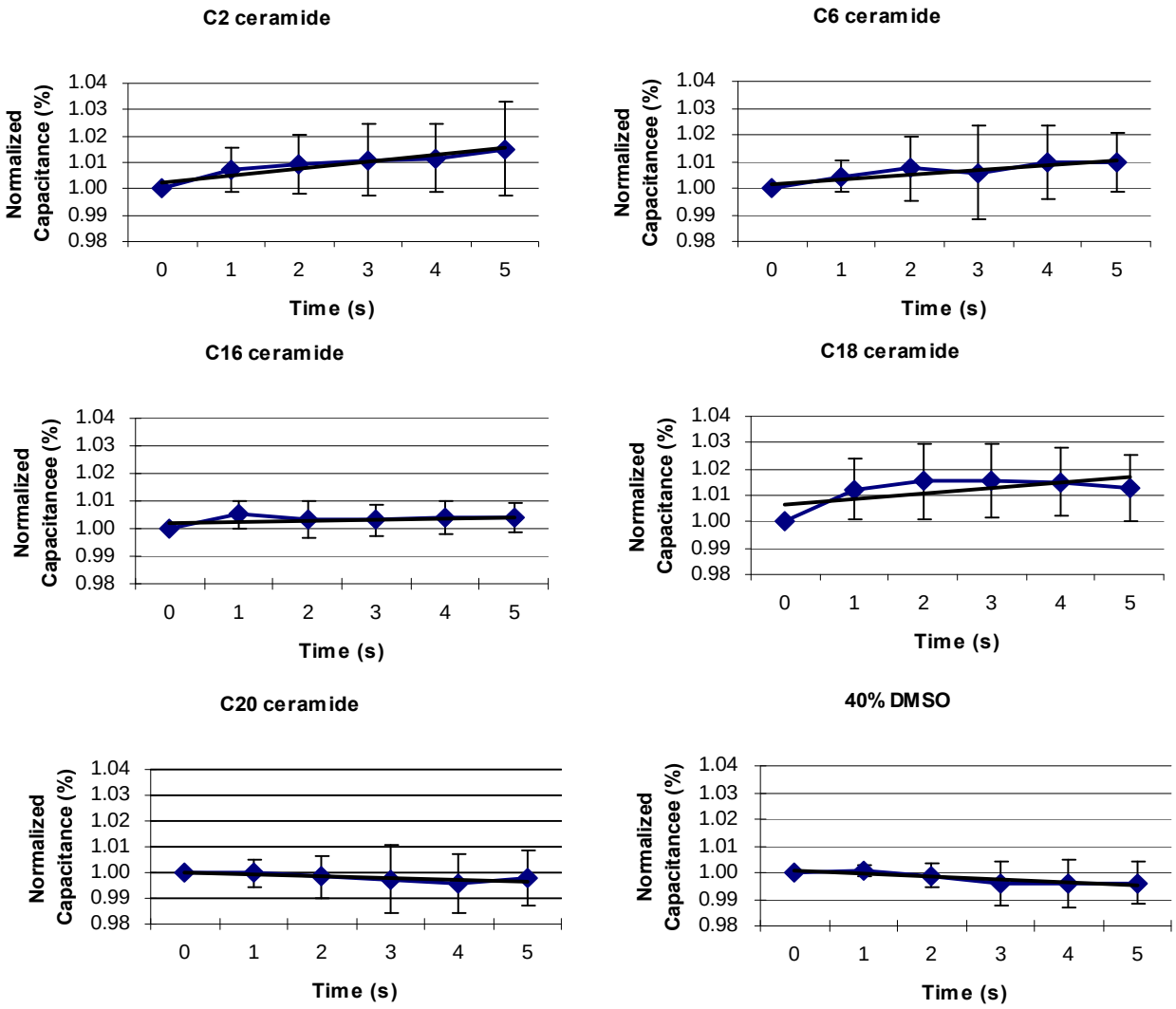

Figure 3.11 Membrane capacitance changes after adding different ceramide species to PC12 cells. Significant increase in capacitance was observed after addition of C2, C6 and C18 ceramide. Y axes indicate capacitance values normalized to the value before ceramide application. Values indicate mean and standard error. A 'best-fit' line was included in the plots. n = 10 to 13 cells in each treatment. Results were analyzed by Spearman's rank correlation test.

Treatment	n	Coefficient of Determination (R^2)	Correlation Coefficient	P value
C2 Cer	11	0.88	0.41	0.00*
C6 Cer	12	0.82	0.35	0.00*
C16 Cer	11	0.21	0.14	0.27
C18 Cer	10	0.42	0.30	0.02*
C20 Cer	13	0.76	-0.07	0.54
DMSO	10	0.78	-0.20	0.12
M-β-CD + C18 Cer	10	0.88	-0.00	0.98
M-β-CD + DMSO	10	0.21	0.09	0.47

Table 3.11 Effect of ceramide species on exocytosis in PC12 cells. Spearman's rank correlation test was used to calculate the correlation between membrane capacitance and time. A positive correlation indicates increase in capacitance with time, and *vice versa*. Increase in capacitance was observed after addition of C2, C6 and C18 ceramide to PC12 cells. The effect of C18 ceramide was shown to be dependent on the integrity of the lipid raft. Addition of the cholesterol chelating agent / disruptor of lipid rafts, methyl ß cyclodextrin prior to C18 ceramide treatment resulted in no significant increase in capacitance. $P< 0.05$ was considered significant (indicated by *). Abbreviations: Cer: ceramide; M-ß-CD: methyl ß cyclodextrin.

3.1.2. Capacitance changes after adding C18 ceramide to PC12 cells depleted of membrane cholesterol

Pre-treatment of cells with 10 mM M-ß-CD resulted in non-significant increase in capacitance after C18 ceramide addition (Figure 3.12, Table 3.11).

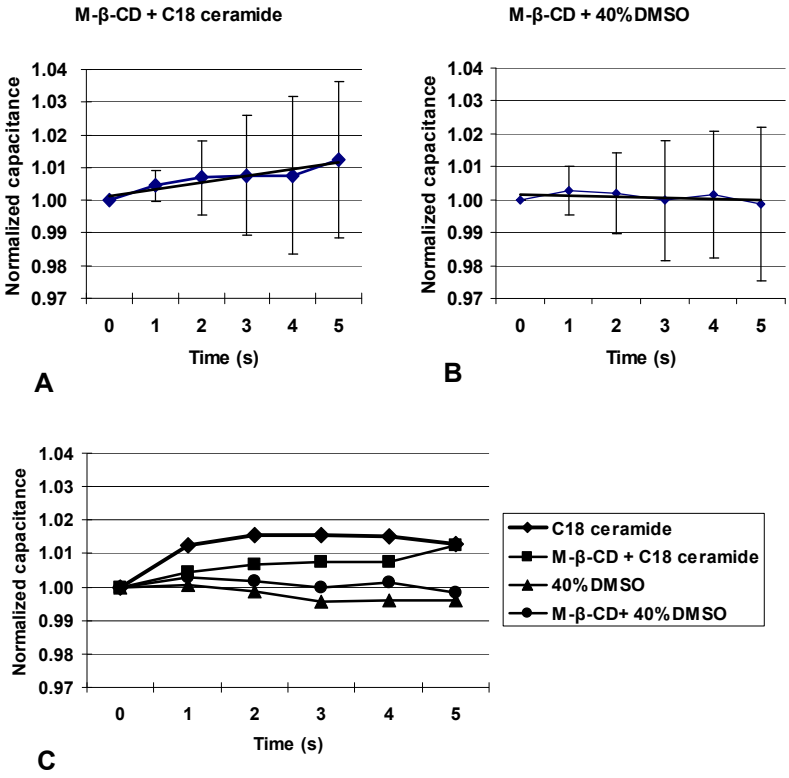

Figure 3.12 Effect of C18 ceramide on membrane capacitance in methyl ß cyclodextrin pre-treated PC12 cells. C18 ceramide (A) or DMSO control (B) could not cause capacitance increase in PC12 cells pre-incubated with methyl ß cyclodextrin. C: summary of capacitance changes on PC12 cells with / without methyl ß cyclodextrin pre-treatment, followed by addition of C18 ceramide / DMSO. n = 10 in each treatment. Results were analyzed by Spearman's rank correlation test, $P < 0.05$ was considered significant. Abbreviation: M-ß-CD: methyl ß cyclodextrin.

3.1.3. Capacitance changes after adding C18 ceramide to primary hippocampal neurons

Significant increase in membrane capacitance with time was observed in primary hippocampal neurons after external addition of C18 ceramide ($P<0.05$), the same species that caused the largest increase in membrane capacitance in PC12 cells. Pre-treatment of neurons with M-ß-CD resulted in non-significant increase in capacitance after C18 ceramide treatment. This finding was similar with the results obtained from PC12 cells (Figure 3.13, Table 3.12).

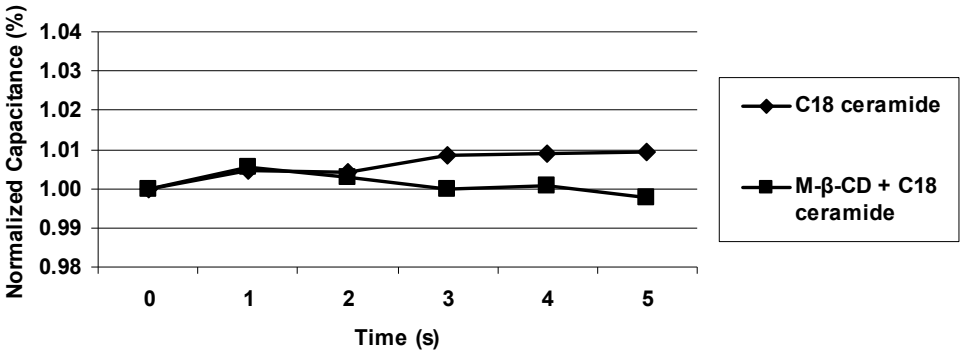

Figure 3.13 Effect of methyl β cyclodextrin on membrane capacitance changes in neurons. C18 ceramide could not cause capacitance increase in methyl ß cyclodextrin pretreated hippocampal neurons. n = 10 in each case. Results were analyzed by Spearman's rank correlation test. $P<0.05$ was considered significant. Abbreviation: M-ß-CD: methyl ß cyclodextrin.

Treatment	n	Coefficient of Determination (R^2)	Correlation Coefficient	P value
C18 Cer	10	0.89	0.40	0.0016*
M-β-CD + C18 Cer	10	0.30	0.15	0.24

Table 3.12 Effect of C18 ceramide on exocytosis in primary hippocampal neurons. Spearman's rank correlation test was used to calculate the correlation between membrane capacitance and time. A positive correlation indicates increase in capacitance with time. Increase in capacitance was observed after addition of C18 ceramide to hippocampal neurons. The effect of C18 ceramide was shown to be dependent on the integrity of the lipid raft. Addition of the cholesterol chelating agent / disruptor of lipid rafts, methyl ß cyclodextrin prior to C18 ceramide treatment resulted in no significant increase in capacitance. $P<0.05$ was considered significant (indicated by *). Abbreviations: Cer: ceramide; M-ß-CD: methyl ß cyclodextrin.

3.2. TIRFM

NPY-EGFP labeled subplasmalemmal vesicles were observed to fuse with the cell membrane, and their numbers quickly decreased after treated with C2, C6, C18 ceramide, indicating exocytosis. The most rapid effect was observed after addition of C18 ceramide. In contrast to the above species, no decrease in vesicle number was detected after addition of C16 or C20 ceramide, and DMSO vehicle. C18 ceramide induced exocytosis was Ca^{2+} dependent, and exocytosis was not observed in cells that were treated with this ceramide in the presence of the Ca^{2+} chelator, EGTA (Figure 3.14, Table 3.13).

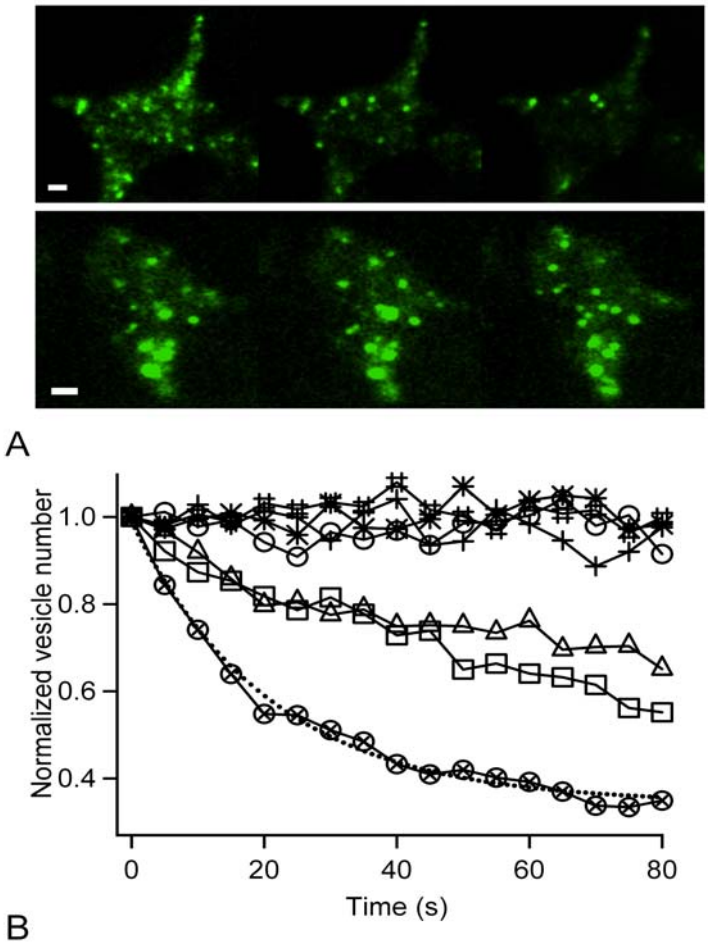

Figure 3.14. Time-lapse total internal reflection fluorescence microscopy (TIRFM) after application of ceramide species. A: Typical recordings of the footprints of living PC12 cells that had been transfected with NPY-EGFP, before (t = 0 s, at the left) and after (t = 30 s in the middle; t = 80 s at the right) addition of 2 μM C18 ceramide (top) or vehicle (0.04% v/v DMSO) (bottom). Upper panels: there was decrease in the number of NPY-EGFP labeled subplasmalemmal vesicles (bright fluorescent dots) after C18 ceramide application indicating release of vesicles. Lower panels: no decrease in number of subplasmalemmal vesicles was seen after application of DMSO (vehicle control). Scale = 2 μm. B: Changes in number of subplasmalemmal vesicles after the application of C18 (⊗), C2 (Δ) or C6 (□) ceramide. The fastest response was observed after application of C18 ceramide. Its kinetics is an exponential (doted line) with a time constant of 20 seconds. In contrast, C16 (#), C20 (+) ceramide and DMSO (*) did not reduce the number of subplasmalemmal vesicles. Depletion of external Ca^{2+} completely eliminated the capability of C18 in triggering vesicle release (○). n = 4 in each group, except the EGTA calcium chelation experiment treated group (n = 6).

Treatment	n	Before treatment	30 s after treatment	P value
C2 Cer	4	1	0.7755	< 0.01
C6 Cer	4	1	0.8154	< 0.01
C16 Cer	4	1	1.0333	0.28
C18 Cer	4	1	0.5109	< 0.01
C20 Cer	4	1	0.9458	0.09
DMSO	4	1	1.0226	0.31
EGTA + C18 Cer	6	1	0.9648	0.20

Table 3.13 Comparison of numbers of subplasmalemmal vesicles in PC12 cells after external application of different ceramide species. Due to slight differences in starting number of vesicles (NPY-EGFP labeled) between individual cells, the numbers of vesicles were normalized to that before treatment (value of 1). Results were analyzed by Student's t-test. Decrease in vesicles, indicating exocytosis, was observed after addition of C2, C6, and C18 ceramide. The effect of C18 ceramide is dependent on external calcium concentration. Addition of a calcium chelator, EGTA prior to C18 ceramide treatment resulted in no significant effect on exocytosis. Abbreviation: Cer: ceramide.

3.3. C18 ceramide's effect on $[Ca^{2+}]_i$ in PC12 cells

Significant increase of $[Ca^{2+}]_i$ was observed after 2 μM C18 ceramide was applied to non-pretreated PC12 cells. $[Ca^{2+}]_i$ peaked at 20-30 seconds after the addition of C18 ceramide. No change of $[Ca^{2+}]_i$ was observed after addition of C18 ceramide to PC12 cells that were pretreated with 1 μM nifedipine. At 420 seconds, there was significant difference in $[Ca^{2+}]_i$ between non-pretreated cells and nifedipine pretreated cells (P<

0.01), indicating C18 ceramide's effect on $[Ca^{2+}]_i$ is dependent on L-type calcium channel (Figure 3.15).

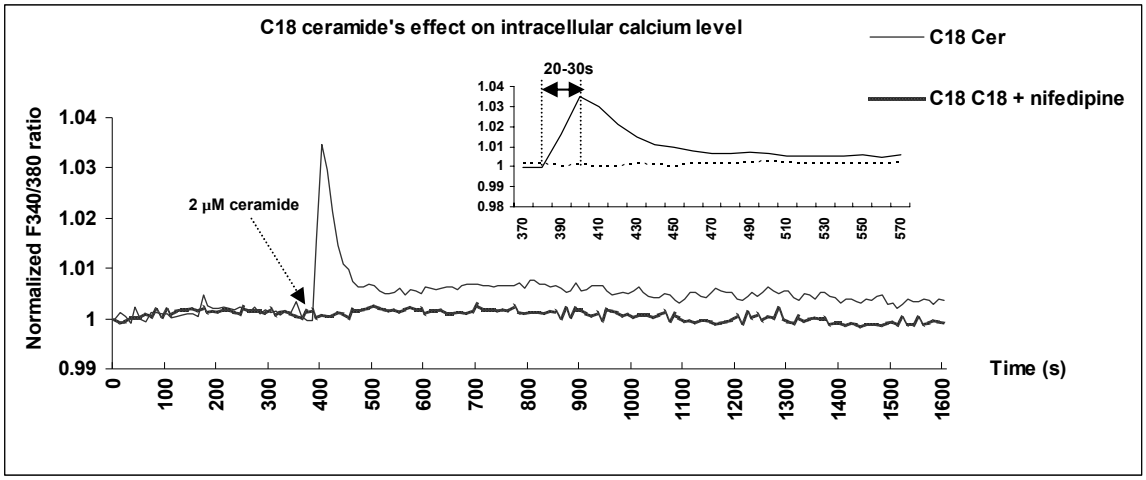

Figure 3.15 Changes of intracellular calcium level after addition of C18 ceramide to PC12 cells. A significant increase of $[Ca^{2+}]_i$ was observed after 2 μM C18 ceramide was added to non-pretreated PC12 cells (n= 13). $[Ca^{2+}]_i$ peaked at 20-30 seconds after C18 ceramide treatment. No change of $[Ca^{2+}]_i$ was observed after addition of C18 ceramide to L-type calcium channel inhibitor nifedipine (1 μM) pretreated PC12 cells (n= 17). At 420 seconds, there was significant difference in $[Ca^{2+}]_i$ between non-pretreated cells and nifedipine pretreated cells ($P< 0.01$), indicating C18 ceramide's effect on $[Ca^{2+}]_i$ is dependent on L-type calcium channel.

4. Discussion

The present study was carried out to determine the effects of various ceramide species on exocytosis and possible underlying mechanism. It was found that C2, C6 and C18 ceramides were effective in triggering exocytosis in PC12 cells, evident by more than 1% increase in membrane capacitance. Similar increase in membrane capacitance was also observed in hippocampal neurons after C18 ceramide treatment, the same species which caused most significant exocytosis in PC12 cells. C16 and C20 ceramide did not show a tendency to cause any changes in membrane capacitance. The ability of

C2, C6 and C18 ceramides to induce exocytosis was confirmed, using TIRFM. These species caused rapid decrease in number of NPY-EGFP labeled subplasmalemmal vesicles, indicating exocytosis. The above results show that any effect of particular ceramide species on exocytosis is highly dependent on the exact length of the fatty acid chain.

Ceramide has been shown to affect the physical properties of artificial lipid membrane. Treatment of model membrane containing sphingomyelin, phosphatidylethanolamine and cholesterol with sphingomyelinase, generated ceramides within seconds, accompanied by vesicle aggregation or efflux of intravascular components (Ruiz-Arguello et al. 1998). Likewise, external- and enzymatically produced ceramides induce release of contents from vesicles which consist of phospholipids and cholesterol (Montes et al. 2002). On the other hand, endocytic vesicles were observed in macrophages when treated with exogenous sphingomyelinase or ceramide (Zhang et al. 1998). Ceramides have also been shown to induce pore formation in model phospholipids bilayers (Siskind and Colombini 2000). In addition, ceramides could affect the movement of proteins into or from rafts, or cause conformational changes in membrane-associated proteins (Cremesti et al. 2002). SNARE complex proteins are clustered in lipid rafts (Chamberlain et al. 2001; Salaun et al. 2005; Gil et al. 2006), and it is possible that changes in their conformation as a result of alteration in ceramide content could affect exocytosis.

A possible role of lipid rafts in the effects of C18 ceramide was studied, using PC12 cells and hippocampal neurons that had been treated with M-ß-CD. The latter binds cholesterol, and is well known to disrupt the function of lipid rafts (Ko et al. 2005; Sun et

al. 2005; Shvartsman et al. 2006). C18 ceramide induced a significant increase in capacitance after external application to PC12 cells/ hippocampal neurons, but no significant increase was observed after C18 ceramide treatment when cells were pre-incubated with M-ß-CD. This suggests that the increase in capacitance was dependent on the integrity of lipid rafts. It could involve calcium sensors associated with SNARE complex proteins in lipid rafts (Chamberlain et al. 2001; Salaun et al. 2005; Gil et al. 2006), since C18 induced exocytosis was also found to be dependent on external calcium.

The ceramide species which most significantly increases cell membrane capacitance and decreases subplasmalemmal vesicles, i.e., C18 ceramide, was chosen for study further the effect of ceramide on calcium channel. It was found that C18 ceramide could cause an increase of intracellular calcium concentration in PC12 cells and this effect was found to be L-type calcium channel dependent, which further supports the idea that C18 ceramide-induced exocytosis is calcium dependent.

C18 is also the ceramide species that showed the greatest increase, by non-targeted lipid profiling analysis (lipidomics) of the rat hippocampus after kainate-induced excitotoxic injury (Guan et al. 2006). It is postulated that C18 ceramide might facilitate exocytosis of glutamate from damaged neurons, thus propagating neuronal injury. Treatment of hippocampal slices with inhibitors of ceramide biosynthesis resulted in attenuation of increased C18 ceramide levels, and partial protection against neuronal death, after kainate injury (He et al. 2007). Further studies are necessary to elucidate the precise effect of various ceramide species on the physicochemical properties on cell membranes or the function of membrane raft-related proteins, and how they could affect exocytosis.

Chapter 3.3 Role of Central Nervous System Peroxynitrite in a Mouse Model of Orofacial Pain

1. Introduction

Nitric oxide (NO) is a gaseous mediator involved in a variety of physiological functions (Schuman and Madison 1994; Moncada 1997). It is produced from L-arginine by nitric oxide synthases (NOS) and is involved in a variety of physiological processes in the cardiovascular, immune and nervous systems. Decreased NOS expression has been shown in the trigeminal ganglion but accumulation of the enzyme at the injury site occurs after inferior alveolar nerve injury (Leong et al. 2000; Davies et al. 2004). In contrast, increased numbers of NOS positive neurons are present in the spinal trigeminal nucleus after hyperalgesia induced by formalin injection (Leong et al. 2000), or loose ligation of the trigeminal nerve (Yonehara et al. 2003).

NO is involved in macrophage cytotoxicity and nociceptive signaling. Injury to the distribution area of the trigeminal nerve has been shown to result in changes in NO amount at the injury site or the trigeminal ganglion. Increased levels of NO are present in synovial fluid of the painful temporomandibular joints (Suenaga et al. 2001; Arinci et al. 2005). NO produced in the trigeminal nucleus likely plays a role in nociceptive transmission, since increased levels of excitatory amino acids are detected in the spinal trigeminal nucleus after nerve ligation, which could be inhibited by local infusion of the NO scavenger, carboxyl PTIO (Fujita et al. 2004). On the other hand, cGMP formed by NO could have an anti-nociceptive effect (Ferreira et al. 1991; Duarte et al. 1992).

NO could also combine with the superoxide radical in macrophages to form peroxynitrite ($ONOO^-$), a highly toxic and reactive intermediate (Radi et al. 1991; Lipton

et al. 1993; De Groote et al. 1995). The latter could affect neuronal proteins, resulting in changes in nociceptive responses. Peroxynitrite and its derivates can oxidize and nitrate lipids (Radi et al. 1991), proteins (Ischiropoulos and al-Mehdi 1995), and DNA (Spencer et al. 1996; Szabo et al. 2007). This could affect the function of signaling molecules in the CNS. It has been shown that nitration of glutamate transporters by peroxynitrite inhibits their ability to transport glutamate from the synaptic cleft to the neurons where it is then metabolized to non-toxic glutamine by glutamine synthase (Kennedy et al. 1974). The latter can also be nitrated by peroxynitrite and lost its enzymatic activity (McBean et al. 1995; Minana et al. 1997; Gorg et al. 2005). These reactions result in the accumulated glutamate in the synaptic cleft, leading to neurotoxicity.

It is postulated that microglia in the nociceptive pathway could be activated in response to neuronal activity (Bessis et al. 2007), leading to peroxynitrite formation and effects on nociceptive transmission. An elevated activation of microglia / macrophage has also been observed in its nucleus, after formalin injection (Yeo et al. 2001). It is, however, unclear whether the increased peroxynitrite could lead to any changes in nociception. The present study was therefore carried out, using intracerebroventricular (ICV) injection of $ONOO^-$ donor or scavenger into the third ventricle of brain, to elucidate the effect of CNS peroxynitrite on nociception, in a facial carrageenan injection induced orofacial pain model (Yeo et al. 2004).

2. Materials and methods

2.1. Chemicals

3-Morpholinosydnonimine, HCl (SIN-1), 5,10,15,20-Tetrakis (4-sulfonatophenyl) porphyrinato iron (III), chloride (FeTPPS) were purchased from Calbiochem, San Diego, USA. They were freshly prepared and dissolved in isotonic saline.

SIN-1 is an active metabolite of molsidomine that decomposes spontaneously in solution in the presence of oxygen, releasing NO and superoxide radical under physiological conditions (Hogg et al. 1992). The NO and superoxide radical combine nearly instantaneously to form $ONOO^-$ and SIN-1 is therefore used as an $ONOO^-$ donor (Lipton et al. 1993). FeTPPS is a ferric porphyrin complex that catalytically isomerizes $ONOO^-$ to nitrate both *in vitro* and *in vivo*. It thus serves as a selective $ONOO^-$ scavenger and decomposition catalyst. Intravenous injection of FeTPPS is effective in reducing edema and nitrate formation 6 hours after paw carrageenan injection in rats (Salvemini et al. 1998b). FeTPPS does not complex with NO and exhibits minimal SOD mimetic activity (Misko et al. 1998; Imam et al. 2000).

2.2. Animals and treatment

Altogether 69 adult male C57BL/6J mice, about 6-8 weeks of age and weighing approximately 20-30 g each were purchased from the Laboratory Animals Centre, Singapore. These mice were randomly divided into 12 groups (4 to 8 mice per group). Nine groups were used to study the effects of $ONOO^-$ donor/scavenger on carrageenan induced facial allodynia. 3 groups were used for effect of $ONOO^-$ donor/scavenger on

normal somatosensation (Table 3.14). All these mice were assessed for behavioral responses to von Frey hair stimulation to the carrageenan injected area in face, at 1 day before treatment, and at 6 hours, 1 day and 3 days after treatment.

Treatment		Amount injected (ICV)	n
With CA	SIN-1	2 μg	4
		50 μg	8
	FeTPPS	0.5 μg	4
		1.5 μg	6
		3.0 μg	5
		7.5 μg	7
	SIN-1 + FeTPPS	50 μg + 7.5 μg	4
	Saline	5 μl	7
	CA injection only		7
Without CA	SIN-1	2 μg	6
	FeTPPS	1.5 μg	7
	Saline		4
Summary		12 groups	69 mice

Table 3.14 Treatment group of C57BL/6J mice. Abbreviation: CA: facial carrageenan injection.

The higher doses of SIN-1 (50 μg) used in ICV injections were chosen based on the estimated proportion of the size of the mouse to rat brain. It was half the highest concentrations used in previous studies on intrathecal or ICV injections in rats (Okada et al. 2002). Since FeTPPS has never been administered centrally into the cerebrospinal fluid, four different doses (0.5 μg, 1.5 μg, 3.0 μg and 7.5 μg), equivalent to 1/30, 1/10,

1/5 and ½ of the lethal dose (15 µg, as determined from the pilot experiment) were tested in this study. The half-life of the drug in the CNS is unknown, but is assumed to be similar to the periphery, hence, behavioral testing was carried out 6 hours after injection (see below).

All measures were taken to minimize pain or discomfort, and experiments were conducted in accordance with international standards on animal welfare and compliant with standards defined by the European Communities Council Directive of 24 November 1986 (86/609/EEC).

2.3. von Frey hair stimulation

The method of behavioral assessment was the same as previously described (details in chapter 3.1, page 49-51). Mice were assessed for behavioral responses to von Frey hair (~ 1 g force) stimulation to the right maxillary area at 1 day before injections, and at 6 hours, 1 day and 3 days after injections. The total number of face wash strokes after 20 probes was noted for each mouse, and the mean and standard deviation of each group were calculated. Possible differences between the means were elucidated using one-way ANOVA with Bonferroni's multiple comparison post hoc test, or Student's t-test (SPSS 12.0 for Windows software). $P < 0.05$ was considered significant.

2.4. ICV injections and facial carrageenan injections

The method of injections was the same as previously described (details in chapter 3.1, page 51). Five microliter of solution was delivered to the right lateral ventricle of mouse via ICV injection. The concentration for each treatment is shown in Table 3.14.

Fifty microliter of carrageenan suspension (40 mg/ml in saline) was injected subcutaneously into the right maxilla area of the mice to study effects of the above chemicals on allodynia.

3. Results

3.1. Effect of facial carrageenan injection on control groups

Mice injected with carrageenan alone, showed significantly increased number of face wash strokes at 6 hours (13.4 ± 2.6), 1 day (18.3 ± 2.4) and 3 days (16.7 ± 3.5) after injections, compared with before injections (3.9 ± 2.3) (Figure 3.16A).

Mice injected with saline plus carrageenan showed significantly increased number of face wash strokes at 6 hours (14.6 ± 7.4) and 3 days (20.9 ± 5.7) after injections, compared with before injections (5.9 ± 2.7) (Figure 3.16B).

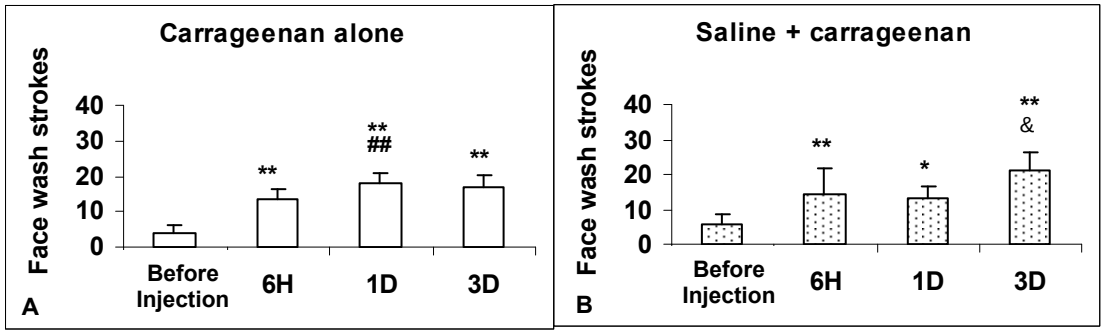

Figure 3.16 Effect of facial carrageenan injection on control groups. Effect of facial carrageenan injection (A), or ICV saline injection plus facial carrageenan injection (B) at different time point is shown (Mean ± SD). Mice in both groups showed significantly increased face wash strokes after facial carrageenan injections. * indicates significant difference compared with before injection (*: $P<0.05$; **: $P<0.01$). # indicates significant difference compared with 6 hours after injection (##: $P<0.01$). & indicates significant difference compared with 1 day after injection (&: $P<0.05$).

3.2. Effect of $ONOO^-$ scavenger on carrageenan injected mice

There were no statistical significant differences in the number of face wash strokes among groups before treatment, i.e., the starting values were matched.

At 6 hours after injections, mice injected with 1.5 μg, 3.0 μg, or 7.5 μg FeTPPS plus carrageenan showed significantly fewer face wash strokes, compared to control mice injected with carrageenan alone or saline plus carrageenan. Those injected with 0.5 μg of FeTPPS showed no significant difference in number of face wash strokes, compared to controls.

At 1 day after injections, mice injected with 1.5 μg FeTPPS plus carrageenan showed significantly fewer face wash strokes, compared to those injected with carrageenan alone (Figure 3.17). The number of face wash strokes at different time point in each group is shown in Table 3.15.

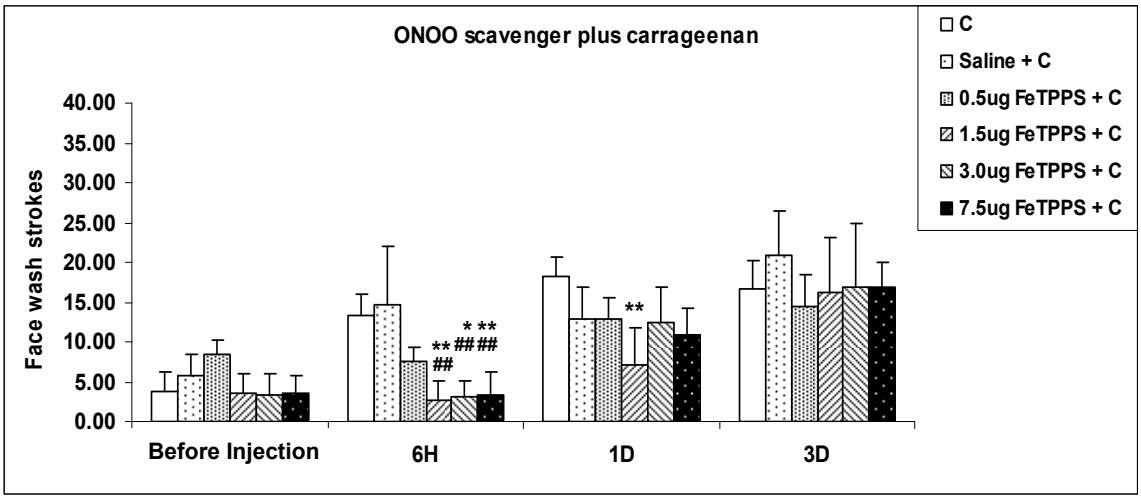

Figure 3.17 Effect of $ONOO^-$ scavenger on carrageenan induced facial allodynia. Mice injected with 1.5 μg, 3.0 μg, or 7.5 μg FeTPPS plus carrageenan showed significantly fewer face wash strokes at 6 hours after injection, compared to control mice. Mice injected with 1.5 μg FeTPPS plus carrageenan showed significantly fewer face strokes compared to those injected with carrageenan alone at 1 day post-injection. Abbreviation: C: carrageenan. * indicates significant difference compared with facial carrageenan injected mice (*: $P<0.05$; **: $P<0.01$). # indicates significant difference compared with ICV saline plus facial carrageenan mice (##: $P<0.01$).

Treatment	n	Before Injection	6H	1D	3D
C	7	3.9 ± 2.3	13.4 ± 2.6$^{\wedge\wedge}$	18.3 ± 2.4$^{\wedge\wedge\#\#}$	16.7 ± 3.4$^{\wedge\wedge}$
Saline + C	7	5.9 ± 2.7	14.6 ± 7.4$^{\wedge}$	13.0 ± 3.8$^{\wedge\wedge}$	20.9 ± 5.7$^{\wedge\wedge\&}$
0.5 μg FeTPPS + C	4	8.5 ± 1.7	7.5 ± 1.9	13.0 ± 2.4$^{\wedge\#\#}$	14.5 ± 4.0$^{\wedge\#}$
1.5 μg FeTPPS + C	6	3.5 ± 2.6	2.7 ± 2.5	7.2 ± 4.5$^{\#\#}$	16.2 ±7.0$^{\wedge\wedge\#\#\&}$
3.0 μg FeTPPS + C	5	3.4 ± 2.7	3.2 ± 1.9	12.4 ± 4.6$^{\wedge\wedge\#}$	16.8 ± 8.0$^{\wedge\wedge\#}$
7.5 μg FeTPPS + C	7	3.6 ± 2.3	3.3 ± 3.0	11.0 ± 3.3$^{\wedge\#\#}$	17.0 ± 2.9$^{\wedge\wedge\#\#\&}$

Table 3.15 Number of face wash strokes after FeTPPs plus carrageenan injection. The Mean ± SD of the number of face wash strokes in each group at different time point is presented in this table. Abbreviation: C: carrageenan. ^ indicates significant difference compared with before injection within the same treatment group (^: $P<0.05$; ^^: $P<0.01$). # indicates significant difference compared with 6 hours after injection within the same treatment group (#: $P<0.05$; ##: $P<0.01$). & indicates significant difference compared with 1 day after injection within the same treatment group (&: $P<0.05$).

3.3. Effect of $ONOO^-$ donor on carrageenan injected mice

No difference in the number of face wash strokes was found between SIN-1 injected mice and control mice at any time point (Figure 3.18). The number of face wash strokes among different time point in each group is shown in Table 3.16.

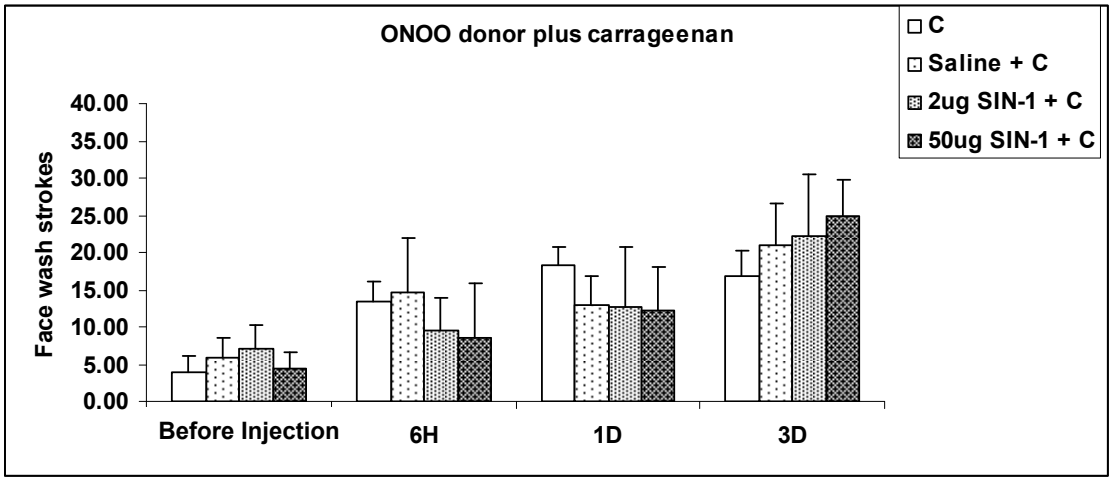

Figure 3.18 Effect of $ONOO^-$ donor on carrageenan induced facial allodynia. No difference in the number of face wash strokes was found between SIN-1 injected mice and control mice. Abbreviation: C: carrageenan.

Treatment	n	Before Injection	6H	1D	3D
C	7	3.9 ± 2.3	13.4 ± 2.6^^	18.3 ± 2.4^^##	16.7 ± 3.4^^
Saline + C	7	5.9 ± 2.7	14.6 ± 7.4^	13.0 ± 3.8^^	20.9 ± 5.7^^&
2 μg SIN-1 + C	4	7.0 ± 3.2	9.5 ± 4.5	12.8 ± 7.9	22.2 ± 8.2^##&&
50 μg SIN-1 + C	8	4.5 ± 2.2	8.5 ± 7.4	12.1 ± 5.8^^	25.0 ± 4.9^^##&&

Table 3.16 Number of face wash strokes after SIN-1 plus carrageenan injection. The Mean ± SD of the number of face wash strokes in each group at different time point is shown. Abbreviation: C: carrageenan. ^ indicates significant difference compared with before injection within the same treatment group (^: $P<0.05$; ^^: $P<0.01$). # indicates significant difference compared with 6 hours after injection within the same treatment group (#: $P<0.05$; ##: $P<0.01$). & indicates significant difference compared with 1 day after injection within the same treatment group (&: $P<0.05$; &&: $P<0.01$).

3.4. Effect of $ONOO^-$ donor or $ONOO^-$ scavenger on mice without carrageenan injection

There were no significant differences in the number of face wash strokes among groups at any time point (Table 3.17).

Treatment	n	Before Injection	6H	1D	3D
Saline	4	6.2 ± 3.8	5.5 ± 3.1	9.2 ± 2.9	12.8 ± 1.0
2 μg SIN-1	6	7.2 ± 4.4	8.0 ± 5.1	10.0 ± 5.9	14.5 ± 6.0
1.5 μg FeTPPS	7	8.0 ± 1.7	7.0 ± 2.6	12.3 ± 6.6	13.6 ± 5.2

Table 3.17 Number of face wash strokes after SIN-1/ FeTPPs injection in mice without facial carrageenan injection. Mean ± SD of the number of face wash strokes in each group at different time point is presented here.

3.5. Effect of the co-injection of the donor and scavenger of $ONOO^-$ on facial carrageenan injected mice

There was no significant difference in the number of face wash strokes among the treated groups at any time point (Table 3.18).

Treatment	n	Before Injection	6H	1D	3D
C	7	3.9 ± 2.3	13.4 ± 2.6$^{\wedge\wedge}$	18.3 ± 2.4$^{\wedge\wedge\#\#}$	16.7 ± 3.4$^{\wedge\wedge}$
Saline + C	7	5.9 ± 2.7	14.6 ± 7.4$^{\wedge}$	13.0 ± 3.8$^{\wedge\wedge}$	20.9 ± 5.7$^{\wedge\wedge\&}$
50 μg SIN-1 + 7.5 μg FeTPPS + C	4	7.8 ± 2.1	11.2 ± 10.0$^{\wedge\wedge}$	14.0 ± 4.1$^{\wedge}$	16.5 ± 3.1$^{\wedge\wedge}$

Table 3.18 Number of face wash strokes after co-injection of SIN-1 and FeTPPs in facial carrageenan injected mice. The Mean ± SD of the number of face wash strokes in each group at different time point is shown in the table. Abbreviations: BI: before injection; C: carrageenan. ^ indicates significant difference compared with before injection within the same treatment group (^: $P<0.05$; ^^: $P<0.01$). # indicates significant difference compared with 6 hours after injection within the same treatment group (##: $P<0.01$). & indicates significant difference compared with 1 day after injection within the same treatment group (&: $P<0.05$)

4. Discussion

The present study aimed to elucidate effects of CNS peroxynitrite on a mouse model of orofacial pain. Facial carrageenan injection was carried out in conjunction with ICV injection of an $ONOO^-$ donor, SIN-1 or an $ONOO^-$ scavenger, FeTPPS, to test possible effects of $ONOO^-$ on nociceptive transmission in facial allodynia. Mice that received ICV injection of three higher doses of FeTPPS (1.5 μg, 3.0 μg, or 7.5 μg), plus facial carrageenan injection showed significantly fewer face wash strokes to von Frey hair stimulation to the carrageenan injected area in right face, compared to control mice that received ICV saline plus facial carrageenan injection, or facial carrageenan injection only. In contrast, mice injected with SIN-1 plus carrageenan, showed no significant difference in the number of face wash strokes, compared to controls. These observations suggest that scavenging of $ONOO^-$ can result in an anti-nociceptive effect on facial allodynia, even though administration of excess $ONOO^-$ did not significantly increase the nociceptive effect. Studies on SIN-1 in the spinal cord have also reported a somewhat ambiguous effect, in that low doses of SIN-1 reduced, whereas higher doses had no effect or increased, mechanical allodynia after chronic ligature of the sciatic nerve in rats (Sousa and Prado 2001; Kina et al. 2005).

The intracerebroventricular injection of SIN-1 or FeTPPS would result in diffusion of these compounds to different parts of the brain via the cerebrospinal fluid circulation, and possible actions at different levels of the pain pathway.

The finding that an $ONOO^-$ scavenger causes a reduction in pain responses is consistent with the results of a recent study which showed that intrathecal injection of a SOD mimetic, M40403 (a compound that converts O_2^- to H_2O_2) reduced hyperalgesia induced by carrageenan injection to the paw in rats (Wang et al. 2004), or intrathecal injection of NMDA (Muscoli et al. 2004). Orally administered FeTPPS was also recently shown to reduce allodynia in a diabetic mouse model (Obrosova et al. 2005).

However, the present results also showed that FeTPPS would not produce the same anti-allodynic effect in mice without facial carrageenan injection, as in facial carrageenan injected mice. This suggests that scavenging of $ONOO^-$ does not affect the basal mechanical sensation in normal mice. The anti-allodynic effect of FeTPPS could be reversed by co-administration of $ONOO^-$ donor SIN-1 in carrageenan injected mice. These data serve as positive controls, and provide indirect evidence that doses of SIN-1 used in the present study were effective in forming $ONOO^-$ in the brain.

In conclusion, the results of the present study suggest that $ONOO^-$ plays a role in nociceptive transmission in orofacial pain. Scavenging of $ONOO^-$ in the CNS can reduce orofacial allodynia caused by facial carrageenan injection.

Chapter IV

CONCLUSIONS

Growing evidences have indicated an important role of CNS lipid mediators and RNS in augmenting the sensitivity of sensory neurons and enhancing pain perception. It is unclear whether these could also play a role in other forms of increased neuronal excitation, such as orofacial allodynia. The main aim of the present study was to evaluate possible effects of CNS ceramide and $ONOO^-$ in nociception in a mouse orofacial allodynia model induced by facial carrageenan injection.

The orofacial pain model of the present study was induced by subcutaneous injection of λ-carrageenan to the right maxilla area of mice, which has been widely used in orofacial pain studies (Yeo et al. 2004; Vahidy et al. 2006). Carrageenan injection produces inflammation, hypersensitivity, and some apparent spontaneous pain with a peak effect at 3–5 hours after injection to the rat hind paw (Tonussi and Ferreira 1992), and persists for at least one week. Directed facial grooming, i.e. uninterrupted series of face wash strokes directed to the stimulated maxillary area, was used as the indicator of unilateral facial pain in freely moving mice in the present study (Vos et al. 1998). To ensure that the experimental methods are consistent and comparable, all chemicals that are involved in the nociception signaling processes have been administered to mice via ICV injection since some of them cannot cross the blood brain barrier.

A flow chart showing the experimental design and main findings of the present study was plotted in order to have an overall view of the central theme of the present investigation (Fig 4.1). The detailed conclusions will then be elaborated in the following paragraphs.

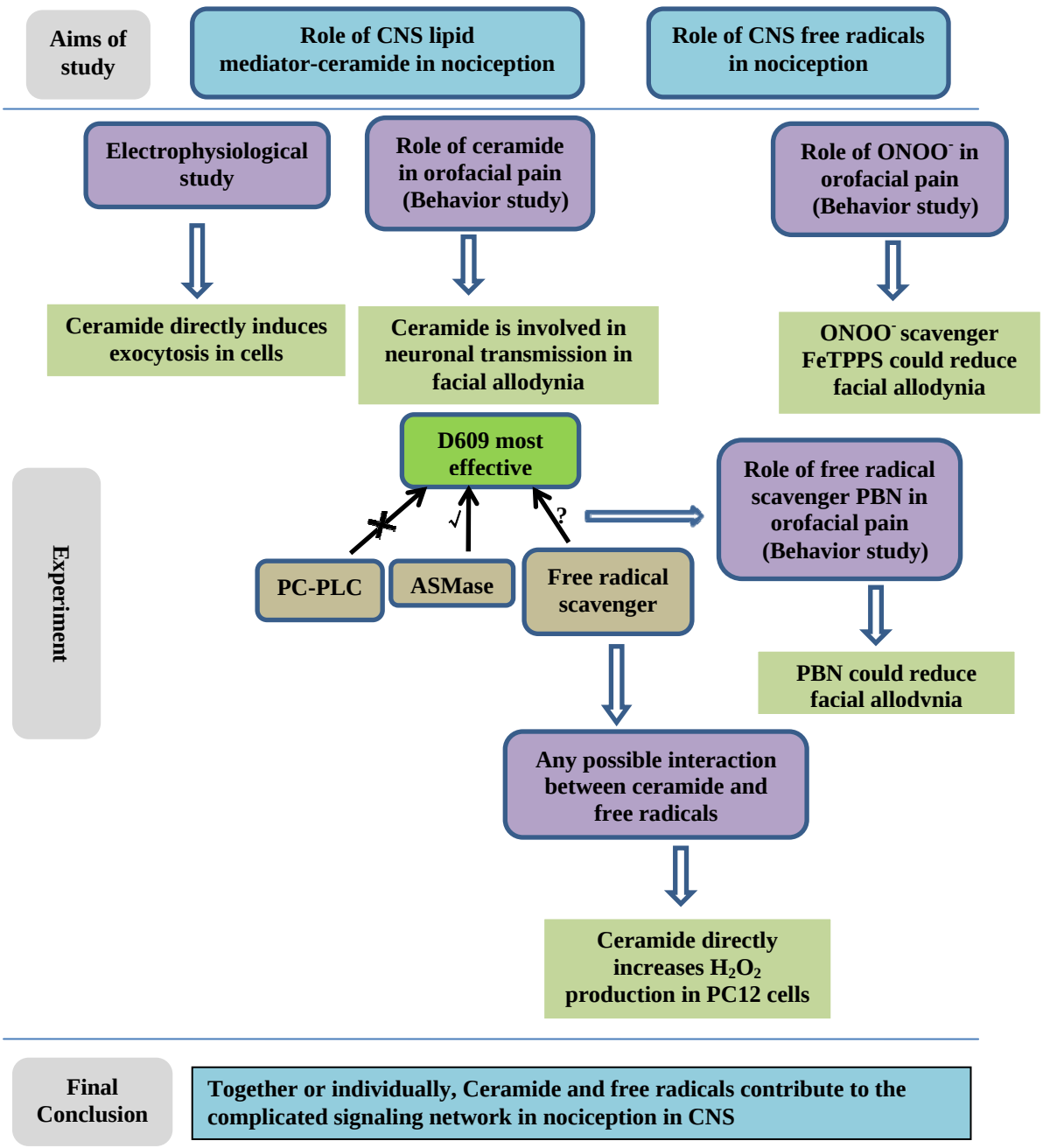

Fig 4.1 Flow chart of the experimental design and main findings of the present study.

It is postulated that ceramide might be an important signaling molecule in nociception in the CNS. ICV injection of inhibitors to enzymes involved in ceramide synthesis was used to investigate possible role of ceramide in orofacial allodynia. Mice received ICV injection of inhibitors to ASMase, NSMase, or SPT showed a significantly reduced face wash strokes compared with vehicle injected mice, at 3 days after injection, indicating that the reduction of ceramide synthesis has an anti-allodynic effect in carrageenan induced facial allodynia. Among these inhibitors, ASMase inhibitor D609 showed the most significant anti-allodynic effect. These results indicate that ceramide plays an important role in nociception in orofacial pain.

The ASMase inhibitor D609 used in the behavior study could also inhibit PC-PLC. However, enzyme activity assay showed no change in PC-PLC activity in brain after facial carrageenan / ICV D609 injection, suggesting that D609's anti-allodynic effect is not via the action of PC-PLC. An increased ASMase activity was observed in the left primary somatosensory cortex at 3 days after facial carrageenan injection. D609 injected mice had reduced ASMase activity in all parts of brain examined (i.e., left and right brain stem, thalamus, and primary somatosensory cortex). These results indicated that D609's anti-allodynic effect might be due to ASMase and reduced production of ceramide. It is postulated that ceramide is an upstream cascade signaling molecule with the ability to amplify downstream signaling molecules/ second messengers at very low concentration. Another possibility might be that D609 modulates allodynia transmission due to its antioxidant properties. Recent studies have shown that D609 is widely used as a

free radical scavenger since it has a very similar structure with glutathione (Zhou et al. 2001; Lauderback et al. 2003; Sultana et al. 2004; Perluigi et al. 2006).

The role of free radicals in nociception was confirmed by the observation that ICV injection of PBN, a free radical spin trap, significantly reduced allodynia in facial carrageenan injected mice. A possible interaction between ceramide and free radicals was also investigated. It was found that incubation of PC12 cells with C18 ceramide led to a significant increase of hydrogen peroxide production. This effect could be inhibited by co-incubation with the L-type calcium channel inhibitor (nifedipine), free radical scavenger (D609 or PBN), or mitochondria permeability transition pore blockers (bongkrekic acid or cyclosporine A). It has been observed that ceramide and its metabolites modulate PLA_2 and COX activities, which regulate the production of free radicals and ROS levels (Farooqui et al. 2007) and may contribute to pathogenesis of neuropathic and inflammatory pain in rats. The complicated interplay and cross-talk between glycerophospholipid- and sphingolipid-derived lipid mediators along with oxidative stress is shown in a hypothetical diagram (Figure 4.2).

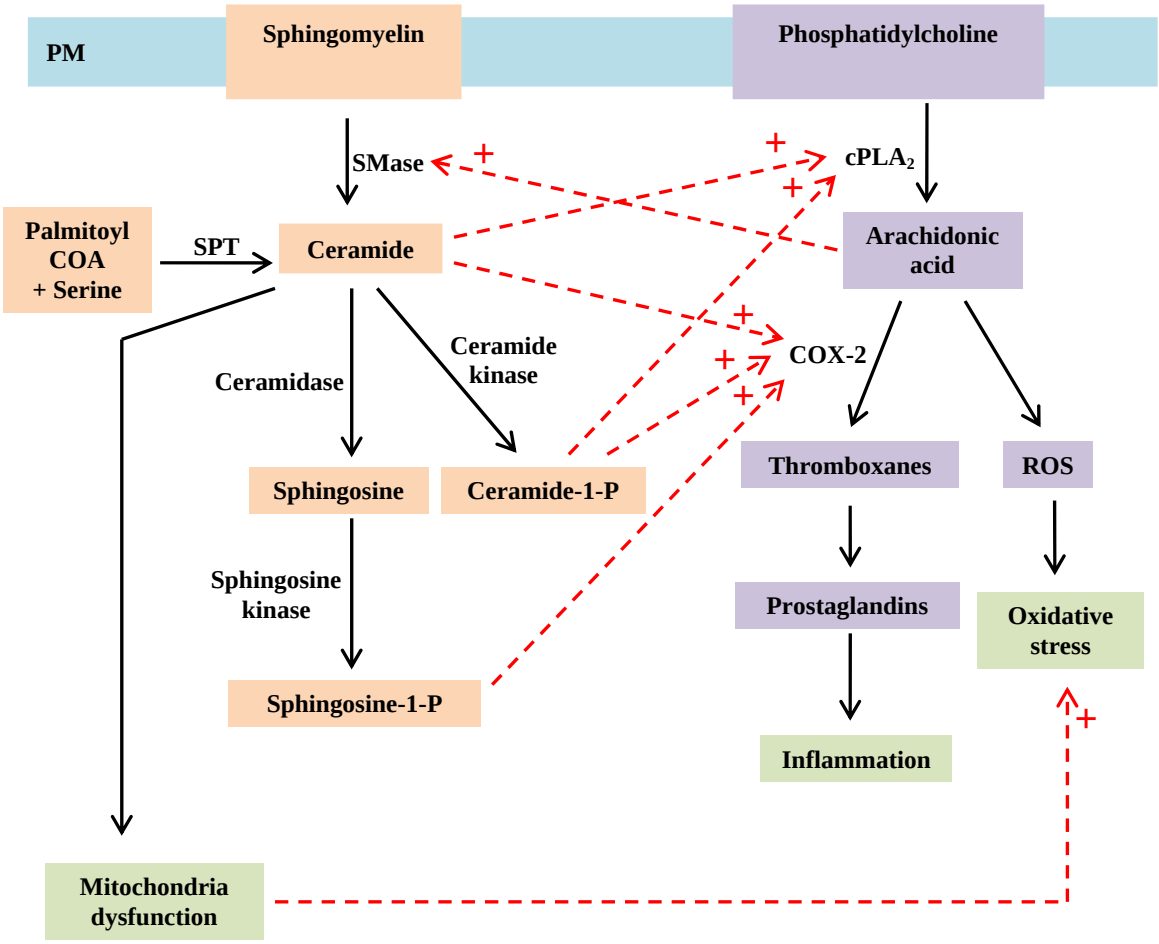

Figure 4.2 Hypothetical diagram showing interplay and cross-talk between glycerophospholipid- and sphingolipid-derived lipid mediators along with oxidative stress (modified from Farooqui et al. 2007 and Farooqui et al. 2010). Abbreviations: PM: plasma membrane; SMase: sphingomyelinase; $cPLA_2$: cytosolic phospholipase A_2; SPT: serine palmitoyltransferase; COX-2: cyclooxygenase-2; Ceramide-1-P: ceramide 1- phosphate; Sphingosine-1-P: sphingosine 1- phosphate. ROS: reactive oxygen species. Plus sign indicates stimulation.

Electrophysiological studies (patch clamp) showed that ceramide has the ability to increase cell membrane capacitance in PC12 cells and hippocampal neurons, indicating exocytosis. Total internal reflection fluorescence microscopy experiments found that, after treating PC12 cells with C18 ceramide, subplasmalemmal vesicles fuse with the cell

membrane, and the number of vesicles quickly decreased. Both experiments found that C18 ceramide is the one that increases exocytosis most significantly. C18 ceramide induced exocytosis was also found to be dependent on extracellular Ca^{2+} and the integrity of the lipid raft. These results showed that ceramide might affect nociception in the CNS by inducing exocytosis of neurons directly.

It is postulated that the role of ceramide in exocytosis is largely determined by its unique structure. The generation or release of ceramide leads to changes of the structure, fluidity, and/or permeability of the cell membrane, which in turn leads to conformational changes of membrane-associated enzymes or receptors, ion influx, and activation of specific local signaling cascade. The concept that ceramide induces ion influx was also confirmed by the present experiments. It was observed that C18 ceramide caused an increase of intracellular calcium concentration shortly after treatment. This effect was also found to be dependent on the L-type calcium channel.

Last, there is also evidence that other forms of free radicals such as RNS mediate pain perception. RNS species such as peroxynitrite ($ONOO^-$) and its derivates can oxidize lipids, nitrate proteins and cause damages to DNA, leading to changes in the function of signaling molecules. Animal behavior studies showed that ICV injection of $ONOO^-$ scavenger FeTPPS significantly reduced the number of face wash strokes in carrageenan injected mice, at 3 days after injection. The effect of FeTPPS can be diminished by co-ICV injection with an $ONOO^-$ donor SIN-1. These results show that scavenging of $ONOO^-$ in the CNS can reduce orofacial allodynia caused by facial carrageenan injection.

Some promising results have been introduced and developed in the present thesis. This investigation might provide a pharmacological basis validating the approach of developing new drugs in the management of pain. For example, it is already known that murine models of opioid tolerance are important for investigating the underlying mechanisms of this phenomenon. Inhibition of ceramide biosynthesis is found to be able to attenuate oxidative stress, which might be crucial for elucidating mechanisms of opioid tolerance in its management of chronic pain (Ndengele et al. 2009). Fabry's disease, where sphingolipids deposit in blood vessels and nerves, can manifest as severe acroparasthesia and pain. Current therapy consists of expensive enzyme replacement which limits its wide application to patients (Pierre-Louis et al. 2009). The work here may be of relevance to future research in its treatment of pain aspects.

However, there are some issues to be explored and solved for understanding the role of lipid mediators and free radicals in pain perception in the future. First, it was found that decreasing ceramide production in the CNS has an anti-allodynic effect, however, whether increased ceramide production in the CNS could increase allodynia need to be investigated. Second, ceramide might affect nociception via increasing exocytosis of neuron directly, or causing conformational changes of the cell membrane, or as an up-stream signaling molecule in nociception processes. However, it is also possible that the allodynic effect of ceramide is due to its effect in regulating oxidative stress. The possible role of ceramide in inducing oxidative stress in the CNS can be examined in the future. Third, scavenging of $ONOO^-$ in the CNS can reduce orofacial allodynia in carrageenan injected mice. Is this because of the excess $ONOO^-$ produced in

the CNS after facial carrageenan injection? Thus a study on whether facial carrageenan injection could induce oxidative stress in the CNS should be carried out in the future.

Chapter V

REFERENCES

Alemany R, Kleuser B, Ruwisch L, Danneberg K, Lass H, Hashemi R, Spiegel S, Jakobs KH, Meyer zu Heringdorf D (2001) Depolarisation induces rapid and transient formation of intracellular sphingosine-1-phosphate. FEBS Lett 509: 239-244

Allen JA, Halverson-Tamboli RA, Rasenick MM (2007) Lipid raft microdomains and neurotransmitter signalling. Nat Rev Neurosci 8: 128-140

Allersma MW, Wang L, Axelrod D, Holz RW (2004) Visualization of regulated exocytosis with a granule-membrane probe using total internal reflection microscopy. Mol Biol Cell 15: 4658-4668

Arinci A, Ademoglu E, Aslan A, Mutlu-Turkoglu U, Karabulut AB, Karan A (2005) Molecular correlates of temporomandibular joint disease. Oral Surg Oral Med Oral Pathol Oral Radiol Endod 99: 666-670

Bajjalieh SM, Martin TF, Floor E (1989) Synaptic vesicle ceramide kinase. A calcium-stimulated lipid kinase that co-purifies with brain synaptic vesicles. J Biol Chem 264: 14354-14360

Balafanova Z, Bolli R, Zhang J, Zheng Y, Pass JM, Bhatnagar A, Tang XL, Wang O, Cardwell E, Ping P (2002) Nitric oxide (NO) induces nitration of protein kinase Cepsilon (PKCepsilon), facilitating PKCepsilon translocation via enhanced PKCepsilon -RACK2 interactions: a novel mechanism of no-triggered activation of PKCepsilon. J Biol Chem 277: 15021-15027

Barsacchi R, Perrotta C, Sestili P, Cantoni O, Moncada S, Clementi E (2002) Cyclic GMP-dependent inhibition of acid sphingomyelinase by nitric oxide: an early step in protection against apoptosis. Cell Death Differ 9: 1248-1255

Beaver DL, Moses HL, Ganote CE (1965) Electron Microscopy of the Trigeminal Ganglion. Ii. Autopsy Study of Human Ganglia. Arch Pathol 79: 557-570

Beckman JS, Beckman TW, Chen J, Marshall PA, Freeman BA (1990) Apparent hydroxyl radical production by peroxynitrite: implications for endothelial injury from nitric oxide and superoxide. Proc Natl Acad Sci U S A 87: 1620-1624

Beckman JS, Koppenol WH (1996) Nitric oxide, superoxide, and peroxynitrite: the good, the bad, and ugly. Am J Physiol 271: C1424-1437

Bessis A, Bechade C, Bernard D, Roumier A (2007) Microglial control of neuronal death and synaptic properties. Glia 55: 233-238

Bielefeldt K, Ozaki N, Gebhart GF (2003) Role of nerve growth factor in modulation of gastric afferent neurons in the rat. Am J Physiol Gastrointest Liver Physiol 284: G499-507

Block ML, Zecca L, Hong JS (2007) Microglia-mediated neurotoxicity: uncovering the molecular mechanisms. Nat Rev Neurosci 8: 57-69

Bock J, Szabo I, Gamper N, Adams C, Gulbins E (2003) Ceramide inhibits the potassium channel Kv1.3 by the formation of membrane platforms. Biochem Biophys Res Commun 305: 890-897

Bradford MM (1976) A rapid and sensitive method for the quantitation of microgram quantities of protein utilizing the principle of protein-dye binding. Anal Biochem 72: 248-254

Brann AB, Scott R, Neuberger Y, Abulafia D, Boldin S, Fainzilber M, Futerman AH (1999) Ceramide signaling downstream of the p75 neurotrophin receptor mediates

the effects of nerve growth factor on outgrowth of cultured hippocampal neurons. J Neurosci 19: 8199-8206

Brearley CA, Hanke DE (1995) Evidence for substrate-cycling of 3-, 3,4-, 4-, and 4,5-phosphorylated phosphatidylinositols in plants. Biochem J 311 (Pt 3): 1001-1007

Bredt DS, Snyder SH (1992) Nitric oxide, a novel neuronal messenger. Neuron 8: 3-11

Brodal P (2004) The Central Nervous System. Oxford University Press

Broton JG, Hu JW, Sessle BJ (1988) Effects of temporomandibular joint stimulation on nociceptive and nonnociceptive neurons of the cat's trigeminal subnucleus caudalis (medullary dorsal horn). J Neurophysiol 59: 1575-1589

Brown GC, Bal-Price A (2003) Inflammatory neurodegeneration mediated by nitric oxide, glutamate, and mitochondria. Mol Neurobiol 27: 325-355

Bulotta S, Barsacchi R, Rotiroti D, Borgese N, Clementi E (2001) Activation of the endothelial nitric-oxide synthase by tumor necrosis factor-alpha. A novel feedback mechanism regulating cell death. J Biol Chem 276: 6529-6536

Burns D, Hill L, Essandoh M, Jarzembowski TM, Schuler HG, Janicki PK (2006) Effect of valdecoxib pretreatment on pain and secondary hyperalgesia: a randomized controlled trial in healthy volunteers [ISRCTN05282752, NCT00260325]. BMC Anesthesiol 6: 3

Capra NF, Dessem D (1992) Central connections of trigeminal primary afferent neurons: topographical and functional considerations. Crit Rev Oral Biol Med 4: 1-52

Cardenas LM, Cardenas CG, Scroggs RS (2001) 5HT increases excitability of nociceptor-like rat dorsal root ganglion neurons via cAMP-coupled TTX-resistant Na(+) channels. J Neurophysiol 86: 241-248

Carlton SM, Zhou S, Coggeshall RE (1996) Localization and activation of substance P receptors in unmyelinated axons of rat glabrous skin. Brain Res 734: 103-108

Cassina AM, Hodara R, Souza JM, Thomson L, Castro L, Ischiropoulos H, Freeman BA, Radi R (2000) Cytochrome c nitration by peroxynitrite. J Biol Chem 275: 21409-21415

Cervero F, Laird JM (1996) Mechanisms of touch-evoked pain (allodynia): a new model. Pain 68: 13-23

Chahl LA, Iggo A (1977) The effects of bradykinin and prostaglandin E1 on rat cutaneous afferent nerve activity. Br J Pharmacol 59: 343-347

Chamberlain LH, Burgoyne RD, Gould GW (2001) SNARE proteins are highly enriched in lipid rafts in PC12 cells: implications for the spatial control of exocytosis. Proc Natl Acad Sci U S A 98: 5619-5624

Chang C, Shyu BC (2001) A fMRI study of brain activations during non-noxious and noxious electrical stimulation of the sciatic nerve of rats. Brain Res 897: 71-81

Chen G, Griffin M, Poyer JL, McCay PB (1990) HPLC procedure for the pharmacokinetic study of the spin-trapping agent, alpha-phenyl-N-tert-butyl nitrone (PBN). Free Radic Biol Med 9: 93-98

Chen P, Gillis KD (2000) The noise of membrane capacitance measurements in the whole-cell recording configuration. Biophys J 79: 2162-2170

Cheng HT, Suzuki M, Hegarty DM, Xu Q, Weyerbacher AR, South SM, Ohata M, Inturrisi CE (2008) Inflammatory pain-induced signaling events following a conditional deletion of the N-methyl-D-aspartate receptor in spinal cord dorsal horn. Neuroscience 155: 948-958

Chik CL, Li B, Karpinski E, Ho AK (2001) Ceramide inhibits the outward potassium current in rat pinealocytes. J Neurochem 79: 339-348

Cho HJ, Park EH, Bae MA, Kim JK (1996) Expression of mRNAs for preprotachykinin and nerve growth factor receptors in the dorsal root-ganglion following peripheral inflammation. Brain Res 716: 197-201

Chuang HH, Prescott ED, Kong H, Shields S, Jordt SE, Basbaum AI, Chao MV, Julius D (2001) Bradykinin and nerve growth factor release the capsaicin receptor from PtdIns(4,5)P2-mediated inhibition. Nature 411: 957-962

Coderre TJ (1992) Contribution of protein kinase C to central sensitization and persistent pain following tissue injury. Neurosci Lett 140: 181-184

Colombaioni L, Garcia-Gil M (2004) Sphingolipid metabolites in neural signalling and function. Brain Res Brain Res Rev 46: 328-355

Cremesti AE, Goni FM, Kolesnick R (2002) Role of sphingomyelinase and ceramide in modulating rafts: do biophysical properties determine biologic outcome? FEBS Lett 531: 47-53

Cridland RA, Henry JL (1986) Comparison of the effects of substance P, neurokinin A, physalaemin and eledoisin in facilitating a nociceptive reflex in the rat. Brain Res 381: 93-99

Cui M, Nicol GD (1995) Cyclic AMP mediates the prostaglandin E2-induced potentiation of bradykinin excitation in rat sensory neurons. Neuroscience 66: 459-466

Cutler RG, Pedersen WA, Camandola S, Rothstein JD, Mattson MP (2002) Evidence that accumulation of ceramides and cholesterol esters mediates oxidative stress-induced death of motor neurons in amyotrophic lateral sclerosis. Ann Neurol 52: 448-457

Cuvillier O (2002) Sphingosine in apoptosis signaling. Biochim Biophys Acta 1585: 153-162

Davies KJ (1999) The broad spectrum of responses to oxidants in proliferating cells: a new paradigm for oxidative stress. IUBMB Life 48: 41-47

Davies SL, Loescher AR, Clayton NM, Bountra C, Robinson PP, Boissonade FM (2004) nNOS expression following inferior alveolar nerve injury in the ferret. Brain Res 1027: 11-17

Dawkins JL, Hulme DJ, Brahmbhatt SB, Auer-Grumbach M, Nicholson GA (2001) Mutations in SPTLC1, encoding serine palmitoyltransferase, long chain base subunit-1, cause hereditary sensory neuropathy type I. Nat Genet 27: 309-312

De A, Krueger JM, Simasko SM (2003) Tumor necrosis factor alpha increases cytosolic calcium responses to AMPA and KCl in primary cultures of rat hippocampal neurons. Brain Res 981: 133-142

De Groote MA, Granger D, Xu Y, Campbell G, Prince R, Fang FC (1995) Genetic and redox determinants of nitric oxide cytotoxicity in a Salmonella typhimurium model. Proc Natl Acad Sci U S A 92: 6399-6403

De Nadai C, Sestili P, Cantoni O, Lievremont JP, Sciorati C, Barsacchi R, Moncada S, Meldolesi J, Clementi E (2000) Nitric oxide inhibits tumor necrosis factor-alpha-induced apoptosis by reducing the generation of ceramide. Proc Natl Acad Sci U S A 97: 5480-5485

Del Fiacco M, Quartu M (1994) Somatostatin, galanin and peptide histidine isoleucine in the newborn and adult human trigeminal ganglion and spinal nucleus: immunohistochemistry, neuronal morphometry and colocalization with substance P. J Chem Neuroanat 7: 171-184

DeLeo JA (2006) Basic science of pain. J Bone Joint Surg Am 88 Suppl 2: 58-62

Di A, Krupa B, Bindokas VP, Chen Y, Brown ME, Palfrey HC, Naren AP, Kirk KL, Nelson DJ (2002) Quantal release of free radicals during exocytosis of phagosomes. Nat Cell Biol 4: 279-285

Dietrich C, Bagatolli LA, Volovyk ZN, Thompson NL, Levi M, Jacobson K, Gratton E (2001) Lipid rafts reconstituted in model membranes. Biophys J 80: 1417-1428

Dix TA, Hess KM, Medina MA, Sullivan RW, Tilly SL, Webb TL (1996) Mechanism of site-selective DNA nicking by the hydrodioxyl (perhydroxyl) radical. Biochemistry 35: 4578-4583

Dobrowsky RT, Werner MH, Castellino AM, Chao MV, Hannun YA (1994) Activation of the sphingomyelin cycle through the low-affinity neurotrophin receptor. Science 265: 1596-1599

Dohrn CS, Mullett MA, Price RH, Beitz AJ (1994) Distribution of nitric oxide synthase-immunoreactive interneurons in the spinal trigeminal nucleus. J Comp Neurol 346: 449-460

Donnerer J, Schuligoi R, Stein C, Amann R (1993) Upregulation, release and axonal transport of substance P and calcitonin gene-related peptide in adjuvant inflammation and regulatory function of nerve growth factor. Regul Pept 46: 150-154

Droy-Lefaix MT, Drouet Y, Geraud G, Hosford D, Braquet P (1991) Superoxide dismutase (SOD) and the PAF-antagonist (BN 52021) reduce small intestinal damage induced by ischemia-reperfusion. Free Radic Res Commun 12-13 Pt 2: 725-735

Duarte ID, dos Santos IR, Lorenzetti BB, Ferreira SH (1992) Analgesia by direct antagonism of nociceptor sensitization involves the arginine-nitric oxide-cGMP pathway. Eur J Pharmacol 217: 225-227

Ebadi M, Sharma SK (2003) Peroxynitrite and mitochondrial dysfunction in the pathogenesis of Parkinson's disease. Antioxid Redox Signal 5: 319-335

Eiserich JP, Hristova M, Cross CE, Jones AD, Freeman BA, Halliwell B, van der Vliet A (1998) Formation of nitric oxide-derived inflammatory oxidants by myeloperoxidase in neutrophils. Nature 391: 393-397

Emmelot P, Van Hoeven RP (1975) Phospholipid unsaturation and plasma membrane organization. Chem Phys Lipids 14: 236-246

Endemann DH, Schiffrin EL (2004) Nitric oxide, oxidative excess, and vascular complications of diabetes mellitus. Curr Hypertens Rep 6: 85-89

Falcone S, Perrotta C, De Palma C, Pisconti A, Sciorati C, Capobianco A, Rovere-Querini P, Manfredi AA, Clementi E (2004) Activation of acid sphingomyelinase and its inhibition by the nitric oxide/cyclic guanosine

3',5'-monophosphate pathway: key events in Escherichia coli-elicited apoptosis of dendritic cells. J Immunol 173: 4452-4463

Farooqui AA, Horrocks LA, Farooqui T (2007) Interactions between neural membrane glycerophospholipid and sphingolipid mediators: a recipe for neural cell survival or suicide. J Neurosci Res 85: 1834-1850

Farooqui AA, Ong WY, Farooqui T (2010) Lipid mediators in the nucleus: Their potential contribution to Alzheimer's disease. Biochim Biophys Acta 1801: 906-916

Fensome AC, Rodrigues-Lima F, Josephs M, Paterson HF, Katan M (2000) A neutral magnesium-dependent sphingomyelinase isoform associated with intracellular membranes and reversibly inhibited by reactive oxygen species. J Biol Chem 275: 1128-1136

Ferreira SH, Duarte ID, Lorenzetti BB (1991) The molecular mechanism of action of peripheral morphine analgesia: stimulation of the cGMP system via nitric oxide release. Eur J Pharmacol 201: 121-122

Floyd RA (1999) Neuroinflammatory processes are important in neurodegenerative diseases: an hypothesis to explain the increased formation of reactive oxygen and nitrogen species as major factors involved in neurodegenerative disease development. Free Radic Biol Med 26: 1346-1355

Forman HJ, Torres M (2002) Reactive oxygen species and cell signaling: respiratory burst in macrophage signaling. Am J Respir Crit Care Med 166: S4-8

Fridovich I (1999) Fundamental aspects of reactive oxygen species, or what's the matter with oxygen? Ann N Y Acad Sci 893: 13-18

Friedrichson T, Kurzchalia TV (1998) Microdomains of GPI-anchored proteins in living cells revealed by crosslinking. Nature 394: 802-805

Fries DM, Paxinou E, Themistocleous M, Swanberg E, Griendling KK, Salvemini D, Slot JW, Heijnen HF, Hazen SL, Ischiropoulos H (2003) Expression of inducible nitric-oxide synthase and intracellular protein tyrosine nitration in vascular smooth muscle cells: role of reactive oxygen species. J Biol Chem 278: 22901-22907

Fujita T, Kamisaki Y, Yonehara N (2004) Nitric oxide-induced increase of excitatory amino acid levels in the trigeminal nucleus caudalis of the rat with tactile hypersensitivity evoked by the loose-ligation of the inferior alveolar nerves. J Neurochem 91: 558-567

Furukawa K, Mattson MP (1998) The transcription factor NF-kappaB mediates increases in calcium currents and decreases in NMDA- and AMPA/kainate-induced currents induced by tumor necrosis factor-alpha in hippocampal neurons. J Neurochem 70: 1876-1886

Galeotti N, Stefano GB, Guarna M, Bianchi E, Ghelardini C (2006) Signaling pathway of morphine induced acute thermal hyperalgesia in mice. Pain 123: 294-305

Garcia-Ruiz C, Colell A, Mari M, Morales A, Fernandez-Checa JC (1997) Direct effect of ceramide on the mitochondrial electron transport chain leads to generation of reactive oxygen species. Role of mitochondrial glutathione. J Biol Chem 272: 11369-11377

Ghosh TK, Bian J, Gill DL (1990) Intracellular calcium release mediated by sphingosine derivatives generated in cells. Science 248: 1653-1656

Gibbs TT, Russek SJ, Farb DH (2006) Sulfated steroids as endogenous neuromodulators. Pharmacol Biochem Behav 84: 555-567

Gil C, Cubi R, Blasi J, Aguilera J (2006) Synaptic proteins associate with a sub-set of lipid rafts when isolated from nerve endings at physiological temperature. Biochem Biophys Res Commun 348: 1334-1342

Gius D, Botero A, Shah S, Curry HA (1999) Intracellular oxidation/reduction status in the regulation of transcription factors NF-kappaB and AP-1. Toxicol Lett 106: 93-106

Gokin AP, Fareed MU, Pan HL, Hans G, Strichartz GR, Davar G (2001) Local injection of endothelin-1 produces pain-like behavior and excitation of nociceptors in rats. J Neurosci 21: 5358-5366

Gold MS, Reichling DB, Shuster MJ, Levine JD (1996) Hyperalgesic agents increase a tetrodotoxin-resistant Na+ current in nociceptors. Proc Natl Acad Sci U S A 93: 1108-1112

Gorg B, Wettstein M, Metzger S, Schliess F, Haussinger D (2005) Lipopolysaccharide-induced tyrosine nitration and inactivation of hepatic glutamine synthetase in the rat. Hepatology 41: 1065-1073

Grassme H, Cremesti A, Kolesnick R, Gulbins E (2003) Ceramide-mediated clustering is required for CD95-DISC formation. Oncogene 22: 5457-5470

Grassme H, Gulbins E, Brenner B, Ferlinz K, Sandhoff K, Harzer K, Lang F, Meyer TF (1997) Acidic sphingomyelinase mediates entry of N. gonorrhoeae into nonphagocytic cells. Cell 91: 605-615

Grassme H, Jekle A, Riehle A, Schwarz H, Berger J, Sandhoff K, Kolesnick R, Gulbins E (2001) CD95 signaling via ceramide-rich membrane rafts. J Biol Chem 276: 20589-20596

Grisham MB, Jourd'Heuil D, Wink DA (1999) Nitric oxide. I. Physiological chemistry of nitric oxide and its metabolites:implications in inflammation. Am J Physiol 276: G315-321

Grushka M, Epstein JB, Gorsky M (2003) Burning mouth syndrome and other oral sensory disorders: a unifying hypothesis. Pain Res Manag 8: 133-135

Guan XL, He X, Ong WY, Yeo WK, Shui G, Wenk MR (2006) Non-targeted profiling of lipids during kainate-induced neuronal injury. FASEB J 20: 1152-1161

Gulbins E, Li PL (2006) Physiological and pathophysiological aspects of ceramide. Am J Physiol Regul Integr Comp Physiol 290: R11-26

Haddad JJ, Land SC (2002) Redox/ROS regulation of lipopolysaccharide-induced mitogen-activated protein kinase (MAPK) activation and MAPK-mediated TNF-alpha biosynthesis. Br J Pharmacol 135: 520-536

Haglind E, Xia G, Rylander R (1994) Effects of antioxidants and PAF receptor antagonist in intestinal shock in the rat. Circ Shock 42: 83-91

Hannun YA, Luberto C (2000) Ceramide in the eukaryotic stress response. Trends Cell Biol 10: 73-80

Hannun YA, Obeid LM (2002) The Ceramide-centric universe of lipid-mediated cell regulation: stress encounters of the lipid kind. J Biol Chem 277: 25847-25850

He X, Guan XL, Ong WY, Farooqui AA, Wenk MR (2007) Expression, activity, and role of serine palmitoyltransferase in the rat hippocampus after kainate injury. J Neurosci Res 85: 423-432

Helme RD, Fletcher JL (1983) Substance P in the trigeminal system at postmortem: evidence for a role in pain pathways in man. Clin Exp Neurol 19: 37-44

Heneka MT, Feinstein DL (2001) Expression and function of inducible nitric oxide synthase in neurons. J Neuroimmunol 114: 8-18

Hering H, Lin CC, Sheng M (2003) Lipid rafts in the maintenance of synapses, dendritic spines, and surface AMPA receptor stability. J Neurosci 23: 3262-3271

Herr I, Martin-Villalba A, Kurz E, Roncaioli P, Schenkel J, Cifone MG, Debatin KM (1999) FK506 prevents stroke-induced generation of ceramide and apoptosis signaling. Brain Res 826: 210-219

Hinrichsen C (2008) A synopsis of regional anatomy. Hackensack, NJ: World Scientific Pub

Hogg N, Darley-Usmar VM, Wilson MT, Moncada S (1992) Production of hydroxyl radicals from the simultaneous generation of superoxide and nitric oxide. Biochem J 281 (Pt 2): 419-424

Holleran WM, Williams ML, Gao WN, Elias PM (1990) Serine-palmitoyl transferase activity in cultured human keratinocytes. J Lipid Res 31: 1655-1661

Holopainen JM, Subramanian M, Kinnunen PK (1998) Sphingomyelinase induces lipid microdomain formation in a fluid phosphatidylcholine/sphingomyelin membrane. Biochemistry 37: 17562-17570

Huwiler A, Pfeilschifter J, van den Bosch H (1999) Nitric oxide donors induce stress signaling via ceramide formation in rat renal mesangial cells. J Biol Chem 274: 7190-7195

Iadarola MJ, Douglass J, Civelli O, Naranjo JR (1988) Differential activation of spinal cord dynorphin and enkephalin neurons during hyperalgesia: evidence using cDNA hybridization. Brain Res 455: 205-212

Imam SZ, Islam F, Itzhak Y, Slikker W, Jr., Ali SF (2000) Prevention of dopaminergic neurotoxicity by targeting nitric oxide and peroxynitrite: implications for the prevention of methamphetamine-induced neurotoxic damage. Ann N Y Acad Sci 914: 157-171

Ischiropoulos H, al-Mehdi AB (1995) Peroxynitrite-mediated oxidative protein modifications. FEBS Lett 364: 279-282

Iwai K, Kondo T, Watanabe M, Yabu T, Kitano T, Taguchi Y, Umehara H, Takahashi A, Uchiyama T, Okazaki T (2003) Ceramide increases oxidative damage due to inhibition of catalase by caspase-3-dependent proteolysis in HL-60 cell apoptosis. J Biol Chem 278: 9813-9822

Jacquin MF, Golden J, Panneton WM (1988) Structure and function of barrel 'precursor' cells in trigeminal nucleus principalis. Brain Res 471: 309-314

Ji RR, Samad TA, Jin SX, Schmoll R, Woolf CJ (2002) p38 MAPK activation by NGF in primary sensory neurons after inflammation increases TRPV1 levels and maintains heat hyperalgesia. Neuron 36: 57-68

Joseph EK, Bogen O, Alessandri-Haber N, Levine JD (2007) PLC-beta 3 signals upstream of PKC epsilon in acute and chronic inflammatory hyperalgesia. Pain 132: 67-73

Joseph EK, Levine JD (2004) Caspase signalling in neuropathic and inflammatory pain in the rat. Eur J Neurosci 20: 2896-2902

Joseph EK, Levine JD (2006) Mitochondrial electron transport in models of neuropathic and inflammatory pain. Pain 121: 105-114

Julius D, Basbaum AI (2001) Molecular mechanisms of nociception. Nature 413: 203-210

Kahle PJ, Shooter EM, Johnson RM, Verity AN (1998) Phosphatidylcholine-specific phospholipase inhibitor D609 differentially affects MAP kinases and immediate-early genes in PC12 cells. Cell Signal 10: 321-330

Kayser V, Guilbaud G (1987) Local and remote modifications of nociceptive sensitivity during carrageenin-induced inflammation in the rat. Pain 28: 99-107

Kennedy AJ, Voaden MJ, Marshall J (1974) Glutamate metabolism in the frog retina. Nature 252: 50-52

Kim HK, Kim JH, Gao X, Zhou JL, Lee I, Chung K, Chung JM (2006) Analgesic effect of vitamin E is mediated by reducing central sensitization in neuropathic pain. Pain 122: 53-62

Kim HK, Park SK, Zhou JL, Taglialatela G, Chung K, Coggeshall RE, Chung JM (2004) Reactive oxygen species (ROS) play an important role in a rat model of neuropathic pain. Pain 111: 116-124

Kina VA, Villarreal CF, Prado WA (2005) The effects of intraspinal L-NOARG or SIN-1 on the control by descending pathways of incisional pain in rats. Life Sci 76: 1939-1951

Kitto KF, Haley JE, Wilcox GL (1992) Involvement of nitric oxide in spinally mediated hyperalgesia in the mouse. Neurosci Lett 148: 1-5

Klede M, Handwerker HO, Schmelz M (2003) Central origin of secondary mechanical hyperalgesia. J Neurophysiol 90: 353-359

Klyachko VA, Jackson MB (2002) Capacitance steps and fusion pores of small and large-dense-core vesicles in nerve terminals. Nature 418: 89-92

Ko M, Zou K, Minagawa H, Yu W, Gong JS, Yanagisawa K, Michikawa M (2005) Cholesterol-mediated neurite outgrowth is differently regulated between cortical and hippocampal neurons. J Biol Chem 280: 42759-42765

Koishi R, Yoshimura C, Kohama T, Serizawa N (2002) Leustroducsin B activates nuclear factor-kappaB via the acidic sphingomyelinase pathway in human bone marrow-derived stromal cell line KM-102. J Interferon Cytokine Res 22: 343-350

Kolesnick R (2002) The therapeutic potential of modulating the ceramide/sphingomyelin pathway. J Clin Invest 110: 3-8

Kolesnick R, Hannun YA (1999) Ceramide and apoptosis. Trends Biochem Sci 24: 224-225; author reply 227

Kolesnick RN, Goni FM, Alonso A (2000) Compartmentalization of ceramide signaling: physical foundations and biological effects. J Cell Physiol 184: 285-300

Kolesnick RN, Kronke M (1998) Regulation of ceramide production and apoptosis. Annu Rev Physiol 60: 643-665

Kolzer M, Arenz C, Ferlinz K, Werth N, Schulze H, Klingenstein R, Sandhoff K (2003) Phosphatidylinositol-3,5-Bisphosphate is a potent and selective inhibitor of acid sphingomyelinase. Biol Chem 384: 1293-1298

Korkotian E, Schwarz A, Pelled D, Schwarzmann G, Segal M, Futerman AH (1999) Elevation of intracellular glucosylceramide levels results in an increase in endoplasmic reticulum density and in functional calcium stores in cultured neurons. J Biol Chem 274: 21673-21678

Lauderback CM, Drake J, Zhou D, Hackett JM, Castegna A, Kanski J, Tsoras M, Varadarajan S, Butterfield DA (2003) Derivatives of xanthic acid are novel antioxidants: application to synaptosomes. Free Radic Res 37: 355-365

Le Bars D, Gozariu M, Cadden SW (2001) [Acute pain measurement in animals. Part 1]. Ann Fr Anesth Reanim 20: 347-365

Lee I, Kim HK, Kim JH, Chung K, Chung JM (2007) The role of reactive oxygen species in capsaicin-induced mechanical hyperalgesia and in the activities of dorsal horn neurons. Pain 133: 9-17

Lenaz G (2001) The mitochondrial production of reactive oxygen species: mechanisms and implications in human pathology. IUBMB Life 52: 159-164

Leong S, Liu H, Yeo J (2000) Nitric oxide synthase and glutamate receptor immunoreactivity in the rat spinal trigeminal neurons expressing Fos protein after formalin injection. Brain Res 855: 107-115

Levine JD, Dardick SJ, Basbaum AI, Scipio E (1985) Reflex neurogenic inflammation. I. Contribution of the peripheral nervous system to spatially remote inflammatory responses that follow injury. J Neurosci 5: 1380-1386

Levy D, Zhang XC, Jakubowski M, Burstein R (2008) Sensitization of meningeal nociceptors: inhibition by naproxen. Eur J Neurosci 27: 917-922

Lipton SA, Choi YB, Pan ZH, Lei SZ, Chen HS, Sucher NJ, Loscalzo J, Singel DJ, Stamler JS (1993) A redox-based mechanism for the neuroprotective and neurodestructive effects of nitric oxide and related nitroso-compounds. Nature 364: 626-632

Lloyd-Evans E, Pelled D, Riebeling C, Bodennec J, de-Morgan A, Waller H, Schiffmann R, Futerman AH (2003a) Glucosylceramide and glucosylsphingosine modulate calcium mobilization from brain microsomes via different mechanisms. J Biol Chem 278: 23594-23599

Lloyd-Evans E, Pelled D, Riebeling C, Futerman AH (2003b) Lyso-glycosphingolipids mobilize calcium from brain microsomes via multiple mechanisms. Biochem J 375: 561-565

Loeser JD, Treede RD (2008) The Kyoto protocol of IASP Basic Pain Terminology. Pain 137: 473-477

Luberto C, Hannun YA (1998) Sphingomyelin synthase, a potential regulator of intracellular levels of ceramide and diacylglycerol during SV40 transformation.

Does sphingomyelin synthase account for the putative phosphatidylcholine-specific phospholipase C? J Biol Chem 273: 14550-14559

Luberto C, Hassler DF, Signorelli P, Okamoto Y, Sawai H, Boros E, Hazen-Martin DJ, Obeid LM, Hannun YA, Smith GK (2002) Inhibition of tumor necrosis factor-induced cell death in MCF7 by a novel inhibitor of neutral sphingomyelinase. J Biol Chem 277: 41128-41139

Macmillan-Crow LA, Cruthirds DL (2001) Invited review: manganese superoxide dismutase in disease. Free Radic Res 34: 325-336

Magnusson KR, Clements JR, Larson AA, Madl JE, Beitz AJ (1987) Localization of glutamate in trigeminothalamic projection neurons: a combined retrograde transport-immunohistochemical study. Somatosens Res 4: 177-190

Malan TP, Jr., Porreca F (2005) Lipid mediators regulating pain sensitivity. Prostaglandins Other Lipid Mediat 77: 123-130

Malan TP, Ossipov MH, Gardell LR, Ibrahim M, Bian D, Lai J, Porreca F (2000) Extraterritorial neuropathic pain correlates with multisegmental elevation of spinal dynorphin in nerve-injured rats. Pain 86: 185-194

Malisan F, Testi R (2002) GD3 ganglioside and apoptosis. Biochim Biophys Acta 1585: 179-187

Malmberg AB, Yaksh TL (1993) Spinal nitric oxide synthesis inhibition blocks NMDA-induced thermal hyperalgesia and produces antinociception in the formalin test in rats. Pain 54: 291-300

Mansat-de Mas V, Bezombes C, Quillet-Mary A, Bettaieb A, D'Orgeix A D, Laurent G, Jaffrezou JP (1999) Implication of radical oxygen species in ceramide generation,

c-Jun N-terminal kinase activation and apoptosis induced by daunorubicin. Mol Pharmacol 56: 867-874

Matata BM, Galinanes M (2002) Peroxynitrite is an essential component of cytokines production mechanism in human monocytes through modulation of nuclear factor-kappa B DNA binding activity. J Biol Chem 277: 2330-2335

McBean GJ, Doorty KB, Tipton KF, Kollegger H (1995) Alteration in the glial cell metabolism of glutamate by kainate and N-methyl-D-aspartate. Toxicon 33: 569-576

McCord JM, Omar BA (1993) Sources of free radicals. Toxicol Ind Health 9: 23-37

McInnis J, Wang C, Anastasio N, Hultman M, Ye Y, Salvemini D, Johnson KM (2002) The role of superoxide and nuclear factor-kappaB signaling in N-methyl-D-aspartate-induced necrosis and apoptosis. J Pharmacol Exp Ther 301: 478-487

Meller ST, Dykstra C, Gebhart GF (1996) Acute thermal hyperalgesia in the rat is produced by activation of N-methyl-D-aspartate receptors and protein kinase C and production of nitric oxide. Neuroscience 71: 327-335

Meller ST, Pechman PS, Gebhart GF, Maves TJ (1992) Nitric oxide mediates the thermal hyperalgesia produced in a model of neuropathic pain in the rat. Neuroscience 50: 7-10

Melzack R, Wall PD (1965) Pain mechanisms: a new theory. Science 150: 971-979

Merrill AH, Jr., Jones DD (1990) An update of the enzymology and regulation of sphingomyelin metabolism. Biochim Biophys Acta 1044: 1-12

Merrill AH, Jr., Nixon DW, Williams RD (1985) Activities of serine palmitoyltransferase (3-ketosphinganine synthase) in microsomes from different rat tissues. J Lipid Res 26: 617-622

Merrill AH, Jr., Wang E (1986) Biosynthesis of long-chain (sphingoid) bases from serine by LM cells. Evidence for introduction of the 4-trans-double bond after de novo biosynthesis of N-acylsphinganine(s). J Biol Chem 261: 3764-3769

Meyer zu Heringdorf D, Niederdraing N, Neumann E, Frode R, Lass H, Van Koppen CJ, Jakobs KH (1998) Discrimination between plasma membrane and intracellular target sites of sphingosylphosphorylcholine. Eur J Pharmacol 354: 113-122

Minana MD, Kosenko E, Marcaida G, Hermenegildo C, Montoliu C, Grisolia S, Felipo V (1997) Modulation of glutamine synthesis in cultured astrocytes by nitric oxide. Cell Mol Neurobiol 17: 433-445

Mishra OP, Delivoria-Papadopoulos M (1999) Cellular mechanisms of hypoxic injury in the developing brain. Brain Res Bull 48: 233-238

Misko TP, Highkin MK, Veenhuizen AW, Manning PT, Stern MK, Currie MG, Salvemini D (1998) Characterization of the cytoprotective action of peroxynitrite decomposition catalysts. J Biol Chem 273: 15646-15653

Miyake Y, Kozutsumi Y, Nakamura S, Fujita T, Kawasaki T (1995) Serine palmitoyltransferase is the primary target of a sphingosine-like immunosuppressant, ISP-1/myriocin. Biochem Biophys Res Commun 211: 396-403

Mizutani Y, Tamiya-Koizumi K, Nakamura N, Kobayashi M, Hirabayashi Y, Yoshida S (2001) Nuclear localization of neutral sphingomyelinase 1: biochemical and immunocytochemical analyses. J Cell Sci 114: 3727-3736

Mogil JS, Wilson SG, Bon K, Lee SE, Chung K, Raber P, Pieper JO, Hain HS, Belknap JK, Hubert L, Elmer GI, Chung JM, Devor M (1999) Heritability of nociception I: responses of 11 inbred mouse strains on 12 measures of nociception. Pain 80: 67-82

Moncada S (1997) Nitric oxide in the vasculature: physiology and pathophysiology. Ann N Y Acad Sci 811: 60-67; discussion 67-69

Montes LR, Ruiz-Arguello MB, Goni FM, Alonso A (2002) Membrane restructuring via ceramide results in enhanced solute efflux. J Biol Chem 277: 11788-11794

Mungrue IN, Bredt DS, Stewart DJ, Husain M (2003) From molecules to mammals: what's NOS got to do with it? Acta Physiol Scand 179: 123-135

Murphy S (2000) Production of nitric oxide by glial cells: regulation and potential roles in the CNS. Glia 29: 1-13

Muscoli C, Cuzzocrea S, Riley DP, Zweier JL, Thiemermann C, Wang ZQ, Salvemini D (2003) On the selectivity of superoxide dismutase mimetics and its importance in pharmacological studies. Br J Pharmacol 140: 445-460

Muscoli C, Mollace V, Wheatley J, Masini E, Ndengele M, Wang ZQ, Salvemini D (2004) Superoxide-mediated nitration of spinal manganese superoxide dismutase: a novel pathway in N-methyl-D-aspartate-mediated hyperalgesia. Pain 111: 96-103

Naik AK, Tandan SK, Dudhgaonkar SP, Jadhav SH, Kataria M, Prakash VR, Kumar D (2006) Role of oxidative stress in pathophysiology of peripheral neuropathy and modulation by N-acetyl-L-cysteine in rats. Eur J Pain 10: 573-579

Ndengele MM, Muscoli C, Wang ZQ, Doyle TM, Matuschak GM, Salvemini D (2005) Superoxide potentiates NF-kappaB activation and modulates endotoxin-induced cytokine production in alveolar macrophages. Shock 23: 186-193

Ndengele MM, Cuzzocrea S, Masini E, Vinci MC, Esposito E, Muscoli C, Petrusca DN, Mollace V, Mazzon E, Li D, Petrache I, Matuschak GM, Salvemini D (2009) Spinal ceramide modulates the development of morphine antinociceptive tolerance via peroxynitrite-mediated nitroxidative stress and neuroimmune activation. J Pharmacol Exp Ther 329: 64-75

Neuberger Y, Shogomori H, Levy Z, Fainzilber M, Futerman AH (2000) A lyso-platelet activating factor phospholipase C, originally suggested to be a neutral-sphingomyelinase, is located in the endoplasmic reticulum. FEBS Lett 469: 44-46

Newton AC (1997) Regulation of protein kinase C. Curr Opin Cell Biol 9: 161-167

Ng CH, Ong WY (2001) Increased expression of gamma-aminobutyric acid transporters GAT-1 and GAT-3 in the spinal trigeminal nucleus after facial carrageenan injections. Pain 92: 29-40

Nishiyama T, Ogawa M (2005) Intrathecal edaravone, a free radical scavenger, is effective on inflammatory-induced pain in rats. Acta Anaesthesiol Scand 49: 147-151

Nurminen TA, Holopainen JM, Zhao H, Kinnunen PK (2002) Observation of topical catalysis by sphingomyelinase coupled to microspheres. J Am Chem Soc 124: 12129-12134

Obrosova IG, Mabley JG, Zsengeller Z, Charniauskaya T, Abatan OI, Groves JT, Szabo C (2005) Role for nitrosative stress in diabetic neuropathy: evidence from studies with a peroxynitrite decomposition catalyst. FASEB J 19: 401-403

Ohtori S, Takahashi K, Moriya H, Myers RR (2004) TNF-alpha and TNF-alpha receptor type 1 upregulation in glia and neurons after peripheral nerve injury: studies in murine DRG and spinal cord. Spine 29: 1082-1088

Oka Y, Ibuki T, Matsumura K, Namba M, Yamazaki Y, Poole S, Tanaka Y, Kobayashi S (2007) Interleukin-6 is a candidate molecule that transmits inflammatory information to the CNS. Neuroscience 145: 530-538

Okada S, Murakami Y, Yokotani K (2002) Centrally applied nitric oxide donor elevates plasma corticosterone by activation of the hypothalamic noradrenergic neurons in rats. Brain Res 939: 26-33

Okamoto K, Imbe H, Morikawa Y, Itoh M, Sekimoto M, Nemoto K, Senba E (2002) 5-HT2A receptor subtype in the peripheral branch of sensory fibers is involved in the potentiation of inflammatory pain in rats. Pain 99: 133-143

Ossipov MH, Lai J, Malan TP, Jr., Porreca F (2000) Spinal and supraspinal mechanisms of neuropathic pain. Ann N Y Acad Sci 909: 12-24

Pal S, Sombati S, Limbrick DD, Jr., DeLorenzo RJ (1999) In vitro status epilepticus causes sustained elevation of intracellular calcium levels in hippocampal neurons. Brain Res 851: 20-31

Parada CA, Yeh JJ, Joseph EK, Levine JD (2003) Tumor necrosis factor receptor type-1 in sensory neurons contributes to induction of chronic enhancement of inflammatory hyperalgesia in rat. Eur J Neurosci 17: 1847-1852

Park ES, Gao X, Chung JM, Chung K (2006) Levels of mitochondrial reactive oxygen species increase in rat neuropathic spinal dorsal horn neurons. Neurosci Lett 391: 108-111

Park KA, Vasko MR (2005) Lipid mediators of sensitivity in sensory neurons. Trends Pharmacol Sci 26: 571-577

Perluigi M, Joshi G, Sultana R, Calabrese V, De Marco C, Coccia R, Butterfield DA (2006) In vivo protection by the xanthate tricyclodecan-9-yl-xanthogenate against amyloid beta-peptide (1-42)-induced oxidative stress. Neuroscience 138: 1161-1170

Pierre-Louis B, Kumar A, Frishman WH (2009) Fabry disease: cardiac manifestations and therapeutic options. Cardiol Rev 17: 31-35

Perry DK, Carton J, Shah AK, Meredith F, Uhlinger DJ, Hannun YA (2000) Serine palmitoyltransferase regulates de novo ceramide generation during etoposide-induced apoptosis. J Biol Chem 275: 9078-9084

Petralia RS, Yokotani N, Wenthold RJ (1994) Light and electron microscope distribution of the NMDA receptor subunit NMDAR1 in the rat nervous system using a selective anti-peptide antibody. J Neurosci 14: 667-696

Petruska JC, Mendell LM (2004) The many functions of nerve growth factor: multiple actions on nociceptors. Neurosci Lett 361: 168-171

Pettus BJ, Bielawski J, Porcelli AM, Reames DL, Johnson KR, Morrow J, Chalfant CE, Obeid LM, Hannun YA (2003) The sphingosine kinase 1/sphingosine-1-phosphate pathway mediates COX-2 induction and PGE2 production in response to TNF-alpha. FASEB J 17: 1411-1421

Pettus BJ, Chalfant CE, Hannun YA (2002) Ceramide in apoptosis: an overview and current perspectives. Biochim Biophys Acta 1585: 114-125

Pollock J, McFarlane SM, Connell MC, Zehavi U, Vandenabeele P, MacEwan DJ, Scott RH (2002) TNF-alpha receptors simultaneously activate Ca2+ mobilisation and stress kinases in cultured sensory neurones. Neuropharmacology 42: 93-106

Pralle A, Keller P, Florin EL, Simons K, Horber JK (2000) Sphingolipid-cholesterol rafts diffuse as small entities in the plasma membrane of mammalian cells. J Cell Biol 148: 997-1008

Prasad VV, Nithipatikom K, Harder DR (2008) Ceramide elevates 12-hydroxyeicosatetraenoic acid levels and upregulates 12-lipoxygenase in rat primary hippocampal cell cultures containing predominantly astrocytes. Neurochem Int 53: 220-229

Qiu H, Edmunds T, Baker-Malcolm J, Karey KP, Estes S, Schwarz C, Hughes H, Van Patten SM (2003) Activation of human acid sphingomyelinase through modification or deletion of C-terminal cysteine. J Biol Chem 278: 32744-32752

Quartu M, Del Fiacco M (1994) Enkephalins occur and colocalize with substance P in human trigeminal ganglion neurones. Neuroreport 5: 465-468

Quartu M, Diaz G, Lai ML, Del Fiacco M (1992) Immunohistochemical localization of putative peptide neurotransmitters in the human trigeminal sensory system. Ann N Y Acad Sci 657: 469-472

Raboisson P, Dallel R, Clavelou P, Sessle BJ, Woda A (1995) Effects of subcutaneous formalin on the activity of trigeminal brain stem nociceptive neurones in the rat. J Neurophysiol 73: 496-505

Radi R (2004) Nitric oxide, oxidants, and protein tyrosine nitration. Proc Natl Acad Sci U S A 101: 4003-4008

Radi R, Beckman JS, Bush KM, Freeman BA (1991) Peroxynitrite oxidation of sulfhydryls. The cytotoxic potential of superoxide and nitric oxide. J Biol Chem 266: 4244-4250

Radi R, Cassina A, Hodara R, Quijano C, Castro L (2002) Peroxynitrite reactions and formation in mitochondria. Free Radic Biol Med 33: 1451-1464

Roccamo AM, Pediconi MF, Aztiria E, Zanello L, Wolstenholme A, Barrantes FJ (1999) Cells defective in sphingolipids biosynthesis express low amounts of muscle nicotinic acetylcholine receptor. Eur J Neurosci 11: 1615-1623

Roche AK, Cook M, Wilcox GL, Kajander KC (1996) A nitric oxide synthesis inhibitor (L-NAME) reduces licking behavior and Fos-labeling in the spinal cord of rats during formalin-induced inflammation. Pain 66: 331-341

Rodrigues-Lima F, Fensome AC, Josephs M, Evans J, Veldman RJ, Katan M (2000) Structural requirements for catalysis and membrane targeting of mammalian enzymes with neutral sphingomyelinase and lysophospholipid phospholipase C

activities. Analysis by chemical modification and site-directed mutagenesis. J Biol Chem 275: 28316-28325

Rossetto O, Morbiato L, Caccin P, Rigoni M, Montecucco C (2006) Presynaptic enzymatic neurotoxins. J Neurochem 97: 1534-1545

Ruiz-Arguello MB, Goni FM, Alonso A (1998) Vesicle membrane fusion induced by the concerted activities of sphingomyelinase and phospholipase C. J Biol Chem 273: 22977-22982

Salaun C, Gould GW, Chamberlain LH (2005) The SNARE proteins SNAP-25 and SNAP-23 display different affinities for lipid rafts in PC12 cells. Regulation by distinct cysteine-rich domains. J Biol Chem 280: 1236-1240

Salvemini D, Doyle TM, Cuzzocrea S (2006) Superoxide, peroxynitrite and oxidative/nitrative stress in inflammation. Biochem Soc Trans 34: 965-970

Salvemini D, Jensen MP, Riley DP, Misko TP (1998a) Therapeutic manipulations of peroxynitrite. Drug News Perspect 11: 204-214

Salvemini D, Mazzon E, Dugo L, Riley DP, Serraino I, Caputi AP, Cuzzocrea S (2001) Pharmacological manipulation of the inflammatory cascade by the superoxide dismutase mimetic, M40403. Br J Pharmacol 132: 815-827

Salvemini D, Riley DP, Lennon PJ, Wang ZQ, Currie MG, Macarthur H, Misko TP (1999) Protective effects of a superoxide dismutase mimetic and peroxynitrite decomposition catalysts in endotoxin-induced intestinal damage. Br J Pharmacol 127: 685-692

Salvemini D, Wang ZQ, Stern MK, Currie MG, Misko TP (1998b) Peroxynitrite decomposition catalysts: therapeutics for peroxynitrite-mediated pathology. Proc Natl Acad Sci U S A 95: 2659-2663

Sang CN, Gracely RH, Max MB, Bennett GJ (1996) Capsaicin-evoked mechanical allodynia and hyperalgesia cross nerve territories. Evidence for a central mechanism. Anesthesiology 85: 491-496

Schaible HG, Schmidt RF, Willis WD (1987) Enhancement of the responses of ascending tract cells in the cat spinal cord by acute inflammation of the knee joint. Exp Brain Res 66: 489-499

Schuman EM, Madison DV (1994) Nitric oxide and synaptic function. Annu Rev Neurosci 17: 153-183

Schwartz ES, Lee I, Chung K, Chung JM (2008) Oxidative stress in the spinal cord is an important contributor in capsaicin-induced mechanical secondary hyperalgesia in mice. Pain 138: 514-524

Sessle BJ (2000) Acute and chronic craniofacial pain: brainstem mechanisms of nociceptive transmission and neuroplasticity, and their clinical correlates. Crit Rev Oral Biol Med 11: 57-91

Shvartsman DE, Gutman O, Tietz A, Henis YI (2006) Cyclodextrins but not compactin inhibit the lateral diffusion of membrane proteins independent of cholesterol. Traffic 7: 917-926

Simarro M, Calvo J, Vila JM, Places L, Padilla O, Alberola-Ila J, Vives J, Lozano F (1999) Signaling through CD5 involves acidic sphingomyelinase, protein kinase

C-zeta, mitogen-activated protein kinase kinase, and c-Jun NH2-terminal kinase. J Immunol 162: 5149-5155

Simone DA, Baumann TK, LaMotte RH (1989) Dose-dependent pain and mechanical hyperalgesia in humans after intradermal injection of capsaicin. Pain 38: 99-107

Simons K, Ikonen E (1997) Functional rafts in cell membranes. Nature 387: 569-572

Siskind LJ, Colombini M (2000) The lipids C2- and C16-ceramide form large stable channels. Implications for apoptosis. J Biol Chem 275: 38640-38644

Smart EJ, Graf GA, McNiven MA, Sessa WC, Engelman JA, Scherer PE, Okamoto T, Lisanti MP (1999) Caveolins, liquid-ordered domains, and signal transduction. Mol Cell Biol 19: 7289-7304

Snell RS (2006) Clinical neuroanatomy. Philadelphia: Lippincott Williams & Wilkins. 6th ed

Sousa AM, Prado WA (2001) The dual effect of a nitric oxide donor in nociception. Brain Res 897: 9-19

Spencer JP, Wong J, Jenner A, Aruoma OI, Cross CE, Halliwell B (1996) Base modification and strand breakage in isolated calf thymus DNA and in DNA from human skin epidermal keratinocytes exposed to peroxynitrite or 3-morpholinosydnonimine. Chem Res Toxicol 9: 1152-1158

Spiegel S, Cuvillier O, Edsall LC, Kohama T, Menzeleev R, Olah Z, Olivera A, Pirianov G, Thomas DM, Tu Z, Van Brocklyn JR, Wang F (1998) Sphingosine-1-phosphate in cell growth and cell death. Ann N Y Acad Sci 845: 11-18

Stephenson D, Rash K, Smalstig B, Roberts E, Johnstone E, Sharp J, Panetta J, Little S, Kramer R, Clemens J (1999) Cytosolic phospholipase A2 is induced in reactive glia following different forms of neurodegeneration. Glia 27: 110-128

Sternbach RA (1975) Psychophysiology of pain. Int J Psychiatry Med 6: 63-73

Strle K, Broussard SR, McCusker RH, Shen WH, Johnson RW, Freund GG, Dantzer R, Kelley KW (2004) Proinflammatory cytokine impairment of insulin-like growth factor I-induced protein synthesis in skeletal muscle myoblasts requires ceramide. Endocrinology 145: 4592-4602

Suenaga S, Abeyama K, Hamasaki A, Mimura T, Noikura T (2001) Temporomandibular disorders: relationship between joint pain and effusion and nitric oxide concentration in the joint fluid. Dentomaxillofac Radiol 30: 214-218

Sultana R, Newman S, Mohmmad-Abdul H, Keller JN, Butterfield DA (2004) Protective effect of the xanthate, D609, on Alzheimer's amyloid beta-peptide (1-42)-induced oxidative stress in primary neuronal cells. Free Radic Res 38: 449-458

Sun JY, Wu LG (2001) Fast kinetics of exocytosis revealed by simultaneous measurements of presynaptic capacitance and postsynaptic currents at a central synapse. Neuron 30: 171-182

Sun JY, Wu XS, Wu LG (2002) Single and multiple vesicle fusion induce different rates of endocytosis at a central synapse. Nature 417: 555-559

Sun ZX, Zhou QH, Sui SF (2005) Cholesterol depletion inhibits the degradation of amyloid beta-peptide in rat pheochromocytoma (PC12) cells. Neurosci Lett 391: 71-75

Szabo C, Ischiropoulos H, Radi R (2007) Peroxynitrite: biochemistry, pathophysiology and development of therapeutics. Nat Rev Drug Discov 6: 662-680

Takeda Y, Tashima M, Takahashi A, Uchiyama T, Okazaki T (1999) Ceramide generation in nitric oxide-induced apoptosis. Activation of magnesium-dependent neutral sphingomyelinase via caspase-3. J Biol Chem 274: 10654-10660

Takemura M, Nagase Y, Yoshida A, Yasuda K, Kitamura S, Shigenaga Y, Matano S (1993) The central projections of the monkey tooth pulp afferent neurons. Somatosens Mot Res 10: 217-227

Tal M (1996) A novel antioxidant alleviates heat hyperalgesia in rats with an experimental painful peripheral neuropathy. Neuroreport 7: 1382-1384

Tallaksen-Greene SJ, Young AB, Penney JB, Beitz AJ (1992) Excitatory amino acid binding sites in the trigeminal principal sensory and spinal trigeminal nuclei of the rat. Neurosci Lett 141: 79-83

Testai FD, Landek MA, Goswami R, Ahmed M, Dawson G (2004) Acid sphingomyelinase and inhibition by phosphate ion: role of inhibition by phosphatidyl-myo-inositol 3,4,5-triphosphate in oligodendrocyte cell signaling. J Neurochem 89: 636-644

Titievsky A, Titievskaya I, Pasternack M, Kaila K, Tornquist K (1998) Sphingosine inhibits voltage-operated calcium channels in GH4C1 cells. J Biol Chem 273: 242-247

Tonussi CR, Ferreira SH (1992) Rat knee-joint carrageenin incapacitation test: an objective screen for central and peripheral analgesics. Pain 48: 421-427

Tornquist K, Blom T, Shariatmadari R, Pasternack M (2004) Ceramide 1-phosphate enhances calcium entry through voltage-operated calcium channels by a protein kinase C-dependent mechanism in GH4C1 rat pituitary cells. Biochem J 380: 661-668

Treede RD, Meyer RA, Raja SN, Campbell JN (1992) Peripheral and central mechanisms of cutaneous hyperalgesia. Prog Neurobiol 38: 397-421

Tschaikowsky K, Meisner M, Schonhuber F, Rugheimer E (1994) Induction of nitric oxide synthase activity in phagocytic cells inhibited by tricyclodecan-9-yl-xanthogenate (D609). Br J Pharmacol 113: 664-668

Turko IV, Murad F (2003) Quantitative protein profiling in heart mitochondria from diabetic rats. J Biol Chem 278: 35844-35849

Turp JC (2005) [Atypical odontalgia]. Schweiz Monatsschr Zahnmed 115: 1006-1011

Usta J, El Bawab S, Roddy P, Szulc ZM, Yusuf, Hannun A, Bielawska A (2001) Structural requirements of ceramide and sphingosine based inhibitors of mitochondrial ceramidase. Biochemistry 40: 9657-9668

Usunoff KG, Marani E, Schoen JH (1997) The trigeminal system in man. Adv Anat Embryol Cell Biol 136: I-X, 1-126

Vadseth C, Souza JM, Thomson L, Seagraves A, Nagaswami C, Scheiner T, Torbet J, Vilaire G, Bennett JS, Murciano JC, Muzykantov V, Penn MS, Hazen SL, Weisel JW, Ischiropoulos H (2004) Pro-thrombotic state induced by post-translational modification of fibrinogen by reactive nitrogen species. J Biol Chem 279: 8820-8826

Vahidy WH, Ong WY, Farooqui AA, Yeo JF (2006) Effects of intracerebroventricular injections of free fatty acids, lysophospholipids, or platelet activating factor in a mouse model of orofacial pain. Exp Brain Res 174: 781-785

van Meer G, Lisman Q (2002) Sphingolipid transport: rafts and translocators. J Biol Chem 277: 25855-25858

Varma R, Mayor S (1998) GPI-anchored proteins are organized in submicron domains at the cell surface. Nature 394: 798-801

Viani P, Giussani P, Ferraretto A, Signorile A, Riboni L, Tettamanti G (2001) Nitric oxide production in living neurons is modulated by sphingosine: a fluorescence microscopy study. FEBS Lett 506: 185-190

Viani P, Giussani P, Riboni L, Bassi R, Tettamanti G (1999) Sphingosine inhibits nitric oxide synthase from cerebellar granule cells differentiated in vitro. FEBS Lett 454: 321-324

Viggiano A, Monda M, Viggiano D, Viggiano E, Chiefari M, Aurilio C, De Luca B (2005) Trigeminal pain transmission requires reactive oxygen species production. Brain Res 1050: 72-78

Vivekananda J, Smith D, King RJ (2001) Sphingomyelin metabolites inhibit sphingomyelin synthase and CTP:phosphocholine cytidylyltransferase. Am J Physiol Lung Cell Mol Physiol 281: L98-L107

Vos BP, Hans G, Adriaensen H (1998) Behavioral assessment of facial pain in rats: face grooming patterns after painful and non-painful sensory disturbances in the territory of the rat's infraorbital nerve. Pain 76: 173-178

Vos BP, Strassman AM, Maciewicz RJ (1994) Behavioral evidence of trigeminal neuropathic pain following chronic constriction injury to the rat's infraorbital nerve. J Neurosci 14: 2708-2723

Wajima Z, Hua XY, Yaksh TL (2000) Inhibition of spinal protein kinase C blocks substance P-mediated hyperalgesia. Brain Res 877: 314-321

Wang ZQ, Porreca F, Cuzzocrea S, Galen K, Lightfoot R, Masini E, Muscoli C, Mollace V, Ndengele M, Ischiropoulos H, Salvemini D (2004) A newly identified role for superoxide in inflammatory pain. J Pharmacol Exp Ther 309: 869-878

Wei S, Ong WY, Thwin MM, Fong CW, Farooqui AA, Gopalakrishnakone P, Hong W (2003) Group IIA secretory phospholipase A2 stimulates exocytosis and neurotransmitter release in pheochromocytoma-12 cells and cultured rat hippocampal neurons. Neuroscience 121: 891-898

Wiertelak EP, Furness LE, Horan R, Martinez J, Maier SF, Watkins LR (1994) Subcutaneous formalin produces centrifugal hyperalgesia at a non-injected site via the NMDA-nitric oxide cascade. Brain Res 649: 19-26

Willis WD, Jr. (2009) The role of TRPV1 receptors in pain evoked by noxious thermal and chemical stimuli. Exp Brain Res

Won JS, Im YB, Khan M, Singh AK, Singh I (2004) The role of neutral sphingomyelinase produced ceramide in lipopolysaccharide-mediated expression of inducible nitric oxide synthase. J Neurochem 88: 583-593

Won JS, Singh I (2006) Sphingolipid signaling and redox regulation. Free Radic Biol Med 40: 1875-1888

Wu SN, Lo YK, Kuo BI, Chiang HT (2001) Ceramide inhibits the inwardly rectifying potassium current in GH(3) lactotrophs. Endocrinology 142: 4785-4794

Xu J, Yeh CH, Chen S, He L, Sensi SL, Canzoniero LM, Choi DW, Hsu CY (1998) Involvement of de novo ceramide biosynthesis in tumor necrosis factor-alpha/cycloheximide-induced cerebral endothelial cell death. J Biol Chem 273: 16521-16526

Yamamoto R, Bredt DS, Snyder SH, Stone RA (1993) The localization of nitric oxide synthase in the rat eye and related cranial ganglia. Neuroscience 54: 189-200

Yang MS, Jou I, Inn-Oc H, Joe E (2001) Sphingomyelinase but not ceramide induces nitric oxide synthase expression in rat brain microglia. Neurosci Lett 311: 133-136

Yeo JF, Liu HP, Leong SK (2001) Sustained microglial immunoreactivity in the caudal spinal trigeminal nucleus after formalin injection. J Dent Res 80: 1524-1529

Yeo JF, Ong WY, Ling SF, Farooqui AA (2004) Intracerebroventricular injection of phospholipases A2 inhibitors modulates allodynia after facial carrageenan injection in mice. Pain 112: 148-155

Yeo JF, Tang FR, Leong SK (1997) Ultrastructural study of NADPH-d positive neurons in laminae I and II of the rat caudal spinal trigeminal nucleus. Int J Neurosci 91: 29-43

Yonehara N, Kudo C, Kamisaki Y (2003) Involvement of NMDA-nitric oxide pathways in the development of tactile hypersensitivity evoked by the loose-ligation of inferior alveolar nerves in rats. Brain Res 963: 232-243

Young KW, Bootman MD, Channing DR, Lipp P, Maycox PR, Meakin J, Challiss RA, Nahorski SR (2000) Lysophosphatidic acid-induced Ca2+ mobilization requires intracellular sphingosine 1-phosphate production. Potential involvement of endogenous EDG-4 receptors. J Biol Chem 275: 38532-38539

Yu SP, Yeh CH, Gottron F, Wang X, Grabb MC, Choi DW (1999) Role of the outward delayed rectifier K+ current in ceramide-induced caspase activation and apoptosis in cultured cortical neurons. J Neurochem 73: 933-941

Zanelli SA, Ashraf QM, Delivoria-Papadopoulos M, Mishra OP (2000) Peroxynitrite-induced modification of the N-methyl-D-aspartate receptor in the cerebral cortex of the guinea pig fetus at term. Neurosci Lett 296: 5-8

Zanelli SA, Ashraf QM, Mishra OP (2002) Nitration is a mechanism of regulation of the NMDA receptor function during hypoxia. Neuroscience 112: 869-877

Zekry D, Epperson TK, Krause KH (2003) A role for NOX NADPH oxidases in Alzheimer's disease and other types of dementia? IUBMB Life 55: 307-313

Zhang C, Zhou Z (2002) Ca(2+)-independent but voltage-dependent secretion in mammalian dorsal root ganglion neurons. Nat Neurosci 5: 425-430

Zhang DX, Zou AP, Li PL (2003) Ceramide-induced activation of NADPH oxidase and endothelial dysfunction in small coronary arteries. Am J Physiol Heart Circ Physiol 284: H605-612

Zhang W, Trible RP, Samelson LE (1998) LAT palmitoylation: its essential role in membrane microdomain targeting and tyrosine phosphorylation during T cell activation. Immunity 9: 239-246

Zhang YH, Nicol GD (2004) NGF-mediated sensitization of the excitability of rat sensory neurons is prevented by a blocking antibody to the p75 neurotrophin receptor. Neurosci Lett 366: 187-192

Zhang YH, Vasko MR, Nicol GD (2002) Ceramide, a putative second messenger for nerve growth factor, modulates the TTX-resistant Na(+) current and delayed rectifier K(+) current in rat sensory neurons. J Physiol 544: 385-402

Zhang YH, Vasko MR, Nicol GD (2006) Intracellular sphingosine 1-phosphate mediates the increased excitability produced by nerve growth factor in rat sensory neurons. J Physiol 575: 101-113

Zhou D, Lauderback CM, Yu T, Brown SA, Butterfield DA, Thompson JS (2001) D609 inhibits ionizing radiation-induced oxidative damage by acting as a potent antioxidant. J Pharmacol Exp Ther 298: 103-109

Zhou Z, Davar G, Strichartz G (2002) Endothelin-1 (ET-1) selectively enhances the activation gating of slowly inactivating tetrodotoxin-resistant sodium currents in rat sensory neurons: a mechanism for the pain-inducing actions of ET-1. J Neurosci 22: 6325-6330